Essential discrimination of vascular and tissue lymphocytes redefines CD8 T cell responses to respiratory infection

A DISSERTATION
SUBMITTED TO THE FACULTY OF THE GRADUATE SCHOOL
OF THE UNIVERSITY OF MINNESOTA
BY

Kristin Gail Anderson

IN PARTIAL FULFILLMENT OF THE REQUIREMENTS
FOR THE DEGREE OF
DOCTOR OF PHILOSOPHY

Advisor: David Masopust, PhD

March 2014

Acknowledgements

The work presented in this thesis would not have been possible without the help and support of many people, from classmates, professors and collaborators, to dear friends and family.

First and foremost, I want to acknowledge how much of my success in graduate school has been a direct result of my mentor, Dave Masopust. His creativity, passion for knowledge and drive to produce excellent research is inspiring. When I started in Dave's lab, I was familiar with the basics of immunology and had a moderate level of experience at the bench, but as I reflect back on the progress I've made, I know I owe the vast majority of my success to Dave. Goethe once said, "If you treat an individual as he is, he will remain how he is. But if you treat him as if he were what he ought to be and could be, he will become what he ought to be and could be." I don't know if Dave did this intentionally, but from my perspective, this was our relationship dynamic. From the very beginning he recognized and praised my strengths, while also acknowledging the areas in which I needed improvement, and challenging me to develop them. While he rewarded small achievements, he constantly pushed me to expect more from myself. His high expectations led me to achieve more than I realized I could in graduate school.

I am also greatly indebted to the other members of my doctoral thesis committee: Marc Jenkins, Steve Jameson, Vaiva Vezys, and Brian Fife. In addition to thought-provoking feedback on my research, they were a great source of support throughout my training. Some of the most empowering experiences I had in graduate school came from interactions outside of lab when these mentors made me feel like a colleague rather than just a trainee.

But Dave and my thesis committee members were certainly not the only people who influenced my scientific growth. Thank you so much to all the members of the Masopust and Vezys lab, both past and present, for all their help when I needed it most: Heungsup Sung, Lalit Beura, Angie Deisinger, Lindor Qunaj, Kerry Casey, Katy Fraser, Jason Schenkel, Lizzie Steinert, Nancy Fares, Jean Porter, JJ Locquiao, Lee Swanson, Emily Thompson, Christine Nelson, and Clare Conemac. I will miss the constructive discussions and the random humor that kept us going on the long days (which far outnumbered the not-long days).

My success in the Microbiology, Immunology and Cancer Biology (MICaB) Program also wouldn't have been possible without the support of many other people at the University of Minnesota in the Microbiology Department and the Center for Immunology. Annette Bethke, the Center for Immunology Executive Administrator, was always a great help any time I needed a room to study or help keeping track of the many nuances of hosting a visiting speaker. I don't think I would have survived my year as a student representative without the support of Louise Shand, the MICaB Program Administrator. Her genuine interest in the students, talent for her job, and drive to go above and beyond is truly inspiring. I

also owe a debt of gratitude to Paul Champoux, the Flow Cytometry Core Operator, and Jason Mitchell, the Center for Immunology Imaging Core Director, for their help in advancing my training in both of these rapidly advancing technologies. Many thanks as well to Yoji Shimizu and Mark Herzberg, the two mentors largely responsible for my acceptance to and success in the Minnesota Craniofacial Research Training (MinnCResT) Program. I would be remiss if I didn't also acknowledge Ann Hagen, the Assistant Program Director for the MinnCResT Program, who planned excellent programs for our fellowship meetings and helped me find creative ways to take advantage of every training opportunity my pre-doctoral fellowship had to offer. In my tenure in the program, I also had the opportunity to work with Steve Jameson, Chris Pennell and Sandy Armstrong who each served terms as the MICaB Director of Graduate Studies. In addition to always showing a heartfelt interest in my training as a scientist, it was clear that each one of them cared about me personally. Finally, many thanks to my MICaB peers and their partners (our behind the scenes support), without whom I might not have maintained my sanity or passed my preliminary exams: Jeff Hall, Val Neff, Cara Skon, Luke Brand, Casey Katerndahl, Ryan Flynn, Megan Multhaup, Adam Spaulding, Kelsey Spaulding, Brandon Leonard, Bobbi Leal, Britnie James, Wade Thomas, and Polly Chuntova. I can sincerely say I wouldn't have graduated without the support of my University of Minnesota/MICaB family.

I also want to sincerely thank some of my previous scientific advisors, without whom I may not have had the courage to pursue a graduate degree in

the first place. Jill Manske, my undergraduate immunology professor, is the primary driver behind my decision to study immunology. She was the first professor I had the opportunity to learn from who made active learning a priority in class, and I think it was this unique approach to teaching that helped me realize my passion for research, despite the challenging nature of the topic. I had several other amazing professors at the University of St. Thomas, Nancy Hartung, Bill Ojala, and Joe Brom, who all contributed in their own ways to my development as a student and future scientist. Their fine-tuned balance between constructive feedback and praise was just the right amount of character-building (read: challenging) advice mixed with support that I needed to persevere during those times when I questioned whether or not science was for me. I also want to thank Julie Curtsinger and Jeffrey S. Miller who were my advisors when I was a junior scientist at the University of Minnesota. Without their training and influence, I might not have been accepted to such a competitive doctoral training program.

My mentors, collaborators and peers were far from the only people who ensured that I had a successful graduate school experience. My parents, Mark Anderson and Barb Anderson, and my younger brother, Eric, have seen me through it all, and they were always there to pick me up when I stumbled and never hesitated or complained, even when I needed them to carry me. Many thanks to Grandma Chale, Grandma and Grandpa Anderson, and the Freedman, Egan, Chale, Swingen, and Anderson families for encouraging my curiosity and supporting my dreams. I am also greatly appreciative of everything my new

family, the Taylor clan, has done to support me. Don, Brenda, Carissa, Kevin, Doni, Sean, Jen, Ollie, Brett and Jack: thank you for treating me like one of the family even before I officially joined it. And, obviously, I want to extend my greatest appreciation to my friends, those listed here and not, for listening to me complain when we were together, for understanding and forgiving my absences when we could not be, and for loving and supporting me through it all: Rachel Reese, Maren MacGregor-Hannah, Sarah Bretl, Grace Friedman, Lindsay Narayan, Nadia Narayan, Brandi Supple, Jessica Fiege, Katie Gundlach, Matt Swords, Erin Kennedy, Holly Stessman, Candice Keimig, Edward Colburn, Charlie Mitchell, Joyce Heckman, Sarah Polcher, Trina Kuriger, Katie Hermanson, Lauren McCarthy, and Lauren Klugherz. Thank you for wanting the best for me and for helping me to achieve it.

Finally, the hardest person to find the words to thank is the (Reverend) Dr. Justin James Taylor, because his contribution to my success goes far beyond his role as my scientific colleague. Justin has a talent for asking questions that help me resolve any hurdle I encounter (scientific or personal), rebuilding my confidence when I doubt myself, making me laugh when I want to scream, reminding me that the struggle is worth it, and redirecting my perspective on life so I take everything one step at a time. He saw me through the hardest battles of graduate school (and life in general), and I will always be grateful for his steadfast confidence and love.

Dedication

After my breast cancer diagnosis in 2011, my aunt shared a story with me about accepting help from others, and I think the metaphor aptly reflects my situation:

> A man led his army into battle. When the man held his hands up, his side prevailed, and when he let his hands down, his side began to lose. But the man's hands were heavy, and he could not hold them up on his own for the entire battle. When his hands began to fall, his friends supported arms, one on one side and one on the other, day and night, until the battle was won.

This work is dedicated to my wonderful family and friends who held my hands up.

Abstract

Characterizing the cellular participants in tissue immune responses is critical for understanding infection, cancer, autoimmunity, allergy, graft rejection, and other immunological processes. Leukocytes recirculate through blood vessels before localizing to tissue sites of immune responses. Thus, in experimental animal models, tissues are often perfused to putatively remove blood-borne leukocytes that may conflate analysis. Here, we develop and validate an intravascular staining methodology that distinguishes between vascular and tissue-localized cells of the immune system. We demonstrate that perfusion both fails to remove many blood-borne leukocytes and also may remove tissue-localized populations of interest, and we provide examples of how this issue distorts interpretation of leukocyte differentiation state, migration, and phenotype in healthy mice, as well as those responding to viral or *Mycobacterium tuberculosis* infection or tumor challenge. Additionally, we utilize intravascular staining to examine resident memory T cells in non-lymphoid tissues, such as the lung, liver and female reproductive tract. This study highlights the breadth and gravity of the issues regarding tissue leukocyte composition, outlines simple methods for identification of various intravascular leukocyte populations, reviews the limitations of the technology, and demonstrates that these methods should be routinely adopted in lieu of perfusion for interpretable and accurate analyses of immune responses in many tissues.

Table of Contents

List of Tables

List of Figures

Chapter 1

Introduction

Respiratory Infections

Lower respiratory tract infections (LRIs or LRTIs), involving the trachea, bronchial tubes, bronchioles and lungs, are the third leading cause of death in the world (behind only ischaemic heart disease and stroke), and they are the leading cause due to infectious disease (*1*). Bronchioles of the lower respiratory tract branch into alveoli, tiny air sacs separated from blood vessels by a cell layer only 2μm thick. This intimate barrier permits efficient gas exchange, a critical function of the lung, but it also allows for a major vulnerability: the only separation between environmental agents and the vascular circulation are a fused alveolar pneumocyte and a capillary endothelial cell with a shared basement membrane. During an infection of the lung, the immune system must maintain a delicate balance between effector functions, which attempt to prevent systemic disease by eliminating or containing the pathogen, and pathology, which may induce fatal damage to the host.

To reduce vulnerabilities to infection, the respiratory tract consists of numerous physical barriers, including tight junctions between epithelial cells and the mucociliary escalator. Mucous-secreting goblet cells (*2*), ciliated epithelium, and commensal bacteria comprising the lung microbiome (*3*) all contribute critical protective functions in the lower respiratory tract. Further, the innate arm of the immune system, consisting of polymorphonuclear cells (PMNs or neutrophils), mononuclear phagocytes (monocytes, macrophages, and dendritic cells), and innate lymphoid cells mount an immediate response to foreign material, which is often sufficient to prevent the spread of infection. However, despite these diverse

defense mechanisms, some pathogens escape elimination. In these cases, antigen-specific T- and B-lymphocytes of the adaptive immune response are often required for pathogen control and clearance.

Immune responses to viral infection

During an infection, cells of the innate and adaptive immune system work in concert to contain and clear the infectious agent. Upon initial exposure to virus, cells of the innate immune system recognize foreign viral material by detecting pathogen associated molecular patterns (PAMPs) through pattern recognition receptors (PRRs). PAMPs can be in the form of nucleic acids (DNA or RNA), proteins, or cellular damage caused by infection. Pathogen recognition results in the recruitment of additional inflammatory cells to the site of infection and activation of naïve lymphocytes in lymphoid tissue.

An immune response against infectious virus is initiated when an aspect of the virus is detected either by infected host cells or by neighboring cells of the innate immune system. The three major classes of phagocytic cells, macrophages/monocytes, granulocytes, and dendritic cells, detect pathogens using PRRs. Viral nucleic acid sensing can occur in the cytoplasm through RIG-I-like receptors (RLRs) and melanoma differentiation-associated 5 (MDA-5), which detect viral RNA (*4*-*7*), or AIM2-like receptors (ALRs), which detect viral DNA (*8*-*15*). Nucleotide-binding oligomerization domain (NOD)-like receptors (NLRs) (*8*, *10*, *12*, *14*-*16*), such as NLRP3, detect cell stress or damage in the cytoplasm and initiate formation of the inflammasome complex. Detection of viral nucleic

acids can also occur in endosomes through toll-like receptors (TLRs), specifically TLR3 (*16-18*), TLR7 (*17-20*) and TLR9 (*19-21*). Detection of viral PAMPs triggers phagocytic cells to produce and secrete anti-microbial peptides, chemokines, and the anti-viral cytokines interferon (IFN)-α and IFN-β, which contribute to the induction and maintenance of inflammation as well as containment of the infection.

Almost all cell types in the body are capable of producing IFN-α and IFN-β, also referred to as type I IFNs, upon detection of viral RNA via the cytoplasmic PRRs RIG-I and MDA-5 (*21-24*). However, some cell types, such as the plasmacytoid subset of dendritic cells, are capable of producing abundant levels of type I IFN during viral infection (*22-26*). IFNs were named for their ability to interfere with viral replication in infected cells in vitro. In vivo, IFN signaling induces resistance to viral infection in nearby uninfected cells by activating genes that degrade cytoplasmic mRNA and inhibit translation. In addition, IFN signaling also increases major histocompatibility complex (MHC) expression and antigen presentation (*25-28*), activates dendritic cells, macrophages, and natural killer (NK) cells (*27-32*), and induces expression of chemoattractant molecules (*29-33*). Collectively, IFN signaling limits viral replication, sustains inflammatory cues, and plays a role in the initiation of the adaptive immune response.

The innate arm of the immune response utilizes numerous PRRs to detect a broad range of foreign material. Lymphocytes of the adaptive immune system, however, express receptors allowing for recognition of unique epitopes, a phenomenon referred to as antigen-specificity. During development, B and T

lymphocytes undergo unique gene rearrangements to express antigen-specific receptors on the cell surface with very specific binding capabilities. B cells express a B cell receptor (BCR) with direct antigen-binding abilities; consequently, BCRs recognize both the peptide sequence and spatial conformation of antigens. T cells, however, express T cell receptors (TCR) that bind to peptide in MHC expressed on the surface of antigen-presenting cells (APC). The TCRs of CD8 T cells bind to peptide in MHC class I (MHC I) molecules, while the TCRs of CD4 T cells bind to peptide in the context of MHC class II (MHC II). CD8 and CD4 T cells are also identified by their expression of the co-receptors CD8 and CD4, respectively, which stabilize TCR interactions with the peptide:MHC complex.

Activation of naïve T cells requires three distinct signals from professional APCs (*34*, *35*) (of note: while macrophages and B cells have the ability to present antigen to T cells in the context of MHC II, professional APCs involved in T cell activation are usually dendritic cells (*33*, *36*, *37*)). PRR ligation and IFN signaling at the site of infection result in dendritic cell maturation and migration to lymphatic tissue and subsequent lymphocyte activation. In this way, dendritic cells form a critical link between the innate and adaptive arms of the immune response.

The first APC:T cell signal consists of a peptide:MHC and TCR interaction (*34*, *38*). The second involves the interaction of co-stimulatory molecules B7.1 (CD80) or B7.2 (CD86) on the APC and CD28 on the T cell (*36*, *37*, *39*, *40*). The third signal comes in the form of cytokines secreted by the APC (*35*, *38*, *41-45*).

This combination of activating signals initiates clonal expansion and differentiation of the activated cells, resulting in an expanded population of T cells with the same antigen specificity. After priming, antigen-specific lymphocytes, which are rare in the naïve repertoire (approximately 20-200 naïve cells of each epitope specificity) (*39*, *40*, *46*), expand 100- to 50,000-fold (*35*, *41-48*), resulting in an abundant population in secondary lymphoid tissue (Figure 1-1). Importantly, if any of the three signals is absent during activation, T cells are programmed to follow an unresponsive fate (*46*, *49*). T cells receiving incomplete activation signals often undergo clonal deletion, anergy induction, tolerization, or differentiation into regulatory cells (*46-48*, *50*).

The signal three cytokines from APCs also initiate a differentiation program in activated cells, allowing for acquisition of effector functions. Once activated, effector cells no longer require co-stimulation to exert their functions. Activated B cells begin to secrete BCR in the form of antibody. Activated CD8 T cells adopt cytotoxic effector functions, such as Granzyme B and IFN-γ production, for defense against intracellular pathogens. CD4 T cells differentiate down effector lineage pathways based on which cytokines were secreted by APCs during activation (*38*, *51*). To date, numerous CD4 T cells subsets have been characterized on the basis of transcription factor expression and cytokine secretion (*49*, *52*). For example, naïve T cells differentiate into T_H1 cells when activated in the presence of IFN-γ and interleukin (IL)-12 (*50*, *53*, *54*). T_H1 cells provide protection against intracellular pathogens, such as viruses and intracellular bacteria, and are defined by the expression of the transcription factor

T-bet and secretion of IL-2 and IFN-γ (*38*, *55-57*). Upon activation, T cells also begin to express receptors that direct egress from the spleen and lymph nodes and promote migration to non-lymphoid tissues (*52*, *58*).

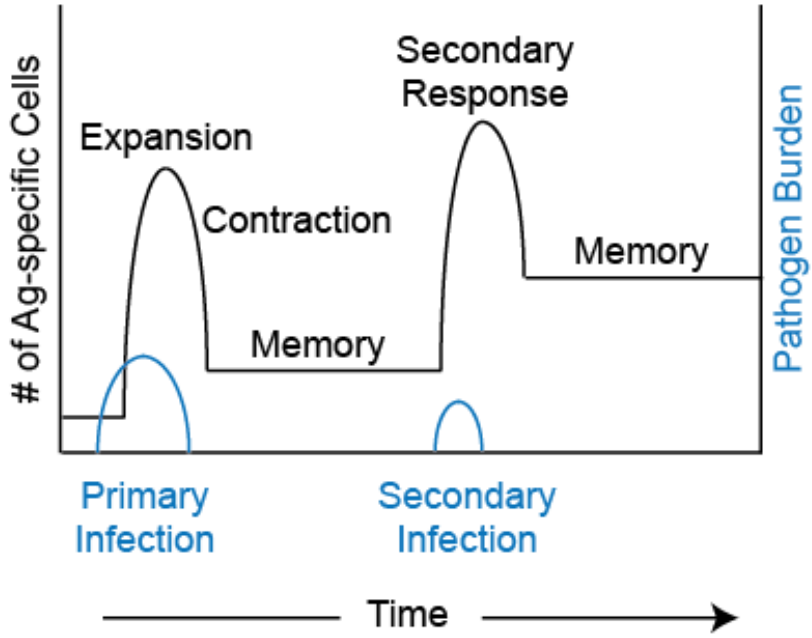

Figure 1-1: T cell expansion, contraction and maintenance after antigen stimulation. The naïve repertoire contains a vast number of T cells that express unique T cell receptors. Prior to antigen exposure, the frequency of these cells in the circulation is very rare. Upon exposure to antigen and activating signals, antigen-specific T cells proliferate and differentiate. After clearance of the antigen, the expanded population contracts, yielding a relatively stable memory pool. These memory cells are capable of rapid expansion and effector function upon repeated exposure to antigen.

In contrast to T cells, which require interactions with mature DCs for priming, B cells undergo activation through interactions with antigen and activated CD4 T cells (*53*, *54*, *59-61*). BCR ligation induces both intracellular signaling and antigen internalization. Antigen is subsequently processed and presented on MHC II molecules to CD4 T cells. Helper T cells previously primed

by mature DCs express co-receptors, such as CD40 ligand (CD40L) and inducible costimulator (ICOS) (*55*-*57*, *62*, *63*), and secrete cytokines, such as IL-4, IL-5, IL-6, and B cell activating factor of the tumor necrosis factor family (BAFF), that induce proliferation and differentiation of B cells expressing cognate peptide:MHC II (*58*, *64*). In the secondary phase of B cell activation, activated B cells migrate into follicles within the secondary lymphoid organ, continue proliferation, and form germinal centers (*59*-*61*, *65*). Further interactions with CD4 T cells of the follicular helper lineage (T_{FH}) in the germinal center initiate somatic hypermutation (*62*, *63*, *66*), affinity maturation, and class switching (*64*, *67*-*69*). Activated B cells differentiate into either antibody-secreting cells (secreting a soluble form of the BCR; also known as plasma cells) or memory cells (*65*, *70*, *71*) (which do not secrete soluble BCR). This process yields long-lived B cell memory as well as the production of both high affinity antibodies and antibodies of different isotypes with distinct effector functions (*66*, *72*).

Effector B and T cells make fundamentally different contributions to the overall immune response. For instance, antibodies contribute to neutralization or opsonization of infectious agents and toxins (*67*-*69*, *73*, *74*). T cells, on the other hand, do not produce soluble TCR. Instead, T cells participate in myriad diverse protective effects within the host. CD8 T cells secrete cytokines and exhibit contact-dependent cytotoxicity during infection, killing infected cells in a controlled manner to prevent pathogen spread (*70*, *71*, *75*). CD4 T cells influence the behavior of other cells by exhibiting cytotoxicity (*76*, *77*), activating macrophages (T_H1) (*72*, *78*, *79*), recruiting and activating eosinophils, mast cells

and basophils (T_H2) (*73*, *74*, *80*), promoting inflammation (T_H17) (*35*, *42*, *75*), providing help to B cells during activation (T follicular helper (T_{FH})) (*35*, *42*, *45*, *76*), or suppressing other lymphocytes (T regulatory cells (Tregs)) (*78*, *79*, *81*). This combination of approaches to preventing pathogen dissemination throughout the body is sufficient to clear the infectious agent in the vast majority of cases. In the event that the innate and adaptive arms of the immune response are unable to clear a pathogen, chronic infection is established within the host; the regulatory capacity of T cells serves to reduce immune-mediated damage within host tissue and establish a new homeostatic equilibrium between host-pathogen interactions (*80-82*).

In acute infections, proliferating lymphocytes reach a peak in population size that correlates with control of the pathogen (Figure 1-1). Upon control or clearance of an infectious agent, the population of effector cells undergoes contraction (*35*, *42*, *83*). Approximately 90-95% of the antigen-specific population undergoes coordinated and controlled cell death, also known as apoptosis (*35*, *42*, *45*, *84-86*). Lymphocytes that remain after contraction form a long-lived memory population, which is maintained in both lymphoid and non-lymphoid tissues, poised to mount a rapid response against future infections.

Lymphocyte migration

Leukocyte migration is a coordinated process involving alterations in expression of a variety of molecules and on a variety of cell types. Despite the great diversity in these molecules at the molecular level, the multistep paradigm

of cellular migration from blood into tissue is remarkably conserved. The central dogma regarding leukocyte migration involves several major steps: rolling, integrin activation, arrest, and transmigration (Figure 1-2). Blood circulating through the body reduces velocity upon entry of post-capillary venules (*81*, *87*), which are wider in diameter than capillaries. Hemodynamic forces, such as shear forces near the edges of endothelial vessels, and interactions with red blood cells (RBC) (*81*, *82*, *88*) also contribute to the reduced velocity of leukocytes traveling in the blood. Interactions between selectins and carbohydrate molecules allow leukocytes to adopt a “rolling” motion along the endothelial surface. This motion allows for ligation of chemokine receptors on leukocytes with chemokines expressed on the vascular endothelium; G-protein coupled intracellular signaling subsequently activates integrins on leukocytes (*83*, *89*). Integrin activation and firm adhesion to the endothelial surface results in cell arrest. Once leukocytes have stopped moving laterally, transmigration (also referred to as extravasation, the process of leukocytes squeezing between endothelial cells, or diapedesis, the process of leukocytes passing through the basement membrane) through the vascular endothelium into the tissue occurs (*90-93*).

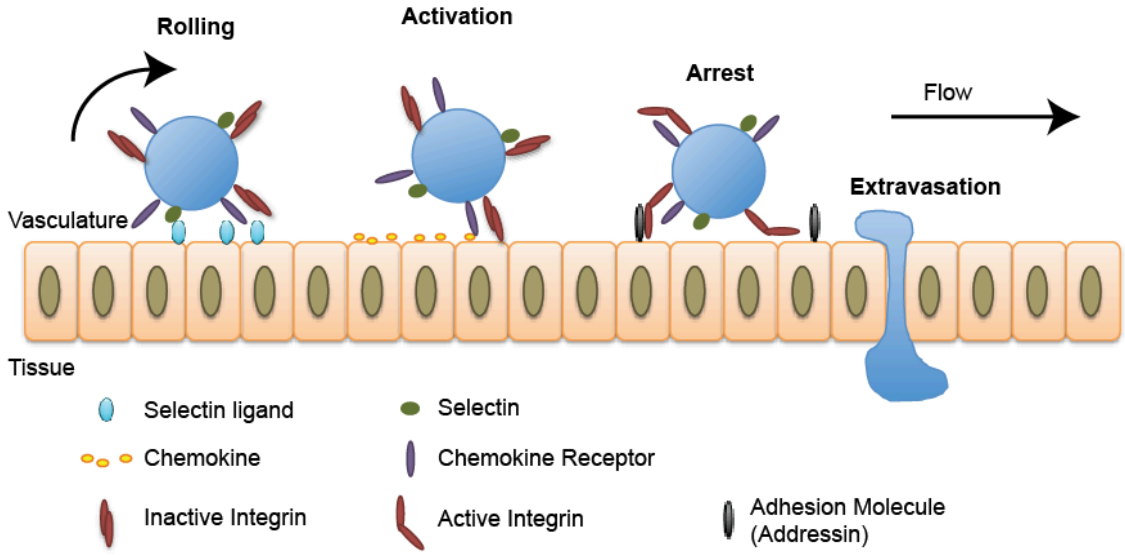

Figure 1-2: T cell migration three-step paradigm. Leukocytes engage in a coordinated process to traffic from blood into tissue. Selectin ligation allows cells to "roll" along the endothelium, chemokine receptor ligation activates integrins on the leukocyte surface, and integrin interactions with addressins on the endothelial surface results in firm adhesion. Upon arrest, cells extravasate into the tissue.

While the specific selectins, chemokine receptors and integrins involved in trafficking from the vasculature into organs of the body vary, the general multi-step migratory process is conserved in lymphoid and non-lymphoid tissues, both under inflamed and steady state (uninflamed) conditions (*94*, *95*). For instance, L-selectin (CD62L) is expressed on naïve lymphocytes and interacts with the carbohydrate moiety sulfated sialyl-Lewis^x on high endothelial venules (HEV) in lymph nodes, which initiates rolling (*96*, *97*). Chemokine receptor 7 (CCR7) on naïve lymphocytes binds to chemokine ligands 19 and 21 (CCL19 and CCL21, respectively), presented on the vascular surface of high endothelial venules in lymph nodes (*84-86*, *98*, *99*). Downstream signaling results in the activation of the leukocyte integrin LFA-1 (composed of the α_L:β_2 heterodimer, also known as

CD11a:CD18). Interactions between LFA-1 on lymphocytes and ICAM adhesion molecules (ICAM-1 and ICAM-2) on the blood vessel wall result in firm adhesion and arrest. [It should be noted that there are some exceptions to this migratory paradigm. For example, in the absence of CD62L, the integrin α_4:β_7, which is expressed at low levels on naïve T cells, can interact with mucosal vascular addressin cell adhesion molecule 1 (MADCAM-1), and is sufficient to initiate rolling and entry of naïve lymphocytes into gut-associated lymphoid organs, such as Peyer's patches and mesenteric lymph nodes (*87*, *100*).] This selective trafficking of naïve lymphocytes to lymphoid tissues increases the likelihood that rare, naive antigen-specific cells will encounter mature APCs and become activated during an immune response.

During a viral infection in the respiratory tract, a subset of activated DCs capable of presenting viral antigens traffics to the draining mediastinal lymph nodes. Five distinct populations of lung DCs have been described in mice to date using a combination of phenotype and location within the lung. Resident cDCs (CD11c+ CD11b+ Langerin+ CD103+), plasmacytoid DCs (pDC; $CD11c^{dim}$, CD11b-, Siglec H+), and alveolar DCs (CD11c+ CD11b+/-) are found in the lung under non-inflammatory conditions. Under inflammatory conditions, inflammatory monocyte-derived DCs (CD11c+ CD11b+ Ly6c+ SIRP-1α) and interferon-producing killer DCs (iKDC; $CD11c^{dim}$ CD11b- B220+ CD19- NK1.1+) are also present (*101*, *102*). Each subset is thought to play a distinct role in T cell activation. For instance, CD103+ cDCs have been shown to be essential for priming of CD8 T cells in the draining lymph node after influenza infection (*103*,

104), while CD11c+ CD11b+ DCs are critical for inducible bronchus associated lymphoid tissue (iBALT) generation and maintenance (*82*, *88*).

Once activated DCs reach the draining lymph node, naïve T and B cells become activated, proliferate, differentiate, and begin to express chemokine receptors and integrins that facilitate migration back to the lung. To date, CCR5 (*89*, *105*, *106*), CXCR6 (*90*, *92*, *93*, *107*), and CXCR3 (*94*, *108*-*110*) have been shown to be important for T cell migration to the respiratory tract. However, CCR5 and CXCR3 have been demonstrated to be important receptors for migration to a variety of non-lymphoid tissues, such as skin and small intestine (*96*, *108*, *109*, *111*). The collagen-binding integrin $\alpha_1\beta_1$ (VLA-1, the α_1 component is also known as CD49a) (*98*, *99*, *112*, *113*), as well as the interaction between lymphocyte function-associated antigen-1 (LFA-1) and very late antigen-4 (VLA-4) (*100*, *114*), have also been implicated as mediators of lung-specific T lymphocyte migration. Whether these or other as of yet unidentified receptors are responsible for lung-specific homing remains to be determined.

Importantly, studies tracking the circulation of neutrophils through the lung vasculature have demonstrated a substantial difference in transit time depending on the route of cell passage. Neutrophils traveling through large blood vessels transit through the lung in roughly 3 minutes, while neutrophils migrating through the capillary beds require closer to 3 hours to completely transit the lung (*101*, *115*-*117*). Consequently, neutrophils are enriched ~100 fold within the lung capillaries over the large lung vessels. In other words, even though capillaries only contain ~40% of the blood volume within the lung, they consist of ~99% of

the blood-borne neutrophils. Erythrocytes, which are of a similar diameter to leukocytes (*103*, *118*), must also transit these narrow capillary segments. However, unlike leukocytes, erythrocytes are capable of deforming (*82*, *119-126*), allowing transit through the lung vasculature without restriction. These results with respect to restricted neutrophil migration through pulmonary capillaries support the hypothesis that lymphocytes may also be sequestered within lung vasculature.

While the paradigm of lymphocyte migration necessitates roles for selectins, chemokines, and integrins, some data suggests that these requirements are dispensable for leukocyte migration to the lung tissue. A role for selectins has been described in lymphocyte migration to the lung (*105*, *106*, *127*), while others suggest that selectins are not critical for trafficking to this tissue (*107*, *128-133*). Although chemokine ligation and integrin activation are thought to be major initiating factors of diapedesis, several reports have indicated this process may be dispensable for lymphocyte migration to the lung (*108-110*, *134-136*). Furthermore, some reports indicate that naïve lymphocytes, which lack expression of the chemokine receptors suggested to be critical for lung homing, are capable of migrating to uninflamed lung tissue (*108*, *109*, *111*, *122*, *137-141*).

In addition to reports suggesting that the requirements for naïve B and T cell migration to the lung tissue are unique, some reports also suggest that cells of the myeloid lineage have unique migratory properties with respect to the lung. For instance, upon extravasation from the circulation, tissue-specific factors induce monocytes to differentiate into macrophages or monocyte-derived DCs

(*142-146*). However, it has also been suggested that monocytes can circulate through the lung tissue without differentiating (*147-149*). These conflicting interpretations of leukocyte homing requirements and differentiation states within the lung tissue necessitate a re-evaluation of this phenomenon. A clear understanding of the mechanism of lymphocyte migration is critical for determining the factors that are important for mounting an effective protective response against infection.

Memory T cell heterogeneity

Upon clearance of a viral infection, expanded primary effector lymphocytes undergoes contraction, resulting in a memory population of antigen-specific cells (Figure 1-1). While this population contains only a fraction of the number of cells that were present during the effector stage (~5-10%), the memory population persists with approximately 100-1000 fold greater frequency than what was initially present in the naïve repertoire (*112*, *113*, *150*, *151*) and remains quite diverse in phenotype and functional capacity (*114*, *144*, *152*).

Immunological memory is long lived (*115-117*, *138*, *153*), and memory cells contribute to rapid protection against subsequent infection. Rapid protection can be attributed to several important differences between naïve and memory T cells: differentiation state, frequency, and proximity to the site of antigen encounter. Like effector T cells, memory T cells are poised to exert effector functions immediately upon TCR recognition of the appropriate peptide:MHC complex without secondary activation signals by APCs. Additionally, the

increased frequency of antigen-specific memory cells in the repertoire (compared to naive cells) increases the chances of antigen encounter. Finally, memory cells are positioned within non-lymphoid tissues, particularly at barrier surfaces, such as the respiratory, digestive, and urogenital tracts, where epithelial breach and infection can occur. This positioning allows memory cells an opportunity to detect and clear an infectious agent before the infection spreads systemically. Thus, there is great interest in understanding the development and maintenance of immunological memory in mucosal tissues, especially for immune-evasive agents such as human immunodeficiency virus (HIV), herpes simplex virus (HSV), *Mycobacterium tuberculosis* (Mtb), and influenza virus.

The T cell memory population was originally defined by expression of the lymphoid homing molecules CD62L and CCR7 (*118*, *138*, *153*, *154*). T cells expressing these molecules are termed central memory T cells (T_{CM}), which retain the ability to circulate through secondary lymphoid organs, blood and lymph. T cells lacking these molecules are termed effector memory T cells (T_{EM}) and may be found circulating throughout the body. Consequently, T_{EM} can be found predominantly in non-lymphoid tissues, blood and lymph. A subset of memory T cells that lack expression of CD62L and CCR7 (hence, cells that were originally classified as T_{EM}) are now known to reside within tissues without egress to the circulation. These cells are known as resident memory T cells (T_{RM}), and they have been identified in many non-lymphoid tissues, including small intestine epithelium, skin, female reproductive tract, brain, kidney, and lung (*119-126*, *155*), as well as some secondary lymphoid organs (*156*). However, within the

memory T cell compartment, "T_{CM}" and "T_{EM}", as well as "T_{RM}", are very broad means of characterizing an extremely diverse population of cells.

Originally, proliferative potential and effector function, in addition to recirculation migration patterns, were used as the primary parameters for distinguishing subsets of memory T cells (*126*, *127*). For example, T_{CM} have been shown to have superior proliferative potential and greater longevity than cells within the T_{EM} category, whereas T_{EM} generally maintain heightened effector capacities (*155*, *157-159*). However, increasing evidence suggests that heterogeneity exists beyond these classifications as well. Many cell-extrinsic conditions, such as the cytokine milieu under which T cells first encountered antigen, the duration and intensity of antigen exposure (*128-133*, *160*), cues unique to the lymphoid site of priming (*119*, *134-136*, *161*), and unique non-lymphoid tissue microenvironment factors (*121-123*, *137-141*, *155*), as well as cell intrinsic characteristics, such as transcription factor expression level (*41*, *42*, *142*, *144-146*), cellular metabolism (*42*, *147*, *149*, *162*), cytolytic capacity (*113*, *118*, *150*, *151*), cytokine secretion profile, cytokine responsiveness (*118*, *144*, *152*, *163*, *164*), and turnover rate, all contribute to diversity within the memory T cell population.

By definition, the T_{RM} subset of the memory T cell population remains within tissues rather than recirculating through the resting host. Studies in the small intestine epithelium and the epidermis of the skin have revealed novel characteristics of T_{RM} populations. Intraepithelial lymphocytes (IEL) of the small intestine reduce expression of the receptors for IL-7 and IL-15, as well as the co-

stimulatory molecule CD27 (*123*, *138*, *153*). IELs also retain cytolytic function and high Granzyme B expression, along with expression of the cell surface molecules CD69 and $\alpha_E\beta_7$ (the α_E integrin is also referred to as CD103) (*138*, *153*, *154*, *165*, *166*). While expression of CD69 is often correlated with recent antigen experience, IELs express CD69 even under germ-free conditions (*155*, *162*, *167*), suggesting that expression of CD69 is not restricted to cells that have recently encountered antigen. In fact, CD69 expression is inversely correlated with expression of the sphingosine-1 phosphate receptor 1 (S1PR1), which in involved in sphingosine-1 phosphate (S1P) mediated egress from tissues (*126*, *168*, *169*). Thus, CD69 is often used as a surrogate marker of T_{RM}. In contrast to CD69, CD103 expression is regulated by tumor growth factor beta (TGF-β), which is expressed constitutively within the small intestine epithelium (*155*, *158*, *159*, *169*, *170*). The integrin CD103 binds to E-cadherin, which is expressed on epithelial cells (*123*, *160*), and is thought to contribute to maintenance of IELs within the epithelium. While T_{RM} isolated from the small intestine epithelium and epidermis of the skin almost unanimously express high levels of CD69 and CD103 (*113*, *119*, *161*), T_{RM} within other non-lymphoid tissues, such as the salivary gland and female reproductive tract (*119*, *121*, *123*, *155*) do not, which suggests that not all T_{RM} express these molecules. Thus, the fidelity of these cell surface molecules as *bona fide* markers of residency remain to be determined.

Memory T cells can exert cytotoxic function in both antigen-specific (*41*, *42*, *171-175*) and bystander manners (*42*, *162*, *176*) to provide protection. Memory T cells that encounter antigen contribute to secondary immune

responses through rapid proliferation (*113*, *118*, *176*), immediate cytotoxic effector mechanisms (*118*, *163*, *164*, *176*), and recruitment of additional immune effectors to the site (*123*, *174*). Importantly, bystander activation via cytokine signaling (*165*, *166*, *176*) or NKGD2 ligation on antigen-nonspecific T cells results in CD8 T cell cytotoxicity (*162*, *167*, *177*) and, in some model systems, protective immunity (*162*, *178*).

During anamnestic responses to respiratory infections, memory T cells are recruited to the lung tissue in an antigen-independent manner (*179-182*). IFN-α signaling promotes Granzyme B expression by recently recruited memory CD8 T cells within the lungs, which contributes to rapid cytotoxicity and control of viral replication (*170*, *183*, *184*). During influenza infections, heterosubtypic immunity provides significant protection against cross-reactive viral serotypes (*168*, *169*, *185*, *186*). Current studies investigating the kinetics of anamnestic responses against respiratory infections suggest that recruitment of memory T cells does not occur until more than 72 hours after infection (*169*, *170*, *187*). However, reports in other model systems have suggested memory T cell recruitment after viral infection can occur within 48 hours (*123*, *188-190*). These kinetic variances may be due to differences in the route of infection or pathogenic agent used during secondary challenge; however, confounding factors, such as the lack of a distinction between vascular and tissue-localized cells in the lung, may also account for these discrepancies. Additional studies involving a more rigorous examination of memory T cell location within the lung are needed.

T_{CM} have also been suggested to play an important role against secondary infections within the lung. For example, Wherry and colleagues performed adoptive transfer of equivalent numbers of sorted T_{CM} and T_{EM} populations, and demonstrated that T_{CM} appeared to have greater protective capacity than T_{EM} in the lung after intranasal infection (*113*, *188*, *191-195*). However, the experimental conditions employed greatly impact the interpretation of these data. For instance, protection was determined by viral titer five days after intranasal challenge; presumably, within this time frame APCs trafficked to secondary lymphoid tissues and reactivated T_{CM}, inducing proliferation and differentiation into new effector T cells, which then likely trafficked to the lung and contributed to control of viral replication. The initial interpretation of the data was that T_{CM} more effectively control viral replication. However, it is possible that the reduced protection afforded by T_{EM} was due to the inability of the transferred memory cells to enter the lung tissue. The transferred memory cells were isolated from mice 45-60d after primary infection and injected into the vascular circulation of the recipient mice. It has been suggested that migration to some tissue compartments is restricted to cells in the effector differentiation state (*119*, *196-199*). Since the requirements for memory T cell migration to the lung tissue have not completely been defined, transferred T_{EM} cells in this system may have been confined to the vasculature, resulting in a delayed protective response.

To thoroughly investigate these incongruities, the employment of a technique distinguishing between T cells confined to the vascular and within the lung tissue is imperative.

Leukocyte responses to *Mycobacterium tuberculosis*

T cells contribute significantly to protection against intracellular pathogens, but these infectious agents are not always viral in origin. For example, both CD4 and CD8 T cells have been shown to make significant contributions to protection against the intracellular bacterium *Mycobacterium tuberculosis* (Mtb) (*171-175*, *200*, *201*). The bacterium infects phagocytic alveolar macrophages and dendritic cells, which fail to fully eliminate the infection (*176*, *202*). Activated T cells specific for Mtb traffic to the lung and secrete the cytokines IFN-γ and TNF-α, which activate infected macrophages to produce nitric oxide synthase (NOS), reactive nitrogen intermediates, and reactive oxygen species (ROS) (*176*, *203*), limiting bacterial replication. However, even the presence of activated Mtb-specific T cells within the lung often fails to completely clear the pathogen (*176*, *204*, *205*); in fact, delayed T cell responses against Mtb have been reported (*174*, *205-207*), and the chronic immunopathology induced by Mtb infection often results in an extended period of transmission to new hosts (*176*, *208-210*). Thus, a thorough understanding of the contributions of lymphocytes to the Mtb immune response is essential for the development of effective preventative vaccines and immune-based treatments.

Numerous subsets of myeloid cells are also involved in defense against Mtb. Neutrophils (Ly6G+, CD11b+ CD68-), inflammatory monocytes/macrophages (CD68+ Ly6C+, CD11b+, CD11c-), cDCs (CD68+, CD11b+/-, CD11c+), tissue-resident CD103+ cDCs (CD68+, CD103+, CD11b-, CD11c+), and inflammatory monocyte-derived DCs (moDC, CD68+, Ly6C+,

CD11b+, CD11c+) can all be isolated from the lungs of mice during Mtb infection (*177*, *211-216*). However, the contributions of each subset to the overall immune response against Mtb are occasionally confounded by the presence of cells in the vasculature that are refractory to perfusion. The ability to distinguish cells in the lung vasculature from those in the Mtb-infected lung may identify major players in the immune response to Mtb.

Leukocyte responses to solid tumors

The immune system also plays a dynamic role in the removal of malignantly transformed cells from the body. Many tumors are detectable by antigen-specific lymphocytes (antigenic) and capable of provoking an immune response in an immune-competent host (immunogenic). Transformed cells are often removed through cytotoxic immune-mediated mechanisms, but tumors have developed myriad evasion techniques to avoid detection and eradication (*178*, *217-220*).

Two categories of tumor escape have been identified: immune exclusion (or ignorance) and immunosuppression (*179*, *181*, *182*, *221*). Many solid tumors contain fibroblast reticular networks, dense collagen matrices, and vascular endothelium that simultaneously support tumor growth and prevent entry of immune cells from the blood. Tumor-associated fibroblasts can express immunosuppressive molecules (*183*, *184*, *222*). Thick collagen networks act as a barrier to T cell interaction with tumor cells (*185*, *186*, *221*). Endothelial vessels associated with tumors express higher levels of endothelin B receptor, which

suppresses T cell adhesion, a critical step in lymphocyte migration to tumor (*187*, *223-225*). Evasion mechanisms preventing immune cell penetration of solid tumors result in immune ignorance of the tumor.

However, tumors are vastly heterogeneous with respect to initiation, expression of tumor-antigen, and microenvironment. In depth analysis of tumor microenvironments has revealed that many solid tumors contain dense immune cell infiltrate; yet, even in these tumors, eradication mechanisms fail. These tumors contain innate and adaptive cells capable of recognizing tumor antigens, but in cases of metastatic melanoma, these tumor-infiltrating effector cells have been shown to be unresponsive (*188-190*, *226*, *227*) and even suppressive (*122*, *188*, *191-195*, *228*).

Regulatory T cells are known negative regulators of tumor immunosurveillance (*120*, *122*, *155*, *196-199*, *228*, *229*). Tregs suppress other immune cells through cell-cell contact dependent mechanisms and secretion of soluble inhibitory factors. Interactions between inhibitory cell surface molecules on Tregs, such as lymphocyte activation gene 3 (LAG-3) (*200*, *201*, *229*, *230*), cytotoxic T lymphocyte antigen 4 (CTLA-4) (*202*, *231*), and Galectin-1 (*110*, *203*), with ligands on DCs (MHC II; CD80 or CD86; and CD45, CD43 or CD7, respectively) have been shown to reduce effective priming of naïve T cells and inhibit T cell function. Tregs expressing membrane bound TGF-β (mTGF-β) suppress the functionality, responsiveness and proliferative ability of both effector T cells and NK cells (*107-109*, *111*, *204*, *205*, *232*). Additionally, soluble factors such as IL-10, TGF-b, prostaglandin E_2, and immunosuppressive metabolites

have been shown to be important for suppression (*205-207*, *233*). Tregs also secrete perforin and granzymes that initiate cytolysis in effector T cells, B cells, monocytes, DCs, and NK cells (*113*, *208-210*). In both human and mouse models of disease, Tregs have been identified within solid and hematological malignancies. In fact, the proportion of Treg to effector T cells has been used for assessing disease severity, tumor burden, and likelihood of treatment effectiveness (*180*, *211-216*). Notably, depletion or blockade of Tregs in cancer models results in increased potency of effector cell function. While Treg plasticity remains controversial, Tregs have been shown to adopt CD4 effector T cell functions in the context of certain inflammatory signals (*217-220*, *234*). Consequently, a more thorough analysis of Tregs and the tumor factors that control differentiation and plasticity is of critical importance for the development of more effective anti-tumor immunotherapies.

In addition to T cells with suppressive functionality, cells of the innate lineage contribute to suppression of anti-tumor immune responses. Myeloid derived suppressor cells (MDSC) are a heterogeneous population of immature myeloid cells capable of suppressing immune responses (*120*, *122*, *155*, *179*, *221*, *228*). In mice, two subsets have been defined based on morphological differences: expression of Ly6C and Ly6G (*113*, *222*, *235*). MDSCs within the granulocytic subset are CD11b+ Ly6C^{low} Ly6G+ while monocytic MDSCs are CD11b+ Ly6C^{high} Ly6G- (*124*, *221*, *236*, *237*). Granulocytic MDSCs use ROS in a contact-dependent manner to suppress immune cell function, whereas monocytic MDSCs induce suppression via nitric oxide (NO) and arginase (*155*, *223-225*).

Notably, MDSCs have also been shown to promote tumor development through non-immunological mechanisms of angiogenesis (*238*, *239*) and metastasis (*138*, *240*).

During chronic infection and cancer, the innate and adaptive immune responses cannot control replication and spread of the pathogen or transformed cells, respectively. A deeper understanding of the immune evasion mechanisms involved in these processes will aid in the discovery of therapeutic reagents. However, our current inability to precisely determine the location of cellular participants in these processes impedes our ability to refine our understanding of these nuanced scenarios. For example, tumor-specific cytotoxic CD8 T cells may be in the circulation but fail to extravasate into the tumor. In this case, CD8 T cells could be isolated from angiogenic tumors containing neovasculature, but the cells would not necessarily be in the appropriate location for optimal function. A method for elucidating the localization of cells within tissue or vasculature will further our understanding of immune evasion processes, such as tumor ignorance.

Intravascular staining overview

We hypothesized that current techniques could not distinguish leukocyte migration to, or differentiation within, the lung tissue from cells present within the lung vasculature. Therefore, we tested the idea that cells within the lung capillaries were refractory to removal by perfusion, and this cellular population confounded the tissue-localized cells during analysis. Intravascular injection of a

non-depleting antibody had previously been used to distinguish between lymphocytes in the blood and tissue (*124*, *155*, *234*, *241-243*); however, these studies were each limited to the analysis of a single lymphocyte subset (e.g. CD8 T cells, CD4 T cells, B cells) during immune responses to infection. As the reliability of this technique had never been confirmed, we aimed to both validate the use and define the limitations of intravascular staining. Moreover, we sought to advance this methodology such that any and all leukocyte subsets could be examined within the same experiment. Additionally, we examined the utility of intravascular staining in non-infectious models of disease. Thus, we adapted this technique for use in numerous lymphoid and non-lymphoid tissues and in multiple disease models. Consequently, we have been able to explore specific phenomena related to leukocyte differentiation, trafficking, and function in several murine models of disease.

Chapter 2

Intravascular staining redefines lung CD8 T cell responses

Non-lymphoid T cell populations control local infections and also contribute to inflammatory diseases, thus driving efforts to understand the regulation of their migration, differentiation, and maintenance. Numerous observations indicate that T cell trafficking and differentiation within the lung is starkly different than what has been described in most non-lymphoid tissues, including intestine and skin. We found that >95% of memory CD8 T cells isolated from mouse lung via standard methods were actually confined to the pulmonary vasculature, despite perfusion. Respiratory route of challenge increased virus specific T cell localization within lung tissue, although only transiently. Removing blood-born cells from analysis by the simple technique of intravascular staining revealed distinct phenotypic signatures and chemokine-dependent trafficking that was restricted to antigen-experienced T cells. These results precipitate a revised model for pulmonary T cell trafficking and differentiation and a re-evaluation of studies examining the contributions of pulmonary T cells to protection and disease.

Introduction

A dense network of pulmonary capillaries underlying the alveoli forms the structural basis of respiration. Gas exchange is most efficient at the thinnest portions of the air-blood barrier where narrow capillaries share a fused basal lamina with alveolar epithelium. This intimate association between the capillary bed, a thin permeable membrane, and the outside world, coupled with the fact that inflammation can disrupt the delicate architecture necessary for gas exchange, creates vulnerabilities. Indeed, lower respiratory infections account for the single greatest cause of death from infectious disease, and the incidence of chronic T cell dependent inflammatory diseases such as asthma are increasing (*119*, *226*, *227*).

T cell differentiation is coupled with anatomic distribution. Naïve and central memory T cells (T_{CM}) recirculate through secondary lymphoid organs, blood, and lymphatic vessels. This restricted homing pattern optimizes interaction with professional APCs and subsequent proliferation in response to cognate antigen recognition. Effector memory T cells (T_{EM}) patrol non-lymphoid tissues where they are positioned for more immediate interception of pathogens at the most common points of exposure (*155*, *157*). Indeed, resident T_{EM} within skin contribute most rapidly to control of local re-infection (*122*, *136*, *228*, *244-247*). Resident T_{EM} populations have been defined in many non-lymphoid tissues, and are characterized by unique phenotypic signatures not represented in blood, including CD69 and CD103/β7 integrin (*120*, *122*, *155*, *228*, *229*, *247-253*).

Regardless of route, infection or immunization give rise to extraordinarily large effector and memory T cell populations that can be isolated from perfused mouse lung (*229*, *230*, *254*). However, lung T cell migration and differentiation is less clear than in tissues such as the intestinal mucosa, skin, brain, or lymph nodes (LNs). In contrast to the stereotypic 3-step model of lymphocyte extravasation (*231*, *254*), some evidence demonstrates that T cell homing to lung is chemokine-independent (*110*, *255-258*). However, expression of chemokine receptors by T cells, including CCR5 and CXCR3, are required for normal distribution and differentiation of lung T cells following local infection (*89*, *101*). In some infection models, the lung contains a large fraction of T_{CM} (*259-261*). In fact, even naïve lymphocytes can be isolated from the perfused lung (*107-109*, *111*, *232*). These observations contrast with most other non-lymphoid compartments, which do not contain T_{CM}, exclude naïve T cells, and require chemokine signaling for entry. This study sheds light on these issues by refining our understanding of the anatomic compartmentalization of CD8 T cells within the lung.

Results

Pertussis toxin treatment of T cells yields increased recovery from lung

We sought to confirm the pertussis toxin (PTx) sensitivity of memory CD8 T cell homing to lung and other tissues, and also to address this issue for naïve CD8 T cells. Gp33-specific P14 memory CD8 T cells were generated in vivo in

response to i.p. lymphocytic choriomeningitis virus (LCMV) infection (referred to hereafter as P14 immune chimeras, see methods). Eight weeks later, splenocytes containing memory P14 CD8 T cells were treated with PTx or control media, then transferred i.v. into naïve recipients (Figure 2-1A). Three days after transfer, various tissues were harvested to assess T cell migration. Consistent with the known requirement for CCR7, migration to inguinal LN (ILN) was blocked by PTx treatment, and there was a reciprocal increase of donor cells among spleen and PBL. As reported previously, PTx treatment did not inhibit migration to lung, and like blood, actually led to an increase in recovered cells (Figure 2-1B). This experiment was repeated with naïve P14 CD8 T cells with similar results (Figure 2-1C). These data suggest that even naïve CD8 T cells home to lung in a chemokine independent process, particularly when LN homing was inhibited.

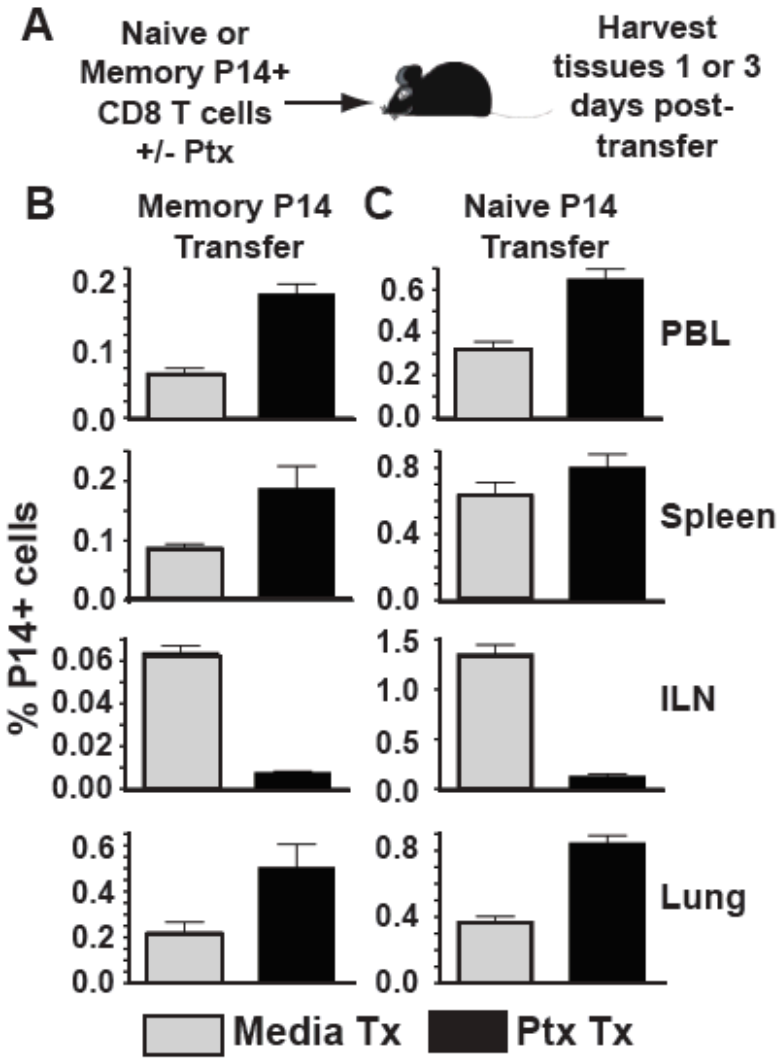

Figure 2-1: Pertussis toxin treatment of transferred T cells yields increased recovery from lung. (A) Naïve or memory P14 splenocytes were treated with pertussis toxin (PTx) or media control and transferred i.v. into naïve recipients. Tissues were harvested 1 (naïve) or 3 (memory) days after transfer. Frequency of memory (B) or naïve (C) P14 cells in PBL, spleen, ILN, or lung. Data are representative of 3 independent experiments totaling >12 mice/condition. Error bars indicate SEM.

In vivo staining distinguishes between anatomic compartments

We wished to define which lung compartment naïve T cells migrated to. We injected anti-CD8α antibody (Ab) i.v. into naïve mice that had received untreated naïve P14 CD8 T cells. Three minutes later, blood was isolated, mice were immediately sacrificed and perfused with PBS, and tissues were quickly dissected, minced, and rinsed of free Ab. Lymphocytes were isolated via standard methods then stained with anti-CD8α surface Ab and other markers of interest. The permissiveness of donor naïve T cells to i.v. staining varied among distinct tissues (Figure 2-2): 100% of donor cells within blood, a subset of cells within spleen, and virtually no cells within LN were labeled. Like blood, 100% of naïve donor cells isolated from lung labeled with injected anti-CD8α Ab.

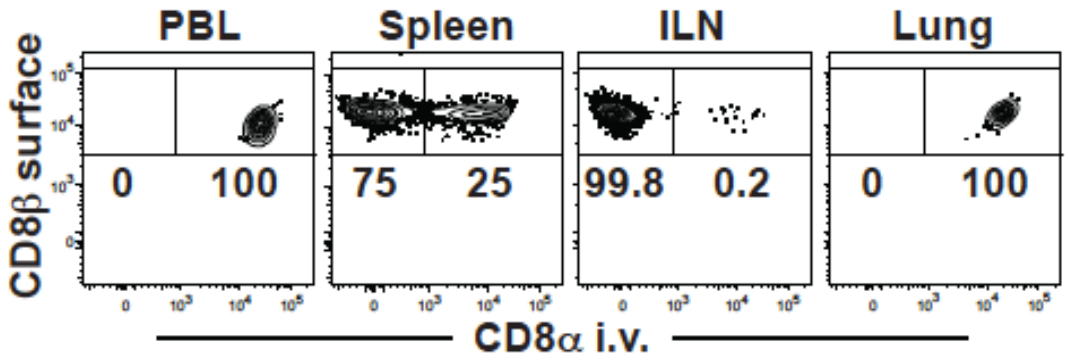

Figure 2-2: Intravascular staining distinguishes between anatomic compartments. Naïve Thy1.1+ P14 splenocytes were transferred i.v. into C57Bl/6J mice. Anti-CD8α was injected i.v. Three minutes later, tissues were harvested. Cells were isolated and then stained ex vivo with anti-CD8β. Plots gated on Thy1.1+ lymphocytes. Data are representative of 3 independent experiments totaling ≥12 mice/condition.

PTx treatment increased the number of labeled donor cells recovered from blood, spleen and lung, but reduced the number of unlabeled cells recovered from spleen and ILN (Figure 2-3).

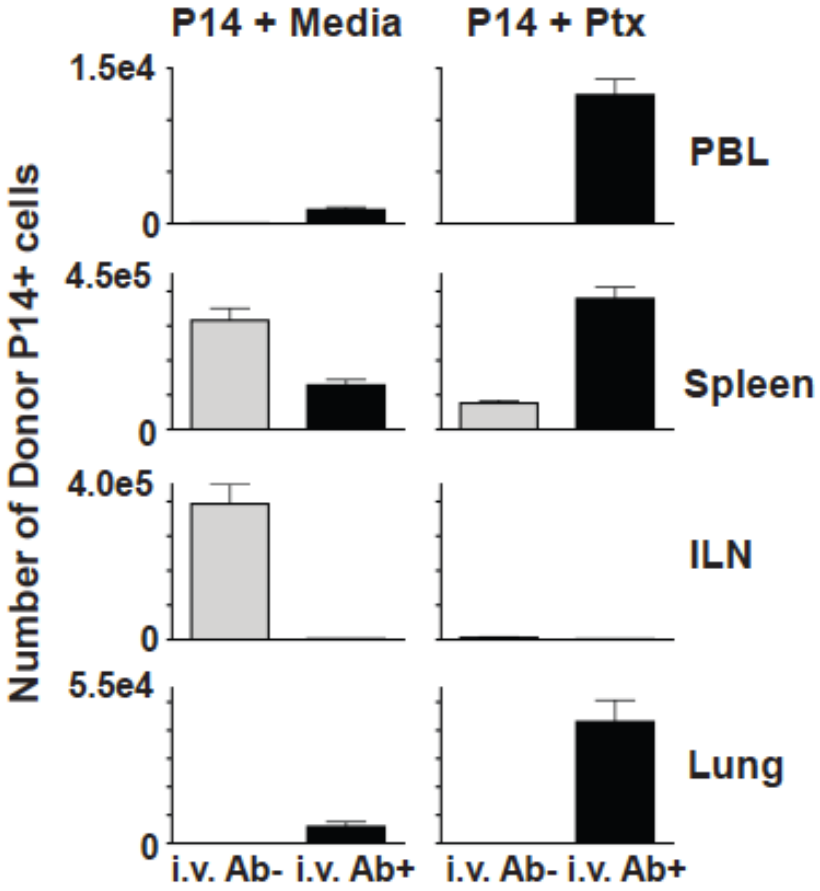

Figure 2-3: PTx treatment prevents memory T cell entry to lymph nodes and white pulp of the spleen, resulting in more memory T cells in the blood and red pulp of the spleen. Memory P14 splenocytes were treated with PTx or media control and transferred i.v. into naïve recipients. Tissues were harvested 3 days after transfer. Anti-CD8α was injected i.v. to distinguish between tissue compartments. Cells were isolated and then stained ex vivo with anti-CD8β. Number of i.v. Ab+ and i.v. Ab- naïve P14 cells, ± PTx treatment, isolated from tissues after transfer. Data are representative of 3 independent experiments totaling ≥12 mice/condition.

To assess whether intravascular staining was associated with distinct anatomic compartments, we injected anti-CD8α-PE Ab into P14 immune chimeras, sacrificed and perfused recipients, then immediately froze spleen and lung for immunofluorescence. Injected Ab labeled CD8 T cells in red pulp but not those in white pulp of spleen (Figure 2-4A). Lung tissue sections were also surface stained for CD8α-AF488, CD31-AF647 (which labels vascular endothelium), and DAPI (which labels cell nuclei). Analysis of the lung revealed that the vast majority of CD8 T cells were labeled only with injected Ab. Closer inspection revealed that these cells (red) appeared to be closely associated with pulmonary capillaries (blue, Figure 2-4B-E). These data indicate that most cells were exposed to injected Ab, and that in vivo staining blocked ex vivo surface staining on tissue sections. However, a small fraction of CD8α+ cells, typically surrounding airways and large blood vessels, were only labeled by ex vivo staining (green) of tissue sections, suggesting that they were protected from i.v. injected Ab (Figure 2-4 D&E).

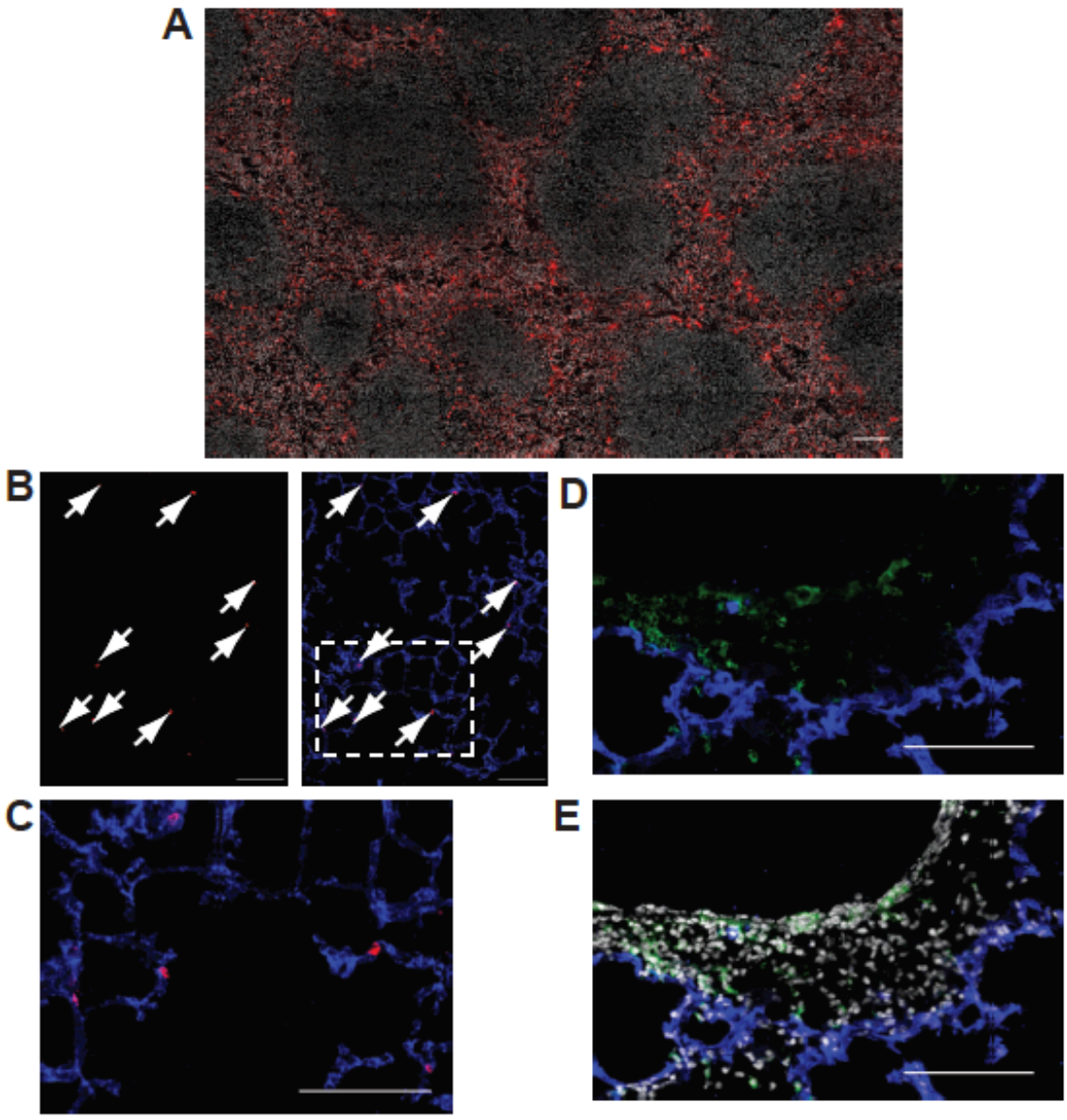

Figure 2-4: In vivo staining distinguishes between anatomic compartments. (A) Spleen after anti-CD8α-PE i.v. injection. (B-E) Lungs of P14 immune chimeras were analyzed. CD8 T cells that stain with i.v. injected Ab (red) co-localize with blood vessels (CD31, blue, see B and C), whereas those protected from i.v. Ab (green surface stain) are spatially distinct (D and E, ± DAPI, respectively). Arrows designate red i.v. Ab+ cells. Images are representative of 2 independent experiments totaling 6 mice. Scale bars represent 100μm.

Migration to lung tissue is chemokine dependent

Based on these data, it was possible that intravascular labeling of cells in the lung was restricted to cells contained within pulmonary capillaries or other blood vessels that were refractory to removal by perfusion. Alternatively, injected Ab may have leaked or been exported out of the pulmonary capillary bed, thereby staining perivascular cells. A collagen IV containing basement membrane underlies the lung vascular endothelium (as revealed by surface staining, Figure 2-5, lower left panel). We injected anti-collagen IV Ab and found that the basement membrane remained unlabeled, suggesting that the capillary bed did not allow rapid perivascular leakage of Abs (Figure. 2-5, lower right panel). For controls, we examined surface and injected collagen IV staining in the spleen (where only red pulp was exposed to injected Ab) and liver (which contains fenestrated endothelium within sinusoids, which permitted intravascular staining of basement membrane, Figure 2-5).

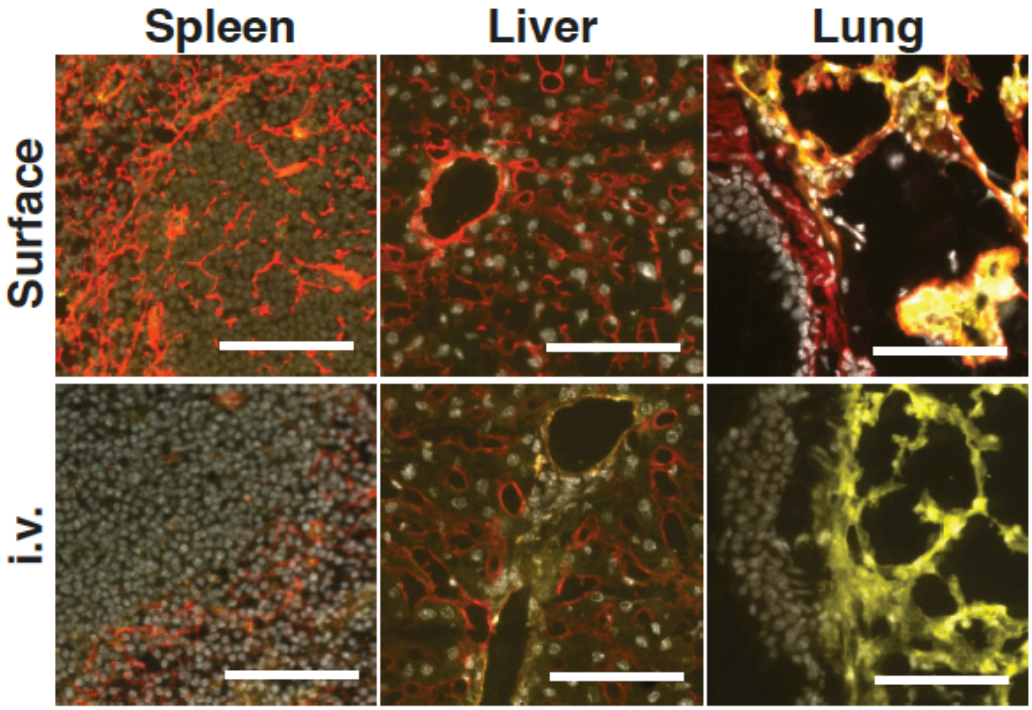

Figure 2-5: Intravascularly injected Ab does not label lung tissue under non-inflammatory conditions. Anti-collagen IV Ab (red) was injected i.v. prior to tissue harvest or tissue sections were surface stained ex vivo along with anti-CD31 (yellow) and DAPI (gray). Images are representative of 2 independent experiments totaling 4 mice. Scale bars represent 100μm.

To further test the interpretation that intravascular staining identifies cells contained within the capillary bed of the lungs of perfused mice, we revisited the issue of PTx insensitive lung trafficking. As in figure 1 A, PTx-treated or control memory CD8 T cells were transferred i.v. and recipient tissues were harvested three days later. The vast majority of untreated donor cells harvested from lung became labeled with injected Ab. However, a small fraction (~6%) was within a compartment of the lung that was protected from injected Ab. Importantly, appearance of this subset was PTx sensitive (Figure 2-6A&B), suggesting that it represented a chemokine dependent trafficking event.

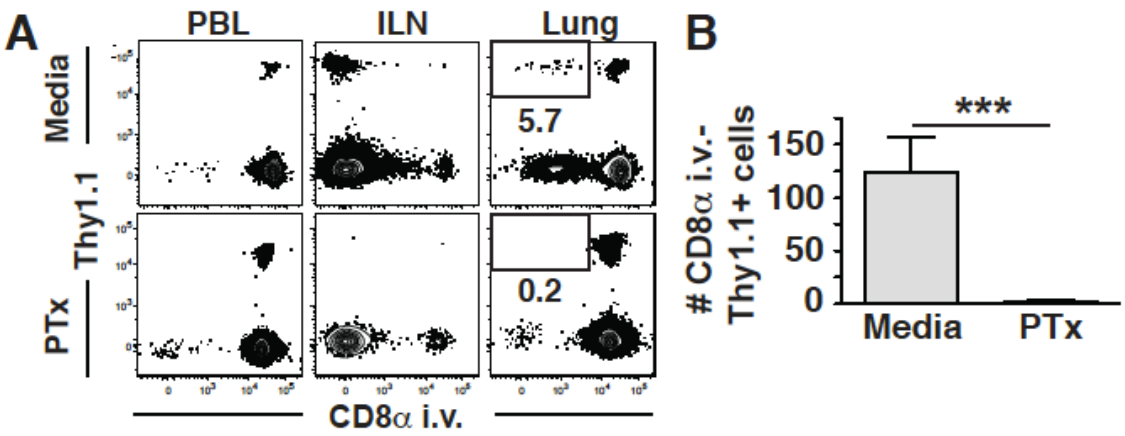

Figure 2-6: Migration of memory CD8 T cells to uninflamed lung tissue is chemokine dependent. Thy1.1+ memory P14 splenocytes were treated with PTx or media and transferred i.v. into naïve C57Bl/6J mice. Intravascular anti-CD8α staining and tissue harvest occurred 3 days later. (A) Representative flow cytometric analysis of the indicated recipient tissues. Plots gated on CD8b+ lymphocytes. (B) Number of donor memory P14 cells recovered from lung that were protected from intravascular staining (intravascular anti-CD8α negative). Plots are representative of 3 independent experiments totaling ≥12 mice/condition. ***, P=0.006 unpaired Student's t test. Error bars represent SEM.

Most lung memory CD8 T cells are capillary-associated after infection

Our results thus far indicate that the vast majority of transferred CD8 T cells recovered from perfused lung were actually present within the narrow capillary network associated with alveoli. We next sought to determine what proportion of memory CD8 T cells recovered from the lungs of infected mice were within blood. To this end, we generated P14 immune chimeras using an i.p. route of infection. We found that >96% of LCMV-specific CD8 T cells isolated from the lung were labeled with intravascular Ab (Figure 2-7). To determine whether this vascular-biased localization was unique to an i.p. infection, mice were instead infected via the intra tracheal (i.t.) route. Although local infection

established a significantly greater CD8 T cell response in the lung stroma and inducible bronchus-associated lymphoid tissue (iBALT), the majority of cells isolated from lung were still capillary-derived (Figure 2-7).

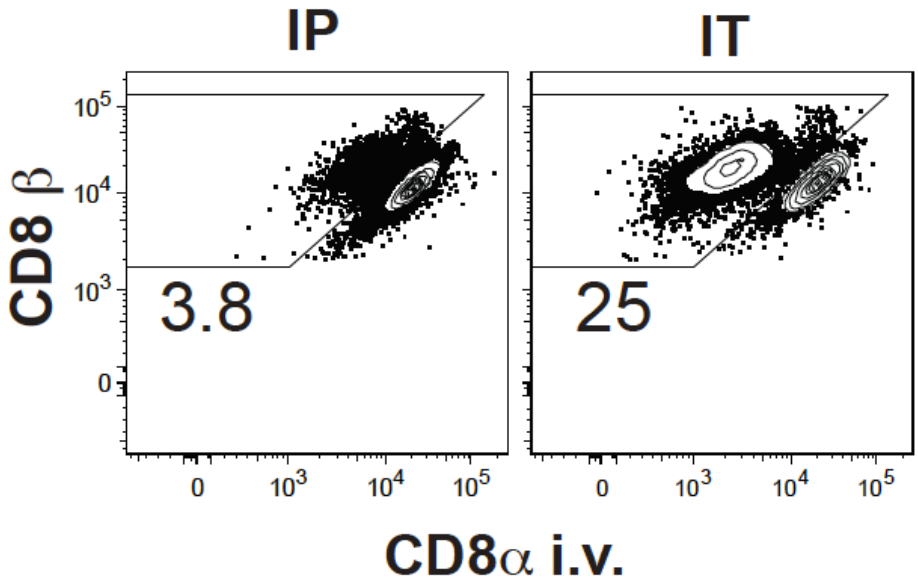

Figure 2-7: Most lung memory CD8 T cells are capillary-associated after infection. P14 immune chimeras were infected with LCMV via the i.p. or i.t. route. 15 days later, mice were subject to intravascular staining and lymphocytes were isolated from perfused lung. Plots are gated on Thy1.1+ P14 cells. Data are representative of 2-3 independent experiments totaling ≥8 mice per condition.

Intratracheal infection with LCMV establishes infection in the lung

LCMV is naturally transmitted between mice through a variety of routes including bites, social grooming, milk, nasal secretions, and airborne transmission (*233*, *242*, *254*, *262*). To confirm that i.t. injection of LCMV was establishing a local respiratory infection, spleen and lungs of C57Bl/6J mice were frozen prior to or two days after i.t. injection of LCMV and immunohistochemical analysis was performed with an Ab specific for LCMV (Figure 2-8).

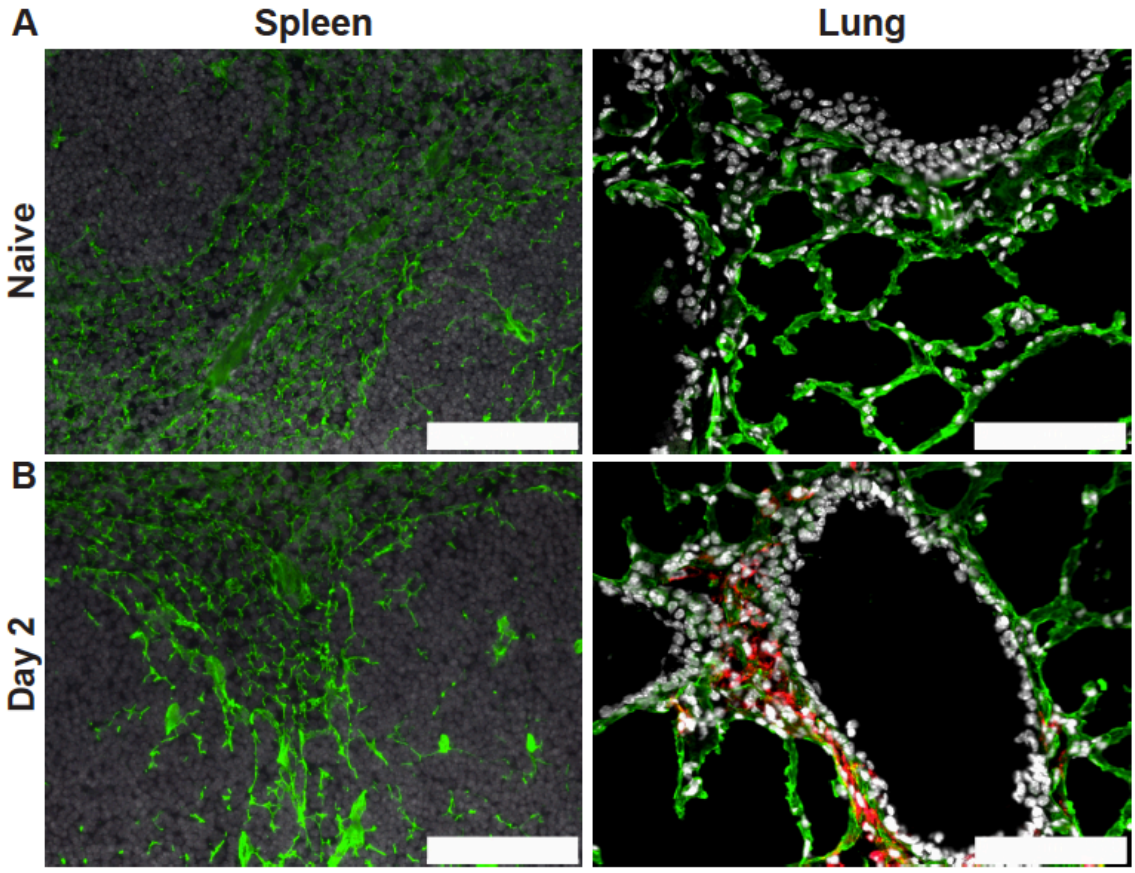

Figure 2-8: Intratracheal injection of LCMV establishes infection in the lung. Anti-collagen IV (green), -LCMV (red) and DAPI (gray) staining in the (A) spleen and (B) lung of C57Bl/6J mice before or two days after i.t. LCMV infection. Images are representative of 2 independent experiments totaling 4 mice. Scale bars represent 100μm.

After infection, mice inoculated i.p. maintained a constant proportion of P14 CD8 T cells in the lung tissue vs. capillaries. In contrast, i.t. infected mice experienced a dynamic elevation and contraction in the proportion of P14 CD8 T cells within lung tissue relative to capillaries (Figure 2-9 A), correlating with the transient presence of iBALT (data not shown). In spleen, P14 CD8 T cells initially predominated in red pulp, then gradually shifted to white pulp (Figure 2-9 B), correlating with T_{CM} differentiation (*113*, *155*, *229*).

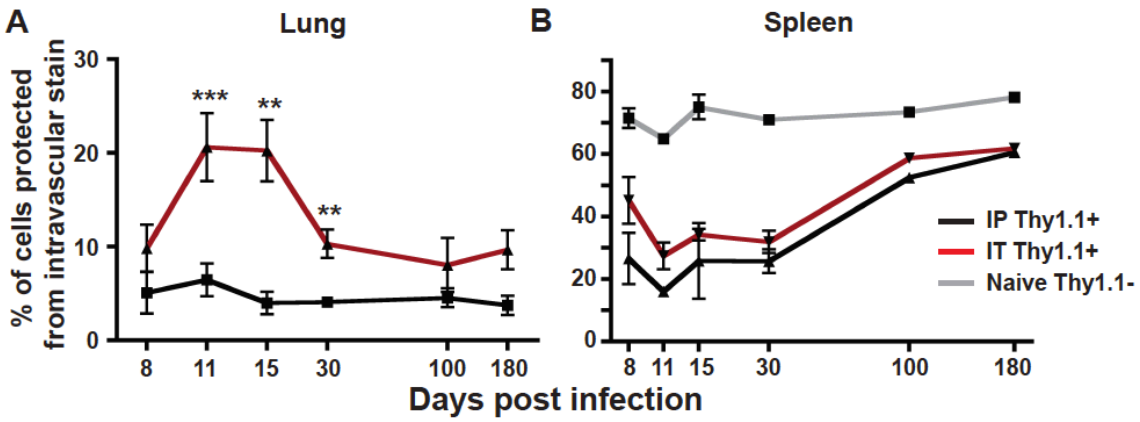

Figure 2-9: The proportion of antigen-specific T cells in lung tissue and splenic red pulp decreases over time. P14 immune chimeras were infected with LCMV via the i.p. or i.t. route. 15 days later, mice were subject to intravascular staining and lymphocytes were isolated from perfused lung. (A) Frequency of P14 cells that were protected from intravascular staining isolated from lung or (B) spleen after i.p (black) or i.t. (red) infection. Proportion of naïve (CD44lo) CD8 T cells (gray) that were protected from intravascular staining was also determined in spleen. Data are representative of 2-3 independent experiments per time point totaling ≥8 mice per condition. ***, P=0.0003; **, P<0.006 unpaired Student's t test. Error bars represent SEM.

Differential phenotype of lung tissue and vascular CD8 T cells

We then examined the phenotype of P14 CD8 T cells 15 days after i.t. LCMV infection. P14 cells present in peripheral blood bore a striking resemblance to those cells isolated from the lung that stained with injected Ab (Figure 2-10 A-D, rows 1 and 2). In contrast, cells protected from i.v. staining were distinct, contained subsets of CD103 and CD69+ cells, and were uniformly CXCR3+ (Figure 2-10 A-D, rows 2 and 3). Airway T cells (removed prior to lung digestion) exhibited a distinct phenotype, including pronounced down-regulation of CD11a as previously described (Figure 2-10 A-D, rows 3 and 4) (*155*, *180*). P14 CD8 T cells isolated from the liver or small intestine epithelium that were

protected from i.v. staining (~5% or >99% of total P14s isolated from each tissue, respectively, data not shown) were also uniformly CXCR3+ but were distinct from lung tissue cells in many respects (Figure 2-10 A-D, rows 5 and 6).

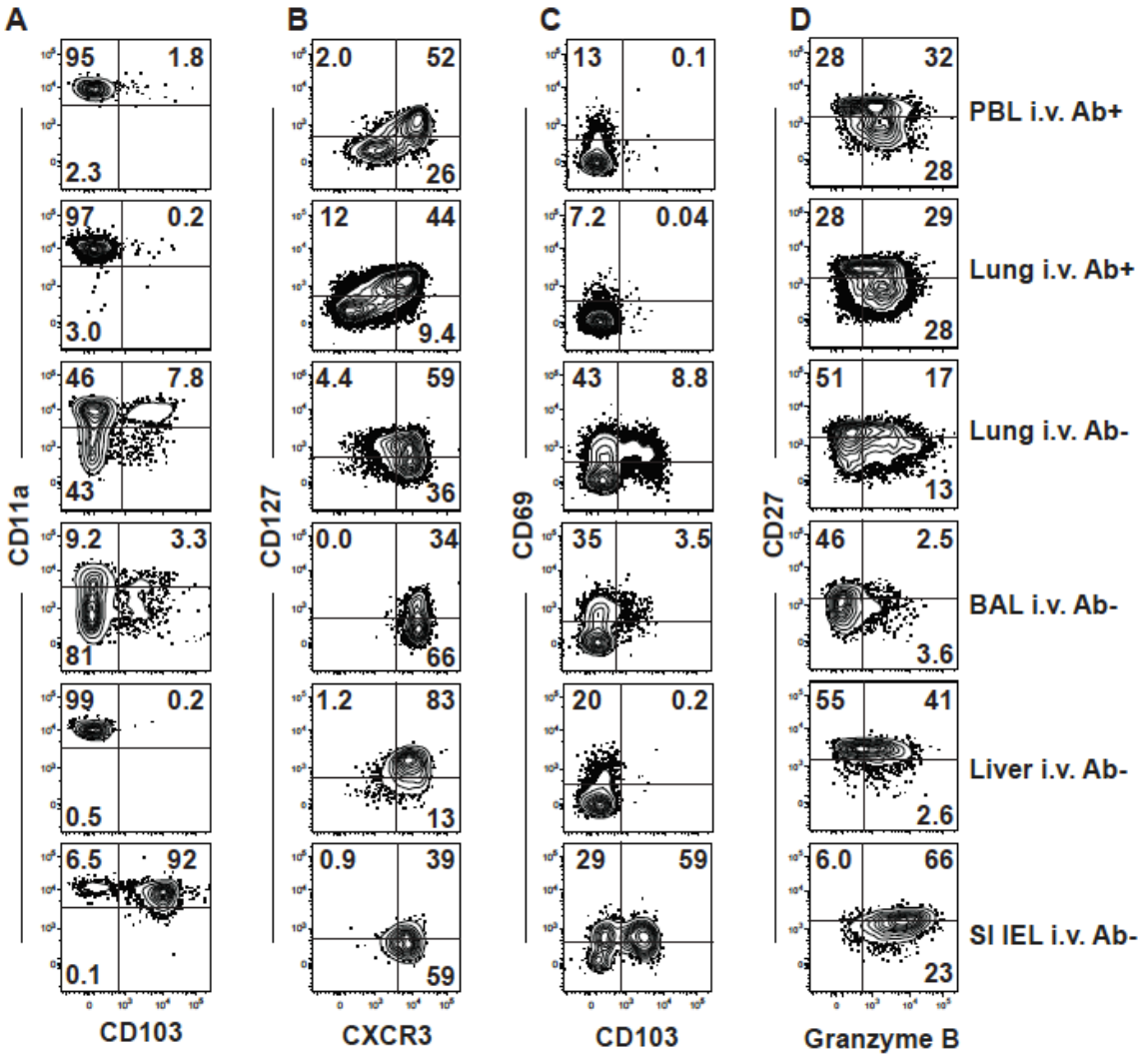

Figure 2-10: Blood and tissue compartments of non-lymphoid tissues contain CD8 T cells with distinct phenotypes. The phenotype of P14 cells was evaluated in the indicated tissues 15 days after i.t. LCMV infection. Data are representative of 2-3 independent experiments per time point totaling ≥8 mice per condition.

Discussion

A previous report quite elegantly demonstrated that CD8 T cells stimulated in vitro under varying conditions, and then transferred i.v., were differentially labeled by intravascular staining when recovered from lung, and exhibited distinct homing requirements (*234*, *263*). Our study validates that intravascular staining discriminates between CD8 T cells present within the lung tissue from those trapped in the vasculature. We utilized this approach to re-evaluate the anatomic distribution of CD8 T cells isolated from lung after in vivo infection. This analysis revealed the major finding that, in some contexts, up to 96% of effector or memory T cells isolated from lung represent cells in the capillary vessels rather than lung tissue. Unique phenotypic signatures were expressed among cells protected from labeling, including CD69 and CD103/β7 integrin expression, which has been associated with resident T_{EM} populations (*120*, *122*, *155*, *228*, *264*). Moreover, only a small fraction of memory CD8 T cells transferred into naïve recipients that were recovered from lung actually migrated into the tissue. This process was chemokine dependent, and naïve T cells were excluded. These results precipitate a re-evaluation of previous studies that examined the distribution, phenotype, and homing requirements of pulmonary T cells, and also have ramifications for T cell-dependent protection studies that may overestimate localization of transferred or established T cell populations within lung tissue (*113*, *235*, *265*). The development of vaccine modalities that enhance true T cell homing to lung tissue, which may be evaluated by intravascular staining, may enhance protection against respiratory infections (*124*, *236*, *237*, *266*, *267*).

In summary, our results demonstrate that intravascular staining is a useful tool to define vascular and tissue pulmonary lymphocytes, indicate that the majority of T cells are often within the vasculature of perfused lung, and support a revised model of the regulation of cellular immunity within the respiratory mucosa.

Materials and Methods

Mice and infections

P14 chimeric immune mice were generated as described (*155*, *254*). Mice were either infected intraperitoneally (i.p.) with 2 x 10^5 PFU LCMV or intratracheally (i.t.) with 1 x 10^5 PFU LCMV (*107-109*, *111*, *238*). The University of Minnesota IACUC approved all experiments.

Intravascular staining and cell isolations

3 µg of Anti-CD8α-APC or anti-CD8α-PE (clone: 53-6.7 from eBioscience) or purified rabbit anti-mouse collagen IV (Novus Biologicals) were injected intravenously (i.v.). Three minutes later, the animals were sacrificed, lavaged to remove cells in the airway, bled, and perfused with 10 ml of cold PBS. The spleen, LNs, lung, liver, and small intestine were harvested within 12min, and lymphocytes were isolated as described (*138*, *268*). Immunofluorescence staining was performed as described (*155*, *269-273*).

Pertussis Toxin Treatment

Purified splenocytes from P14 immune chimeric mice or naïve P14 transgenic mice were incubated in RPMI containing 10% FBS +/- 25 ng/ml pertussis toxin (R&D Systems) at a concentration of $1.5x10^7$ cells/ml for 1h at 37°C as described (*119*, *256-258*, *274*). Following incubation, $1.5\text{-}3.5x10^7$ cells were injected i.v. into C57Bl/6 recipient mice.

Immunofluorescence Microscopy

Immunofluorescence staining was performed as described (*122*, *124*, *155*, *251*, *252*). Briefly, tissues were frozen in O.C.T. on dry ice. 7µm frozen sections were cut using a Leica cryostat. Slides were fixed in cold acetone for 10 minutes. Prior to staining, slides were rehydrated for 10 minutes in PBS. All slides were blocked for 60-90 minutes with 5% bovine serum albumin (BSA) in PBS. Purified pAb goat anti-collagen type IV (AB769, Millipore), rat anti-LCMV nucleoprotein (VL-4, Bioxcell), or conjugated mAb anti-CD31-AF647 (clone: 390, Biolegend), anti-CD31-AF488 (clone: MEC13.3, Biolegend), anti-CD90.1-AF647 (Thy1.1, clone: OX-7, Biolegend), anti-CD8β-AF647 (clone: YTS156.7.7, Biolegend), anti-CD4-AF647 (clone: RM4-5, BioLegend) or anti-CD90.1-eF450 (Thy1.1, clone: HIS51, eBioscience), were used for primary staining. Primary antibodies were used for 60 minutes at room temperature. Goat anti-rabbit AF488, goat anti-rabbit AF555, donkey anti-goat AF488, donkey anti-goat AF555, and donkey anti-rat AF488 (Invitrogen) or donkey anti-rabbit AF647 (Jackson Immuno Research Laboratories) were used for secondary staining. Secondary antibodies were used for 30 minutes at room temperature. DAPI staining was performed for 10

minutes. Cover slips were mounted with Prolong Gold Anti-Fade mounting reagent (Invitrogen). A Leica DM5500B epifluorescent microscope with Leica Acquisition Suite Advanced Fluorescence software was used for image acquisition. Adobe Photoshop was used for image analysis.

Chapter 3

Intravascular staining for essential discrimination of vascular and tissue leukocytes

Characterizing the cellular participants in tissue immune responses is critical for understanding infection, cancer, autoimmunity, allergy, graft rejection, and other immunological processes. Leukocytes recirculate through blood vessels before localizing to tissue sites of immune responses. Thus, in experimental animal models, tissues are often perfused to putatively remove blood-borne leukocytes that may conflate analysis. Here, we show via intravascular staining that perfusion both fails to remove many blood-borne leukocytes and also may remove tissue-localized populations of interest. We provide examples of how this issue distorts interpretation of tissue leukocyte composition and phenotype in healthy mice, as well as those responding to viral or *Mycobacterium tuberculosis* infection or tumor challenge. This study highlights the breadth and gravity of this issue, outlines simple methods for identification of various intravascular leukocyte populations, and demonstrates that these methods should be routinely adopted in lieu of perfusion for interpretable analyses of immune responses in many tissues.

Introduction

Cells of the immune system act locally to ameliorate, prevent, or exacerbate disease (*136*, *244-247*, *275*). Thus, immune responses must be characterized directly within affected tissues. However, cells of the immune system also continuously recirculate throughout the vasculature, which includes an abundant capillary network that permeates every organ. Immune cells in blood, compared to those in tissues, exhibit vastly different phenotypes, functions, and differentiation states (*247-253*, *276-278*). Those within blood are typically (although not always) recirculating cells rather than participants in local immune responses. Thus, blood-borne cell contamination of tissues significantly confounds the identification and purification of leukocytes that are truly participating in local immunological processes. A common solution to this problem in animal models is the putative removal of blood-borne leukocytes by perfusing tissues with a cell-free solution post mortem.

We recently utilized an intravascular staining approach (*234*, *279*) and demonstrated that perfusion fails to remove many CD8 T cells from the lung vasculature during the course of an anti-viral response (*177*, *254*, *280*). Rather unexpectedly, up to 97% of the CD8 T cells that were thought to be located within the lung were not in the tissue (*253*, *254*, *281*), an observation that questions the interpretation of previous studies on CD8 T cell migration, differentiation, maintenance, and correlates of protective immunity against respiratory infections.

The present study addresses whether vascular contamination is an issue in other perfused tissues besides the lung and whether vascular populations conflate interpretation of the other major lineages of the adaptive and innate arms of the immune system. Negative consequences of perfusion are revealed. The strengths and weakness of different staining strategies for different leukocyte subsets and for different tissues are documented, and new intravascular staining applications are defined. Moreover, this study demonstrates that all future analyses of all immune cell lineages in tissues should dispense with perfusion and substitute intravascular staining, for which straightforward methods are described.

Applications of the Method

Discriminating between tissue-localized and blood-borne cells is relevant for studies examining cellular processes in non-lymphoid tissues. Our protocol outlines methods of intravascular staining for identification of vascular T and B cells, neutrophils, and mononuclear phagocytes in mice. Since cells in blood borne compartments may also play important roles in immune responses (*177*, *255-258*), intravascular staining may also be useful for those interested in including these populations of cells in analyses rather than eliminating them via perfusion.

Intravascular staining can be applied to studies of viral and bacterial infections as well as solid tumors in mice, but investigations of many other diseases processes, such as models of graft versus host disease, allergy and autoimmunity, as well as studies of cell migration, may also greatly benefit from

this type of analysis. While our research was limited to immune responses in mice, this protocol may be adaptable to other species, and additional applications and refinements are likely to develop as intravascular staining is applied to different settings.

Comparison with other Methods

Previous work examining neutrophil migration through the lung vasculature demonstrated that neutrophils transited the large vessels of the lung in ~3min, but required 3h if routed through the capillary bed (*101*, *177*). As a result, the ratio of neutrophils:RBCs in lung capillaries is 100-fold higher than in peripheral blood or large lung vessels (1:100 vs. 1:10,000). Consequently, even though capillaries only comprise 40% of the blood volume of the lung, they contain 99% of the lung blood-borne neutrophils. These data indicate that hemodynamic forces greatly influence the transit rate of leukocytes in the microvasculature. Such forces may sequester lymphocytes within pulmonary vasculature as well, perhaps due to the expression of adhesion molecules or the fact that the volume of a lymphocyte is greater than an RBC (~290 femtoliters (fl) vs. ~90 fl) (*259*, *261*, *282*, *283*).

Perfusion, a method of flushing the pulmonary vasculature with buffer, has been used to remove RBCs and leukocytes from the lung vasculature. However, we recently showed that the vast majority of CD8 T cells isolated from the lung of perfused mice were likely trapped within the vasculature because they were rapidly stained with i.v. injected monoclonal antibody (mAb) (*221*, *254*). These results call into question several studies reporting that naïve lymphocytes are

present within the lung tissue of specific pathogen free (SPF) mice that lack inducible bronchus associated lymphoid tissue (iBALT) (*107*-*109*, *111*, *284*, *285*): observations that violate the central dogma that naïve lymphocytes are excluded from non-lymphoid tissues (NLTs) and which were proposed to have major biological implications. Here, we show how intravascular staining can be employed to address these issues.

Experimental Design

When incorporating intravascular staining, critical staining controls must be included in every experiment. Peripheral blood (from retro-orbital or cardiac puncture) should be sampled from every mouse. One should observe that >99% of the cell population targeted by the intravascular Ab will stain positively within the peripheral blood. A negative staining control, such as lymph nodes, should also be sampled. One should observe less than 10% of cells isolated from lymph nodes staining positively with intravascular Ab. For a discussion of Ab selection, see Figure 3.

Limitations

We have used intravascular injection of anti-collagen type IV Ab to test for vascular leakage in all the models examined in this manuscript. While the conditions we tested allow for reliable intravascular staining, there could be conditions under which vascular leakage may compromise the integrity of staining. For instance, there may be inflammatory contexts or angiogenic tumor models that allow rapid exudation of Ab into tissues, which could compromise

interpretation of intravascular staining. Investigators examining unique conditions would be advised to perform appropriate validating controls, such as histological analysis after injection of anti-collagen Ab or injection of Evans Blue Dye (EBD), as described (*221*, *242*, *254*, *262*). A collagen basement membrane surrounds endothelial vessels in tissues such as the lung and intestine and is not exposed to intravascular Ab under conditions that we have tested. Collagen staining in the liver sinusoids, glomerular capillaries of the kidney, and red pulp of the spleen can be used as positive staining controls, as these are exposed to vascular Ab under steady state conditions (data not shown and Anderson et. al., 2012). As an alternative approach, one could consider using Evans Blue dye, as described. Evans Blue dye stains the serum protein albumin, which is only found in blood vessels under conditions with intact endothelium, but which permeates into tissues when vascular permeability is increased. Histological analysis or a quantitative comparison of EBD levels in sample tissues compared to healthy controls can be used to validate the appropriateness of intravascular staining.

Intravascular Staining Procedure

The sample preparation and flow cytometry acquisition steps described in the following procedure are for CD8$\alpha\beta$ T cells isolated from a spleen, as an example application.

1. Prepare Ab dilution in sterile 1x DPBS and keep on ice. For most procedures, 3μg of Ab in 300μl of DPBS per mouse is sufficient. If the Ab is conjugated to a

fluorescent molecule, protect from light. Titration of untested Ab clones or fluorochromes is recommended prior to performing large experiments.

CAUTION: do not dilute the Ab in buffer containing sodium azide, as high azide concentrations are toxic.

2. Inject 300μl of Ab dilution intravenously into a mouse via the tail vein.

3. Kill the mouse 3 min after injection using isoflurane. Euthanasia with inhaled isoflurane should be performed in a closed container with an absorbent material soaked in the anesthetic (the amount of isoflurane to use will vary with container size). Avoid contact between the mouse and the anesthetic.

CRITICAL STEP: Longer wait times have not been validated.

CAUTION: Isoflurane **(**2-chloro-2-(difluoromethoxy)-1,1,1-trifluoro-ethane) is used for inhalational anesthesia. It is liquid at room temperature and vaporizes readily. Isoflurane is a powerful anesthetic and should always be used inside a laminar flow hood. Only approved containers should be used for euthanasia with inhaled anesthetics.

CAUTION: Isoflurane euthanasia should be approved by an Institutional Animal Care and Use Committee and Institutional Biosafety Committee.

4. Harvest tissues of interest into appropriate containers (petri dishes, conical tubes, or gentleMACS tubes, etc.) containing RPMI + 5% Fetal Bovine Serum (FBS).

CRITICAL STEP: mouse euthanasia and tissue harvest should be performed quickly to improve cell viability.

5. Immediately smash or mince tissues and wash to rinse free or dilute any excess Ab. Store in RPMI + 5% FBS on ice.

PAUSE POINT: Tissue pieces can be left on ice while additional mice are processed for up to 3 hours, although empirically, faster processing yields better results.

6. If desired, isolate leukocytes from tissues. Numerous protocols have been described and vary depending on the tissue and leukocyte population of interest (*155*, *229*, *286*, *287*). These protocols will not be reviewed here. Each investigator should optimize this protocol for the tissue and cell type of interest. Alternatively, organs may be embedded in freezing medium such as O.C.T. medium for subsequent immunohistochemical analysis (*124*, *155*, *234*, *243*, *254*, *288*).

Sample preparation and analysis

7. Smash spleen and filter through a 70 μm nylon cell strainer to remove clumps. In parallel, process cells suitable for use as controls.

CRITICAL STEP: Compensation controls should be prepared using either compensation particles or cells from an animal that did NOT receive intravascular antibody because injected animals will already contain fluorescent Ab.

CRITICAL STEP: CD8αβ T cell isolation from spleen is described here as a typical example. Adapt this protocol to the cells and tissue of interest to you.

8. Spin down the cells at 550 x *g* for 5 minutes. Pour off supernatant.

9. Resuspend pellet of cells by vortexing. Lyse the red blood cells with 2 mL Ack lysis buffer for 2 minutes at room temperature. Add 10 mL RPMI + 5% FBS to dilute Ack lysis buffer.

10. Spin down the cells at 550 x *g* for 5 minutes. Remove supernatant. Resuspend cells in desired volume of FACS buffer and aliquot cells into 96-well round bottom plates.

11. Stain cells with *ex vivo* Abs, diluted as indicated in Table 1 in FACS buffer, for 30 minutes on ice.

CRITICAL STEP: Do not add *ex vivo* Ab conjugated to the same fluorochrome as the Ab that was injected i.v.

Fluorochrome	Marker	Ab clone	Company	Dilution
PE	CD44	IM7	eBioscience	2 μg/ml (1:100)
PerCP-Cy5.5	CD8β	YTS156.7.7	BioLegend	2 μg/ml (1:100)
APC-eF780	CD62L	MEL-14	eBioscience	2 μg/ml (1:100)
Aqua	Live / dead	-	Invitrogen	Per protocol
APC	CD8α i.v.	53-6.7	eBioscience	-

Table 3-1: Sample CD8ab T cell ex vivo staining panel

12. Dilute stain with 150 μl FACS buffer and spin plate at 858 x *g* for 2 minutes to wash cells. Repeat wash twice. Resuspend in 200 – 300 μl FACS buffer for acquisition.

PAUSE POINT: Cells can be fixed in 2% paraformaldehyde for 30 minutes, washed with FACS buffer (as in Step 12) and stored at 4°C in FACS buffer for up to 48 hours prior to acquisition.

Data Acquisition and Analysis Procedure

CAUTION: Flow cytometry should be performed by trained individuals and in accordance will all institutional biosafety regulations. Refer elsewhere for detailed overviews of flow cytometry acquisition (*241*, *263*) and data analysis (*254*, *264*).

13. Prepare an acquisition template in the flow cytometry software (e.g. BD FACSDiva software) containing the fluorescent parameters in the staining panel.

14. Perform compensation using an unstained control and single-stained samples.

15. Prepare an acquisition layout containing the following plots:

FSC-A vs. SSC-A – create a lymphocyte gate ("lymphocyte" population)

SSC-A vs. SSC-W – display "lymphocyte" population and create a singlet gate ("singlets" population)

CD8β vs. live/dead – display "singlets" population and create a CD8β+ live/dead- gate ("CD8β+" population)

CD8α i.v. versus CD8β – display "CD8β+" population and create CD8α i.v.+ and CD8α i.v.- gates

16. Acquire 10,000 - 20,000 CD8β+ events and export FCS files for analysis in flow cytometry analysis software (e.g. Tree Star FlowJo software).

17. In Flow Jo, create lymphocyte, singlet, live CD8β+ and CD8α i.v.+ and CD8α i.v.- gates as in step **15**.

Step	Problem	Possible Reason	Solution
3	Cell type of interest in peripheral blood staining control is not >99% stained with i.v. injected Ab	Poor intravascular injection, Ab did not circulate long enough, or method of sacrifice disrupted circulation of Ab	Ensure that tail vein injections are performed correctly. Allow Ab to circulate slightly longer (3.5 – 4 minutes) prior to euthanasia. Do not use cervical dislocation to euthanize mice.
5	Cells isolated from peripheral blood have a higher staining intensity than the vascular fraction in non-lymphoid tissues.	Excess Ab was not diluted out immediately or too much Ab was injected.	Dilute peripheral blood immediately after removal. Reduce concentration of Ab to inject.
5	Tissues with low vasculature:tissue ratios have very high intravascular staining frequencies or MFI when compared to negative control samples.	Excess Ab was not rinsed off immediately.	Proceed to rinsing tissues faster during the harvesting process.

Table 3-2: Troubleshooting Tips

Sample preparation and acquisition steps for examining vascular permeability of the lung.

CAUTION: Microscopy should be performed by trained individuals and in accordance will all institutional biosafety regulations. Refer elsewhere for detailed overviews of immunofluorescence staining (*254*, *265*) and microscopy (*266*, *267*, *289*).

1. Follow intravascular staining protocol steps 1-4 using purified polyclonal goat anti-mouse collagen type IV (15μg/mouse). As a control, include a sample slide for *ex vivo* anti-Collagen type IV staining. One of the following should be included as a positive control for intravascular Collagen type IV staining: liver sinusoids, glomerular capillaries of the kidney, or red pulp of the spleen.
2. Embed the lung and spleen in O.C.T. medium.
3. Snap freeze samples in liquid nitrogen or on dry ice.
4. Prepare 7μm sections on microscope slides using a cryostat.
5. Fix slides in cold acetone for 10 min.

PAUSE POINT: Slides can be stored at -20°C or -80°C for at least 18 months.

6. Rehydrate slides with 1x DPBS for 10 minutes.
7. Block slides for 60-90 minutes at room temperature (or overnight in the fridge) with 5% BSA Blocking solution.
8. Stain slides with mAb anti-CD31-AF488 for 60 minutes (dilute anti-CD31 Ab 1:100 in 5% BSA Blocking solution or PBS). The control slide should also be stained with purified polyclonal goat anti-mouse collagen IV (dilute anti-Collagen IV Ab 1:200 in 5% BSA Blocking solution or PBS).
9. Wash slides gently 3 times with 5% BSA Blocking solution or PBS.
10. Stain slides with purified polyclonal donkey anti-goat-AF555 for 30 minutes (dilute anti-goat Ab 1:2000 in 5% BSA Blocking solution or PBS).
11. Wash slides gently 3 times with 5% BSA Blocking solution or PBS.
12. Stain slides with DAPI for 10 minutes.
13. Wash slides gently with 5% BSA Blocking solution or PBS.

14. Gently tap or blot off excess 5% BSA Blocking solution and mount coverslips onto slides with Prolong Gold Anti-Fade mounting reagent.

15. Acquire images using a Leica DM5500B epifluorescence microscope with Leica Acquisition Suite Advanced Fluorescence software.

Timing

From the time of Ab injection until organ isolation may take 5 - 30 minutes per mouse, depending on the number of organs harvested and the experience of the investigator. This does not include subsequent isolation of leukocytes, staining and analysis.

Results

Evidence that perfusion should be avoided

We recently showed that the vast majority of memory CD8 T cells isolated from the lung of perfused mice were likely trapped within the vasculature because they were rapidly stained with i.v. injected monoclonal antibody (mAb) (*254*). To confirm previous reports regarding the presence of naïve T and B cells within the lung tissue(*107-109*, *111*, *177*), we isolated B cells and T cells from the lungs of uninfected mice that were perfused to remove blood from organs. Consistent with what has been published, the majority of lymphocytes isolated from lung did in fact express a naïve phenotype (CD62L+ and CD44lo for T cells and IgD+ and/or IgM+ for B cells). Importantly, when anti-CD45.2 mAb was injected i.v. three minutes before mice were sacrificed and perfused (CD45 is expressed on the surface of all leukocytes), >99% of naïve lymphocytes, regardless of lineage, became labeled (Figure 3-1). We hypothesized that intravascular labeling indicates that cells were confined to the vasculature of mice despite perfusion.

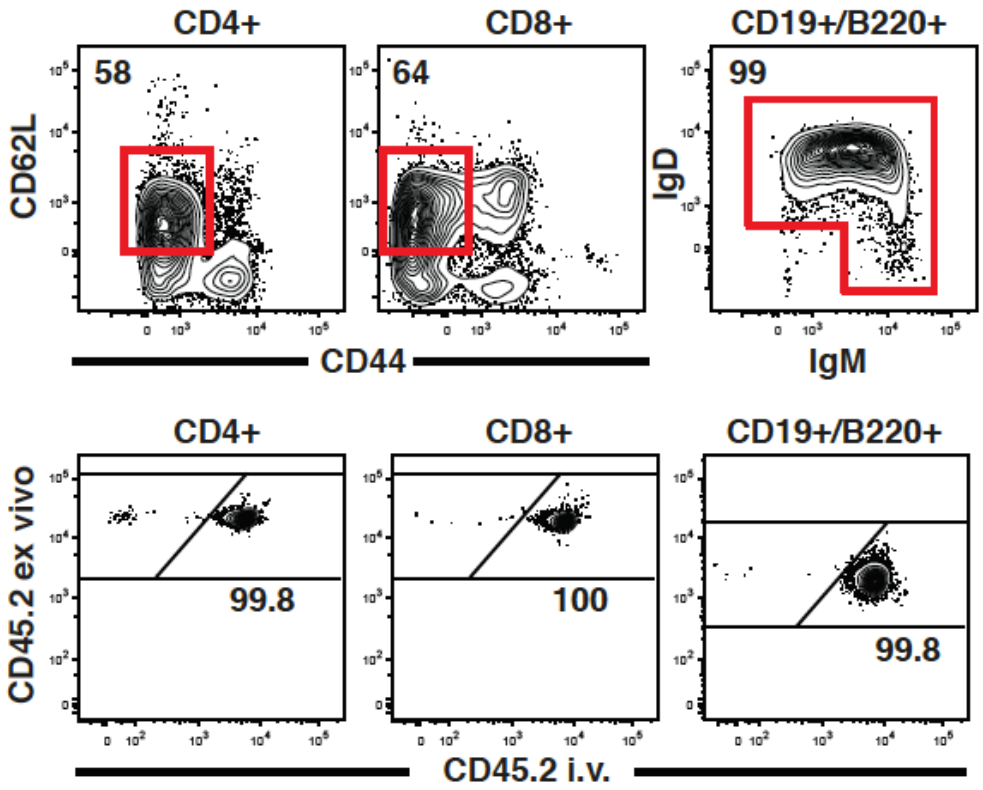

Figure 3-1: Naïve lymphocytes isolated from the lung are confined to the vasculature despite perfusion. Anti-CD45.2 mAb was injected i.v. via the tail vein of naïve C57Bl/6 mice three minutes before perfusion and lymphocyte isolation. Naïve CD4+ and CD8+ T cells and B cells were identified by flow cytometry as indicated and examined for labeling with injected anti-CD45.2 mAb. Representative of 12 mice from two experiments.

After local LCMV infection, iBALT, a transient tertiary lymphoid organ, appears in the lung. iBALT has been well characterized and is classically defined as a collection of lymphocytes and dendritic cells that abuts a large airway, is typically adjacent to large blood vessels, and contains both lymphatic vessels and high endothelial venules (HEV, as detected by Peripheral Node Addressin (PNAd) staining) (*268*, *282*, *283*). We discovered that LCMV infection also induced abundant lymphocyte aggregates that were distinct from iBALT in that

they lacked HEVs, were much smaller, and were not located near large airways. Interestingly, perfusion significantly reduces the abundance of iBALT and alveolar lymphoid aggregates detectable per lung lobe (Figure 3-2), and appeared to reduce the cellularity of those that remained (data not shown). Indeed, alveolar lymphoid aggregates were difficult to detect after perfusion, which may help explain why they have rarely been noted previously (*155*, *269-273*).

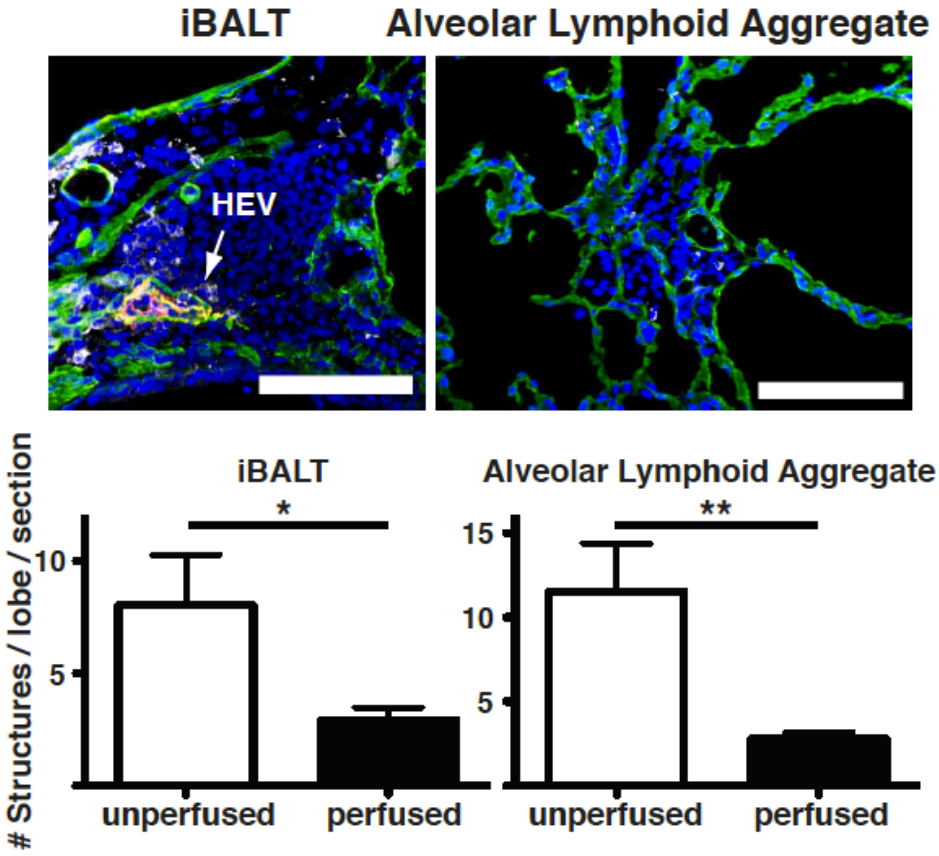

Figure 3-2: Perfusion depletes cells from lung tissue. 15d after i.t. LCMV infection, lungs from P14 chimeras were perfused or left unperfused. Representative immunofluorescence images of iBALT or aggregate structures in lungs stained with anti-collagen type IV (green), -PNAd (red), -Thy1.1 (gray) and DAPI (blue). Arrow designates PNAd+ high endothelial venule. Scale bars = 100μm. Representative of two experiments totaling 10 mice per condition. * $p = 0.05$. ** $p < 0.01$. Error bars indicate SEM.

Collectively, these data show that perfusion not only leaves behind abundant vascular-bound lymphocytes, but also depletes tissue cells and structures that may be of interest.

Validation of intravascular staining

In lung, confocal and epifluorescence microscopy shows that lymphocytes stained with intravascular Ab are present within the vasculature (Figure 3-3).

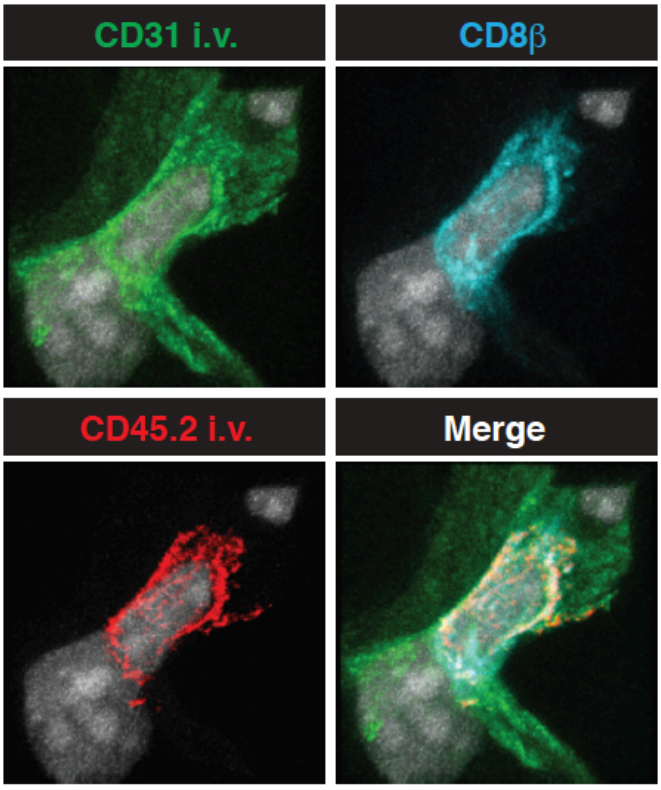

Figure 3-3: Intravascular staining is confined to vascular cells. Anti-CD31 and anti-CD45.2 or (c-g) anti-CD45.2 mAb alone was injected i.v. into C57Bl/6 mice 12d after i.t. LCMV infection. (b) Confocal imaging of lung, anti-CD31 i.v. (green), -CD45.2 i.v. (red), –CD8β (cyan) and DAPI (gray). Representative of three experiments totaling 4 mice.

Cells stained with i.v. mAb were truly confined to CD31+ vessels, whereas cells protected from the i.v. mAb were present outside of capillaries, including the pulmonary epithelium, iBALT, airway lamina propria, surrounding large blood vessels, as well as pericapillary and lung airway compartments (Figure 3-4 A-C, data not shown). These data demonstrate that CD8 T cells stained with intravascular Ab within the lung are confined to vasculature and CD8 T cells protected from intravascular staining are outside of vasculature.

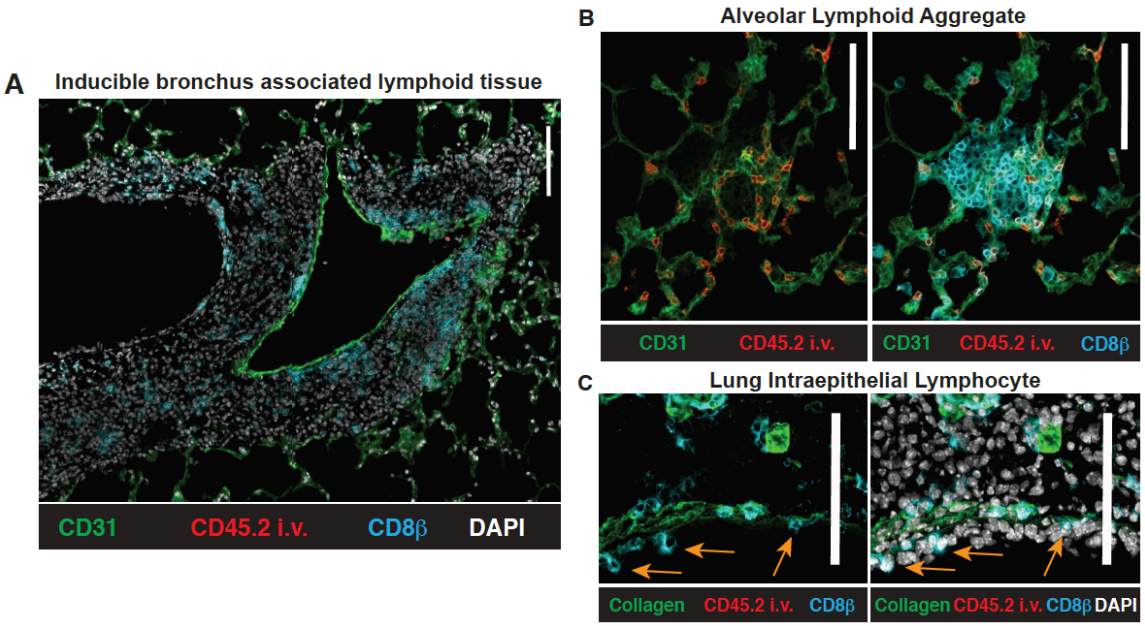

Figure 3-4: CD8 T cells in iBALT, alveolar lymphoid aggregates and epithelium are not accessible by intravascular Ab. (A) iBALT, (B) alveolar lymphoid aggregates, and (C) intraepithelial lymphocytes (IEL) in the lung 12d after i.v. LCMV infection. Orange arrows indicate sample IELs. Data representative of three experiments totaling nine mice.

While perfusion fails to completely remove “contaminating” vascular lymphocytes from many tissues (Figure 3-1), it should also be noted that vascular lymphocytes populations are also often of interest (*155*, *256-258*, *274*). For

example, histological examination of the lymph nodes of mice that were not perfused confirms that i.v. mAb labeled CD8 T cells are largely contained within HEVs (Figure 3-5), and likely represent marginated cells preparing for lymph node (LN) entry. Thus, intravascular staining may be a useful approach to identify this population for further characterization. Permissiveness to intravascular Ab labeling in additional tissues will be shown in Figure 3-8. In summary, perfusion is unnecessary if intravascular staining is incorporated, and neglecting to perfuse has advantages.

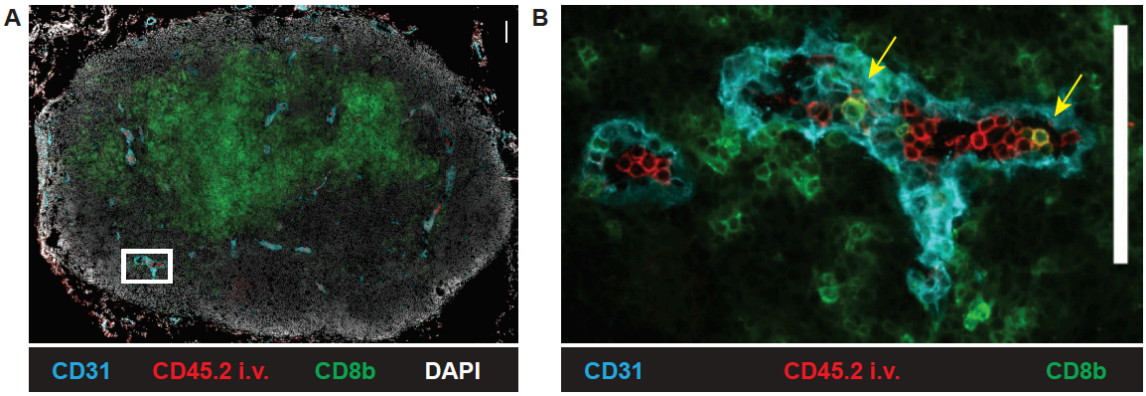

Figure 3-5: Intravascular staining in lymph nodes is confined to HEVs. (A) Inguinal lymph node sections showing anti-CD45.2 i.v. mAb staining (red) and *ex vivo* anti-CD31 (cyan), -CD8β (green), and DAPI (gray). (B) White inset from A without DAPI displayed. Yellow arrows indicate anti-CD45.2 i.v. and -CD8β mAb co-staining. Scale bars represent 100μm. Data representative of three experiments totaling nine mice.

Intravascular staining without perfusion is sufficient to reveal unique lymphocyte subsets in tissues

We next questioned whether perfusion was necessary if intravascular staining was utilized. This issue was examined in the context of polyclonal

endogenous CD4 and CD8 T cell responses twelve days after i.t. LCMV infection. H-2D^b/gp33 MHC I tetramers and I-A^b/gp66 MHC II tetramers were used to identify LCMV-specific CD8 and CD4 T cells responses, respectively (Figure 3-6A). In this case, vascular T cells were identified via injection of anti-CD45.2 mAb, but mice were not perfused. All examined tissues contained LCMV-specific CD4 and CD8 T cells that were labeled by i.v. injected mAb (Figure 3-6, 3-7 and data not shown). However, all cells in non-lymphoid tissues that labeled with vascular injected mAb were contained within endothelial vessels, as confirmed by immunofluorescence imaging (Figure 3-8).

Of note, CD69+ T cells were only found in the compartment of NLT protected from the i.v. mAb, with the exception of cells isolated from the liver. CD69 has been proposed to be a marker of tissue resident T cell populations (*114*, *122*, *124*, *143*, *155*, *251*, *252*), and these results suggest that liver may contain a fraction of sinusoidal resident CD8 T cells. CD69 expression profiles in tissues were similar 12 and 30 days after infection (data not shown). The proportion of i.v. protected LCMV-specific CD4 T cells in tissues was typically greater than observed for CD8 T cells, particularly in lung (Figure 3-7).

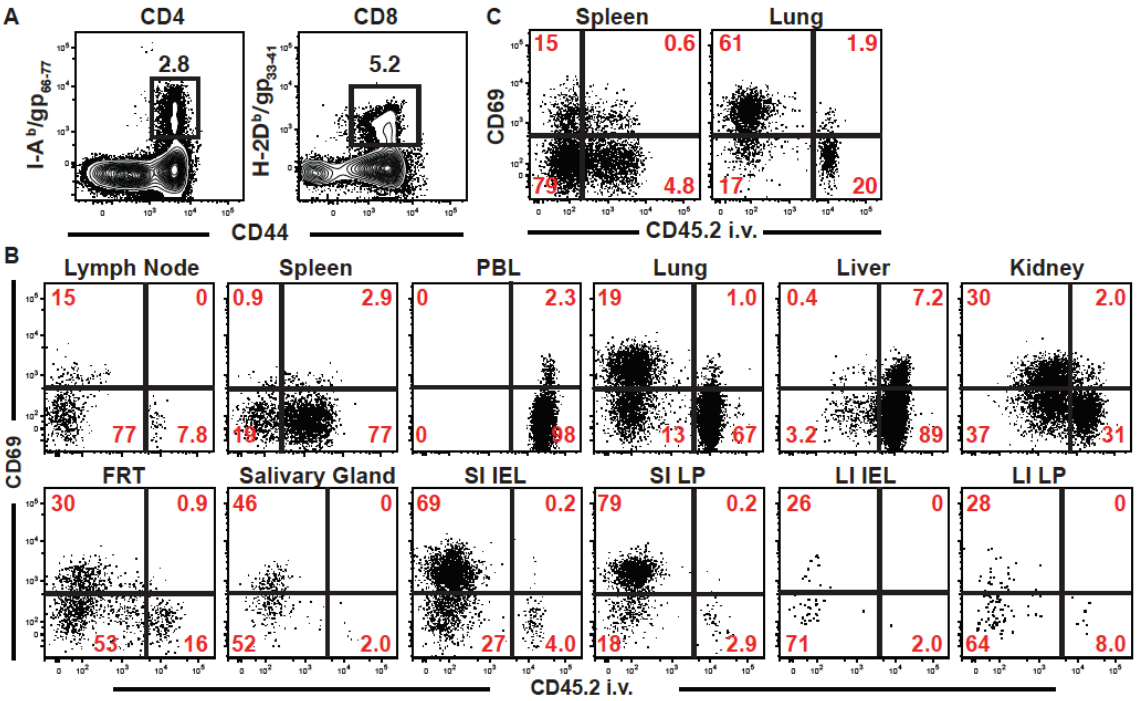

Figure 3-6: Intravascular staining without perfusion is sufficient to reveal unique lymphocyte subsets in tissues. C57Bl/6 mice were injected with anti-CD45.2 mAb i.v. 12 days after i.t. LCMV infection. Lymphocytes were isolated and LCMV-specific CD4+ and CD8+ T cells were identified with I-A^b/gp_{66-77} and H2-D^b/gp_{33-41} MHC tetramers, respectively. (A) Representative tetramer staining in spleen. Anti-CD45.2 i.v. and anti-CD69 mAb staining of (B) H2-D^b/gp_{33-41}-gated CD8 or (C) I-A^b/gp_{66-77} CD4 T cells isolated from the indicated compartments. Data are representative of at least 9 mice from 3 independent experiments.

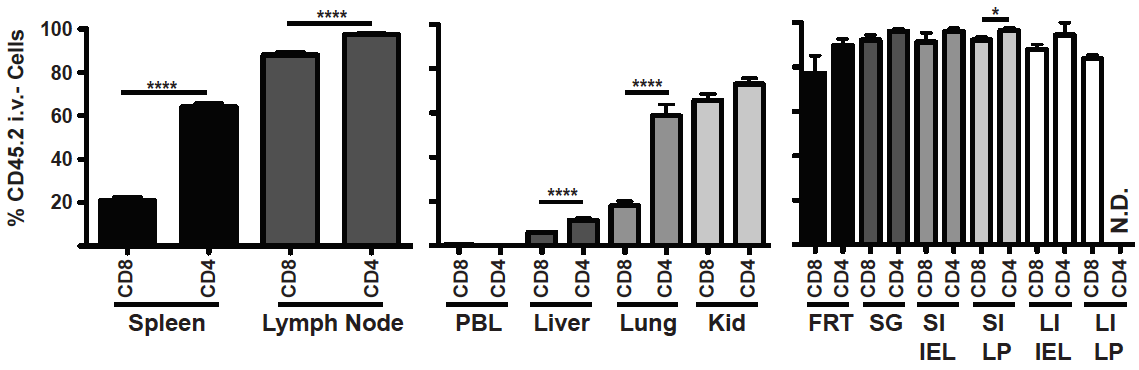

Figure 3-7: Intravascular staining profile of endogenous LCMV-specific CD8 and CD4 T cells isolated from several unperfused tissues. Frequency of tetramer positive cells protected from i.v. mAb staining in lung. Data are representative of at least 9 mice from 3 independent experiments. **** $p < 0.0001$. Error bars indicate SEM.

Technical considerations for intravascular staining

We next examined practical combinations of mAb clones for intravascular staining. When tracking adoptively transferred CD8 T cells in mice, such as P14 T cells, vascular populations can be readily detected by i.v. injection of anti-CD8α mAb (clone 53-6.7), followed by *ex vivo* staining of all isolated populations via anti-CD8β mAb (clone YTS156.7.7, Figure 3-9A). This approach takes advantage of the fact that most CD8+ T cell populations express heterodimeric CD8 consisting of both α and β chains. For tracking CD4 T cells (CD4 consists of a single chain), two anti-CD4 mAb clones that do not compete for the same binding sites are optimal. For example, this can be achieved by i.v. injection of anti-CD4 mAb clone RM4-4 followed by *ex vivo* staining with clone RM4-5 (Figure 3-9B). Alternatively, a mAb specific for CD45 (Figure 3-9C), a pan-

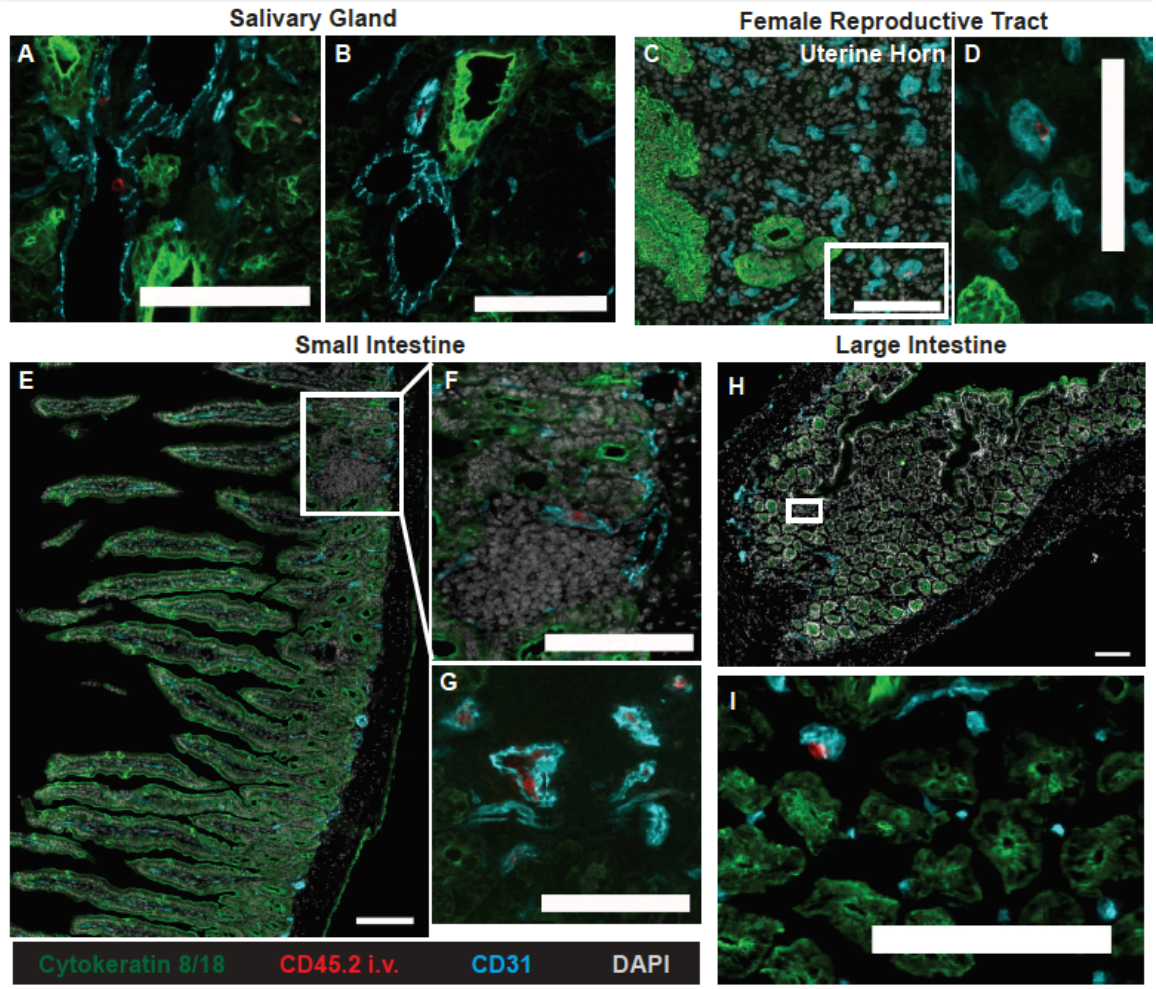

Figure 3-8: Imaging intravascular staining of leukocytes in unperfused tissues. C57Bl/6 mice were injected with anti-CD45.2 mAb i.v. 12d after i.t. LCMV infection. (A,B) Salivary gland, (C,D) female reproductive tract, (E-G) small intestine, and (H,I) large intestine sections showing anti-CD45.2 i.v. mAb staining (red) and *ex vivo* DAPI (gray), anti-cytokeratin 8 and -cytokeratin 18 (green), and -CD31 (cyan) staining. Scale bars represent 100μm. All data are representative of three experiments from nine mice.

leukocyte marker, is useful if contemporaneously examining multiple leukocyte lineages in one mouse or if the use of anti-CD8β must be avoided; for instance CD8β staining can block staining with peptide:MHC I tetramers (*275*, *290*). In this case, we have used the same mAb clone for both intravascular and *ex vivo*

staining (anti-CD45.2 mAb clone 104). This strategy could be pursued for any marker (Figure 3-9D shows dual staining with the anti-CD8α clone 53-6.7 as an example), particularly when mAb clones are limited to markers of interest. However, this approach does diminish the intensity of the *ex vivo* staining, particularly in peripheral blood. While other mAb combinations may suit investigators' unique goals, it is important to avoid i.v. injection of complement-fixing mAb that may rapidly eliminate labeled cells.

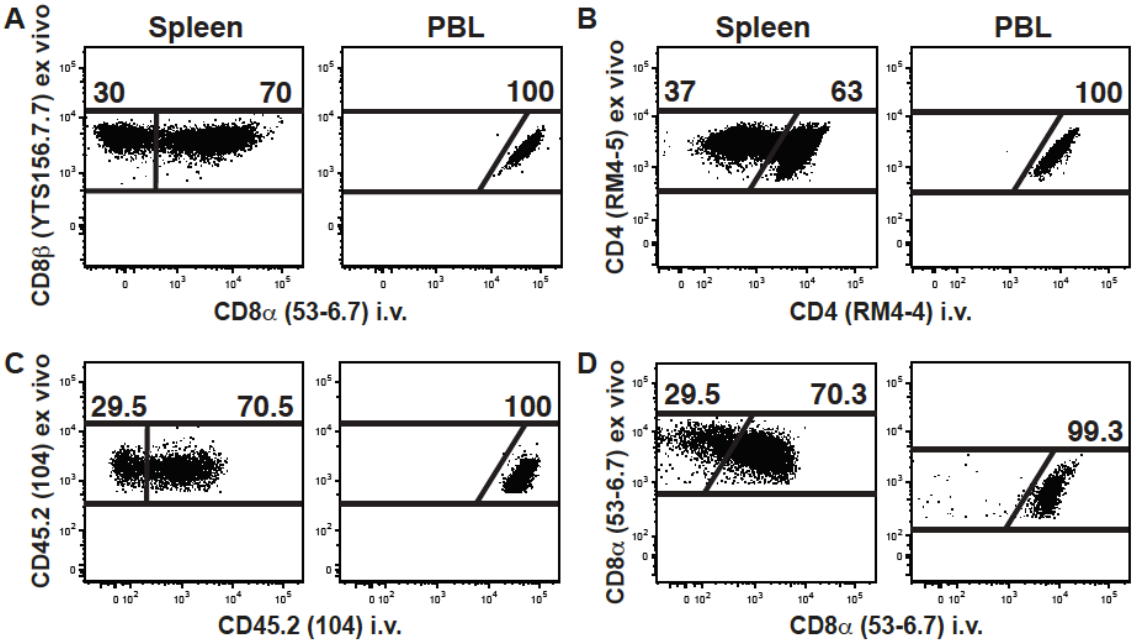

Figure 3-9: Technical considerations for intravascular staining. (A) Thy1.1+ P14 CD8 T cell chimeras, (B) CD45.1+ SMARTA CD4 T cell chimeras, or (C, D) CD45.2+ C57Bl/6 mice were infected with LCMV i.t. After 12-15 days, mice were injected i.v. with the indicated mAb (clones are in parentheses), sacrificed three minutes later, and lymphocytes were isolated and further stained *ex vivo* for flow cytometric analysis. Plots are gated on (A) CD8β+ and Thy1.1+, (B) CD4 (clone RM4-5)+ and CD45.1+, (C) CD45.2+ (clone 104, stained *ex vivo*), CD8α+, and H2-D^b/gp_{33-41} MHC I tetramer+, (D) or CD8α+ (stained *ex vivo*) and H2-D^b/gp_{33-41} MHC I tetramer+ lymphocytes. Plots are representative of at least three experiments and nine mice per condition.

When examining the spleen, intravascular staining discriminates between cells occupying red pulp (i.v. stain positive) and white pulp (i.v. stain negative, Figure 3-10). When injecting anti-CD45 mAb, the marginal zone is stained particularly brightly. However, among T cells, CD45 staining in splenic red pulp is less intense than the vascular compartments of other tissues (lung, for example) or peripheral blood (Figure 3-11).

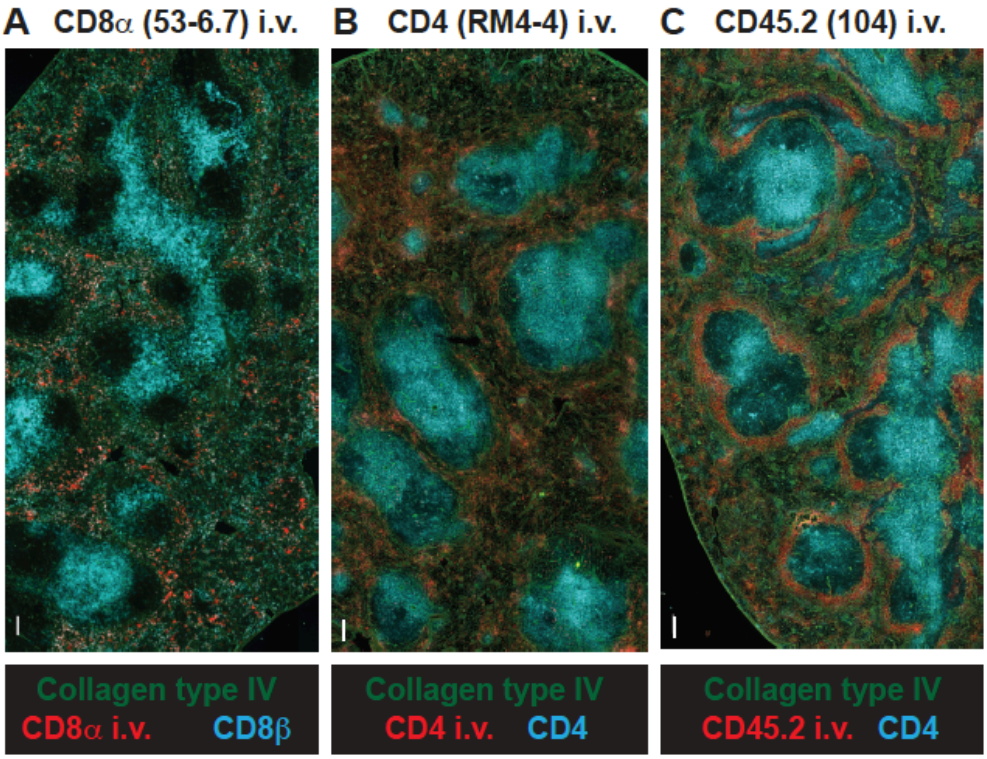

Figure 3-10: Immunofluorescence images of spleens after intravascular staining. After 12-15 days, mice were injected i.v. with the indicated mAb (clones are in parentheses), sacrificed three minutes later, and lymphocytes were tissue sections were examined by epifluorescence microscopy. mAb specific for collagen type IV (green) and CD8β or CD4 (cyan, as indicated) stained *ex vivo*, and the indicated i.v. injected mAb (red) on spleen sections. Images are representative of at least three experiments and eight mice per condition. Scale bars = 100μm.

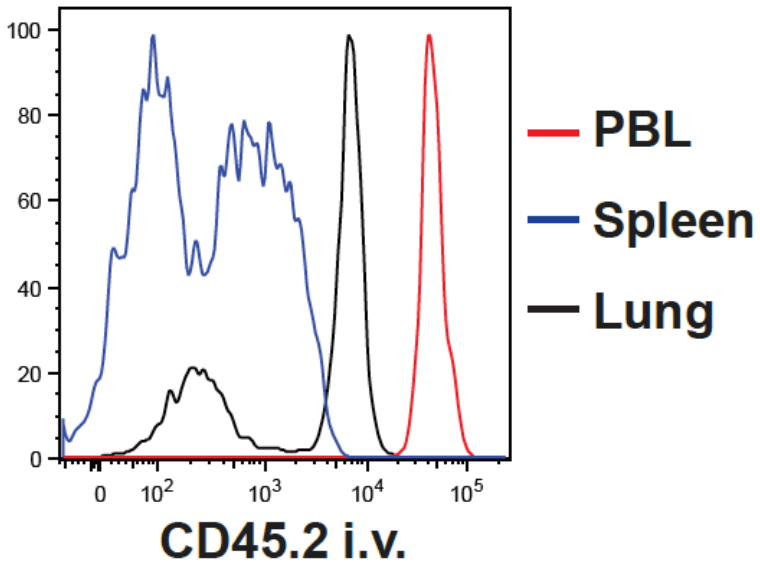

Figure 3-11: Intravascular staining intensity differences in distinct organs. 30d after i.t. LCMV infection of C57Bl/6 mice, anti-CD45.2 i.v. mAb staining intensity was examined on CD8α+ H2-D^b/gp_{33-41} MHC I tetramer+ lymphocytes isolated from blood (PBL, red), spleen (blue), and lung (black). Representative of three experiments totaling nine mice.

Intravascular staining indicates anatomic localization of B cells

Our next study determined the extent to which intravascular staining could be applied to refine the anatomic compartmentalization of different B cell subsets. A thirteen parameter flow-cytometry panel was used to phenotypically identify Ab-secreting (Intracellular Ig high), B1 (B220 low, CD43+), germinal center (B220+, CD43 low, CD38 low, GL7+), switched memory (CD19+, B220+, CD38+, IgM/IgD-) or naïve and unswitched memory (CD19+, B220+, CD38+, IgM/IgD+) B cells after LCMV infection (Figure 3-12A).

In the spleen, Ab-secreting and germinal center B cells were protected from i.v. anti-CD45.2 mAb (12 days after i.t. challenge with LCMV, Figure 3-12B

and D), consistent with preferential localization to white pulp follicles (*276-278*, *291*). Although B1, naïve, unswitched memory, and switched memory B cells were also predominantly protected from i.v. mAb staining, ~30% of each subset was exposed to i.v. mAb (Figure 3-12C, E-F). These data extend the applications of intravascular staining to B cells.

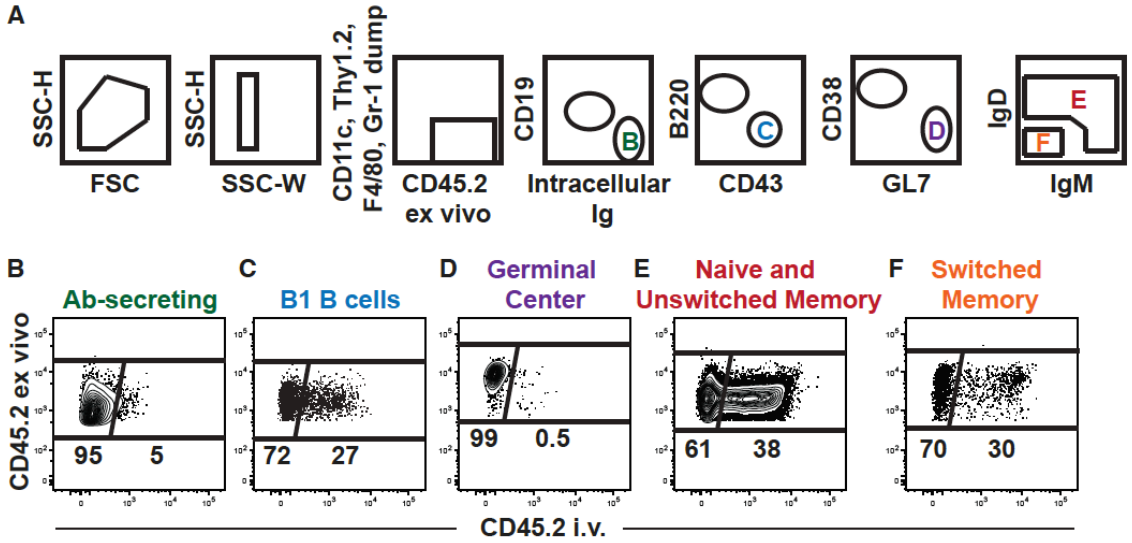

Figure 3-12: Intravascular staining indicates anatomic localization of B cells. Anti-CD45.2 mAb was injected i.v. into C57Bl/6 mice 12 days after i.t. LCMV infection. (A) Gating strategy. Lymphocytes were isolated from spleen and anti-CD45.2 mAb staining was examined on the following B cell lineages that were identified by 13-parameter flow cytometry (defining markers indicated in parentheses): (B) Ab-secreting cells (intracellular Ig+, IgM-, IgD-), (C) B1 B cells (intracellular Ig+, CD19+, B220-, CD43+), (D) germinal center B cells (intracellular Ig+, CD19+, B220+, CD43-, CD38-, GL7+), (E) unswitched naïve and memory B cells (intracellular Ig+, CD19+, B220+, CD43-, CD38+, GL7-), or (F) isotype switched memory B cells (intracellular Ig+, CD19+, B220+, CD43-, CD38+, GL7-, IgM-, IgD-). Plots are representative of three experiments totaling nine mice.

Intravascular staining during Mycobacterium tuberculosis infection reveals tissue-specific myeloid and lymphoid cell subsets

To examine the extent to which intravascular staining could delineate differences between vascular and tissue cells of the myeloid lineage, we used fourteen-parameter flow cytometry to measure markers characteristic of neutrophils (Ly6G, clone IA8) and mononuclear phagocytes (intracellular CD68+, these include monocytes, macrophages and dendritic cells, DCs) (Figure 3-13A). Neutrophils could be isolated from the lungs of naïve mice, regardless of perfusion (Figure 3-13B). This is surprising, as neutrophils do not occupy most healthy tissues. However, employing intravascular staining revealed that all of the isolated neutrophils from the naive lung were labeled with the i.v. mAb, suggesting that they were not in the pulmonary tissue of uninfected mice and that perfusion failed to remove them from vasculature (Figure 3-13C). Both i.v. mAb labeled and unlabeled CD68+ mononuclear phagocytes were recovered, consistent with the fact that certain myeloid cells are present both in blood and in tissue parenchyma and airways at steady state (*238*, *279*)(Figure 3-13D).

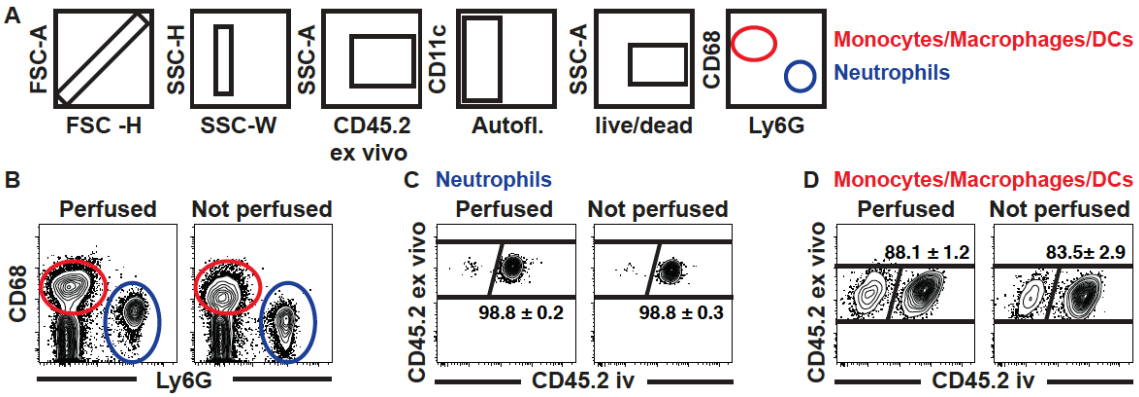

Figure 3-13: Perfusion fails to remove myeloid cells from lung vasculature. (A) Gating strategy for myeloid neutrophils and mononuclear phagocytes. (B) Neutrophils and mononuclear phagocytes were recovered from the lungs of naïve C57Bl/6 mice with or without perfusion. Intravascular staining of (C) neutrophils or (D) mononuclear phagocytes from lungs of perfused (left plots) or unperfused (right plots) naïve mice. Representative of nine mice per condition from two independent experiments.

To confirm that *bona fide* pulmonary neutrophils would be protected from intravascular staining, we evaluated the i.v. staining technique in a situation in which neutrophils localize to lung tissue. *Mycobacterium tuberculosis* (Mtb) causes a chronic lung infection that is contained, but not eliminated, by local immune responses. 12 week old C57Bl/6 mice were infected with 100-150 CFU of aerosolized Mtb (strain H37Rv), anti-CD45.2 mAb was injected i.v. 24 days later, and leukocytes from the lungs, bronchioalveolar lavage (BAL) of the lung airways, and blood were evaluated. Unlike uninfected mice, approximately half the neutrophils recovered from lung were now protected from i.v. mAb (PBL and BAL served as positive and negative staining controls, respectively, Figure 3-14A A&B). Similarly, and consistent with enhanced recruitment of myeloid cells to the lung between three to four weeks after Mtb infection (*177*, *238*, *280*), the

proportion of unlabeled CD68+ mononuclear phagocytes also increased after Mtb infection compared to naïve mice (Figure 3-14C).

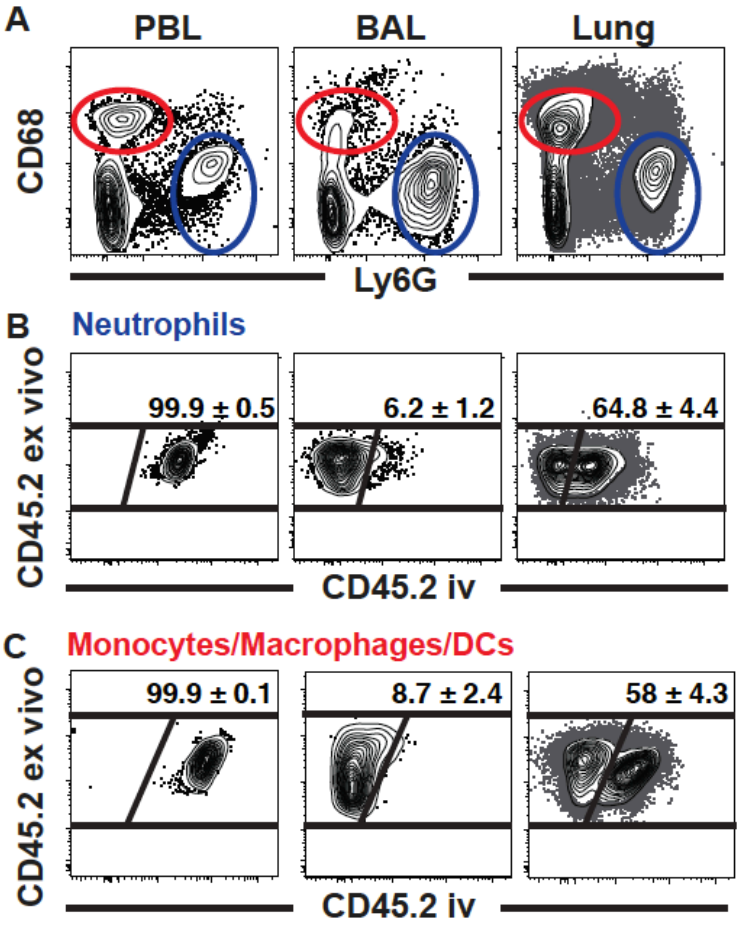

Figure 3-14: Intravascular staining of myeloid cells isolated from PBL, BAL or lungs of C57Bl/6 mice 24d after *Mtb* infection without perfusion. (A) Neutrophils and mononuclear phagocytes isolated from lung 24d after infection with 100-150 CFU of aerosolized *Mtb* (strain H37Rv) were identified by staining for CD68 and Ly6G. Intravascular staining of (B) neutrophils or (C) mononuclear phagocytes isolated from blood (PBL), airways (BAL) or lung tissue. Representative of nine mice per condition from two independent experiments.

Amongst CD68+ cells we then further discriminated various pulmonary myeloid subsets, such as inflammatory monocytes/macrophages (Ly6C+, CD11b+, CD11c-), conventional DC (cDC, CD11b+/- and CD11c+), tissue

resident CD103+ cDC (CD103+, CD11c+, CD11b-) and inflammatory monocyte-derived DCs (moDC, Ly6C+, CD11c+ CD11b+) (*168*, *169*, *253*, *281*). As expected, CD103+ cDCs isolated from the lung were indeed protected from intravascular mAb staining (Figure 3-15A&C). Interestingly, Ly6C+, CD11c- monocytes/macrophages were largely contained in the i.v. labeled fraction (Figure 3-15B&C) suggesting that the majority of this subset represents true monocytes present in pulmonary blood vasculature, while only a minority were tissue-localized *bona fide* macrophages. It should be noted that previously the Ly6C+, CD11c- population was found to be seemingly homogeneous with uniform expression of over 50 phenotypic markers of interest (*122-124*, *169*, *177*, *292*) (data not shown), highlighting the critical importance of the intravascular staining technique in distinguishing pulmonary Ly6C+ inflammatory monocytes from macrophages.

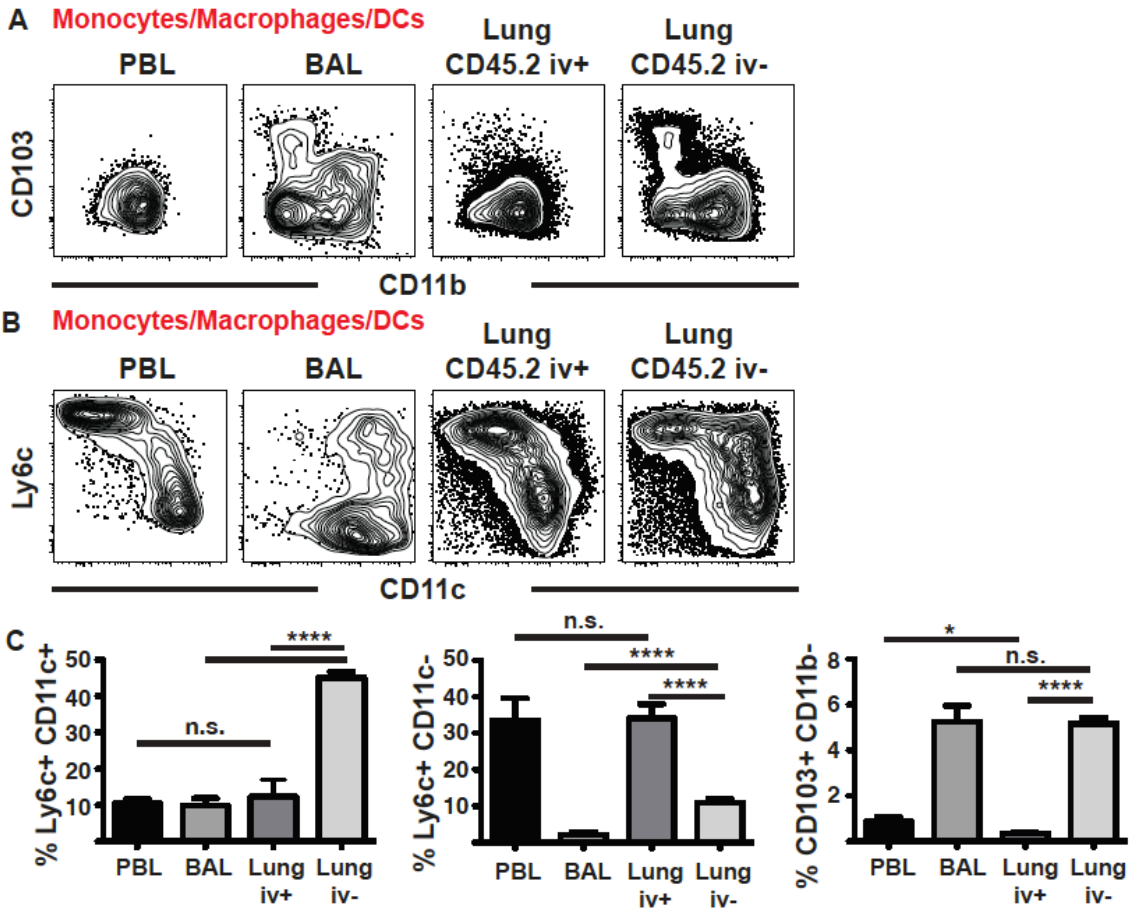

Figure 3-15: Intravascular staining during *Mycobacterium tuberculosis* infection reveals tissue-specific myeloid cell subsets. (A) CD11b and CD103 or (B) CD11c and Ly6C staining on mononuclear phagocytes isolated from the indicated compartments. (C) Summary of CD68+ mononuclear phagocyte subsets as defined in A,B. Plots are representative of two experiments totaling nine mice. * $p<0.05$. **** $p<0.0001$. n.s. = not significant. Error bars indicate SEM.

Moreover, inflammatory moDCs (CD11b+, CD11c+, Ly6C+) represent the major myeloid cell type truly present in the lungs of Mtb infected mice, since they were completely protected from i.v. mAb labeling (Figure 3-15B&C). These inflammatory moDCs have recently been shown to be highly multifunctional, producing IL-1α, IL-1β, TNFα, iNOS, and IL-10 and are phenotypically

characterized by high TLR2, CD13, Ly6C and CD64 expression (*126*, *177*, *254*, *293*). Thus, utilization of the intravascular staining technique uniquely enabled us to enrich and uncover inflammatory moDCs as myeloid effector cells in lung tissue in response to Mtb infection, another observation otherwise obscured by the presence of large numbers of myeloid cells in the lung blood vasculature.

In the context of Mtb infection, intravascular staining also discriminated between the function and phenotype of local T cells truly within the lung as compared to those in vasculature (Figure 3-16 and data not shown). For example, intravascular staining revealed that I-A^b ESAT-6_{1-20} and K^bTB10.3/4_{4-11} tetramer+ T cells (which identify Mtb-specific CD4 and CD8 T cells, respectively) had profound differences in PD-1 expression, a receptor that inhibits T cell function and is regulated by antigen-stimulation (Figure 3-16 B&C). Among both antigen-specific CD4 and CD8 T cells, PD-1 was more highly expressed on cells protected from intravascular staining compared to i.v. labeled cells present in vasculature (Figure 3-16 B&C). Taken together, these data clearly indicate that intravascular staining has the potential to change our understanding of local immune control over Mtb.

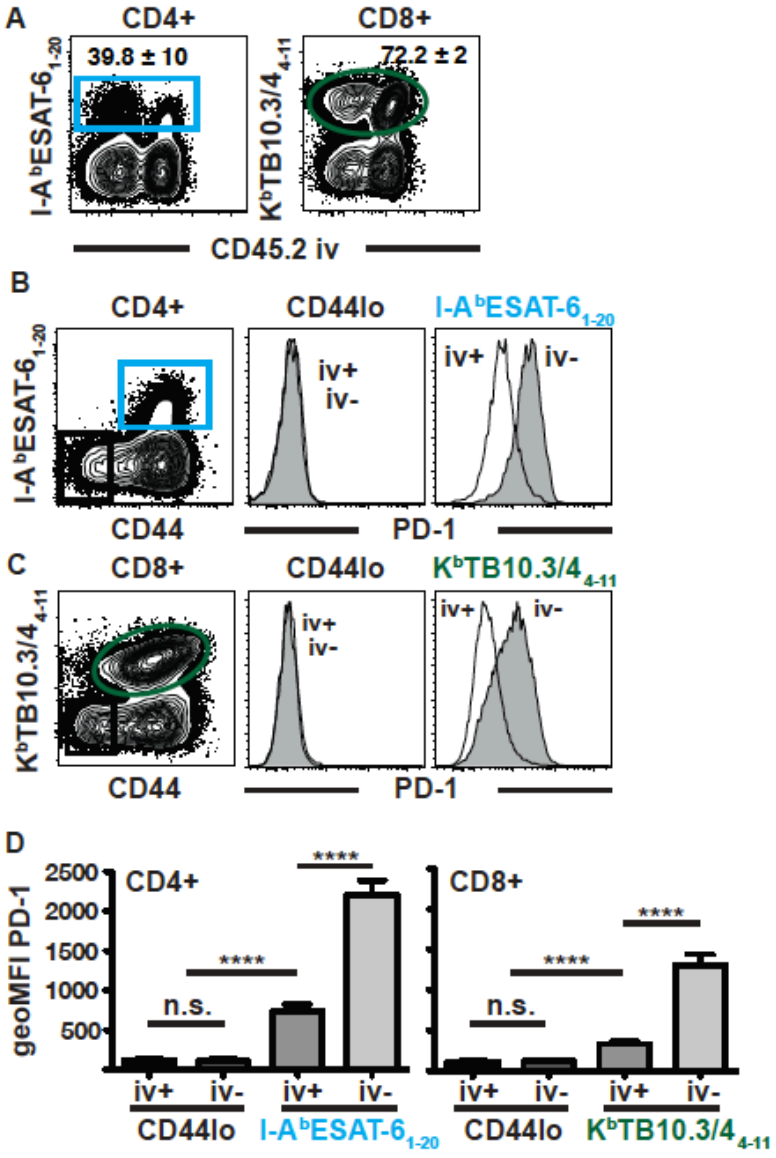

Figure 3-16: Intravascular staining without perfusion is sufficient to reveal unique lymphocyte subsets in lung tissue after *Mtb* infection. *Mtb*-specific CD4+ and CD8+ T cells isolated from lung 24d after infection with 100-150 CFU of aerosolized *Mtb* (strain H37Rv) were identified by staining with I-A^{b}ESAT-6$_{1-20}$ and K^{b}TB10.3/4$_{4-11}$ MHC tetramers, respectively. (A) Representative anti-CD45.2 i.v. mAb and MHC tetramer staining. PD-1 expression on (B) CD4+ and (C) CD8+ T cells from lungs. Shaded histograms are anti-CD45.2 i.v. mAb-, and black line indicates anti-CD45.2 i.v. mAb+. (D) Geometric mean fluorescence intensity (geoMFI) of PD-1 expression on naïve (CD44lo) or *Mtb* MHC tetramer+ CD4 and CD8 T cells. Plots are representative of two experiments totaling nine mice. **** $p<0.0001$. n.s. = not significant. Error bars indicate SEM.

Intravascular staining reveals myeloid and lymphoid tissue-specific subsets in tumor-bearing tissue

To determine the extent to which intravascular staining can distinguish tissue from vascular immune cells in a non-infectious disease model, we phenotypically analyzed T cells and myeloid cells in a solid tumor model of renal cancer (*282*, *283*, *294*). Murine renal adenocarcinoma cells (Renca) were injected into the left kidneys of 8 week old BALB/c mice. Tumor nodules were detectable histologically in the left kidneys 14 days later (Figure 3-17).

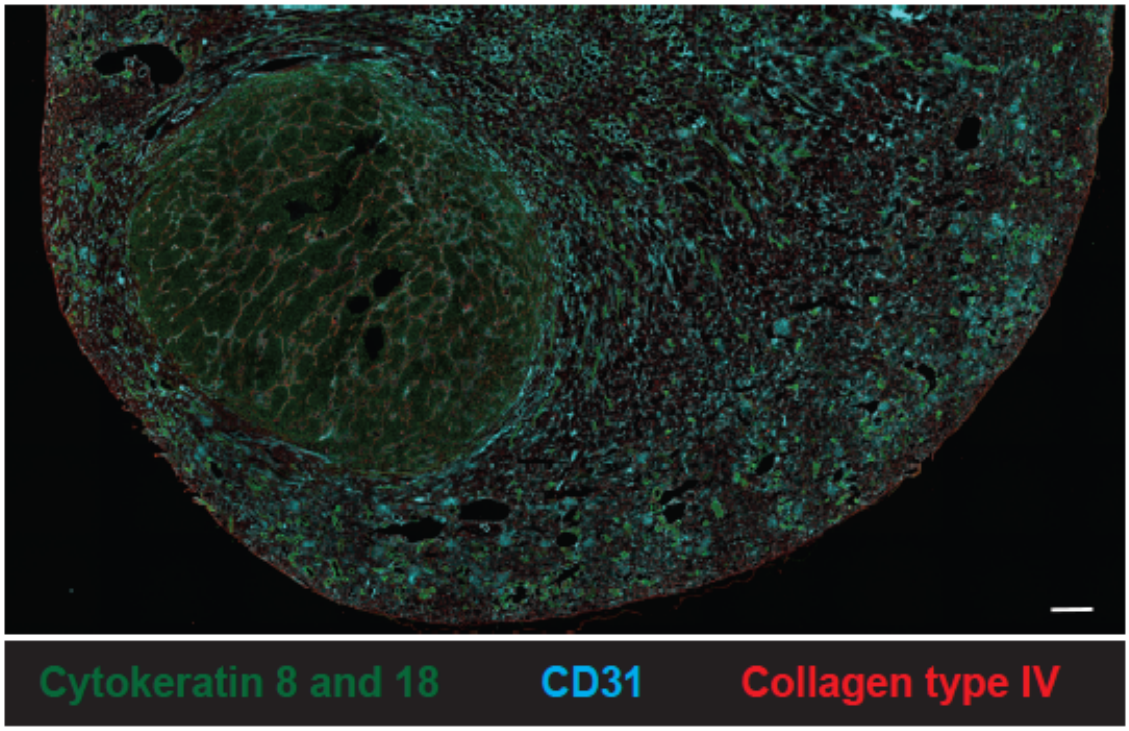

Figure 3-17: Immunofluorescence imaging of renal adenocarcinoma tumor model in mouse kidney. Non-metastatic Renca cells were injected into the kidney of Balb/c female mice in order to establish solid tumors. After 14 days, kidneys were removed and sections were stained *ex vivo* for cytokeratin 8 and 18 (green), collagen type IV (red), CD31 (cyan), and DAPI (gray). Scale bar = 250μm. Representative of five mice analyzed from three experiments.

When a polyclonal Ab (pAb) against collagen was injected i.v., it labeled glomerular basement membrane, but did not infiltrate the tumor (data not shown), indicating that i.v. injected Ab staining was limited to vascular-localized epitopes. In separate mice, anti-CD45.2 mAb was injected i.v. and cells isolated from blood, tumor-bearing kidneys, and non-tumor-bearing contralateral kidneys were examined. Intravascular staining revealed striking phenotypic differences among T cells within tumor-bearing kidney compared to those in control kidney tissue and also blood (Figure 3-18). For instance, ~30% of CD4 T cells protected from i.v. mAb staining isolated from tumor-bearing tissue co-expressed CD69 and CD103, a phenotype suggestive of regulatory T cells that may interfere with tumor immune responses. The inhibitory molecule PD-1, which is expressed upon cognate Ag stimulation, was expressed by most CD45.2 unlabeled T cells in tumor-bearing kidneys. This observation provides further evidence that intravascular staining may be used to identify tumor-infiltrating lymphocytes.

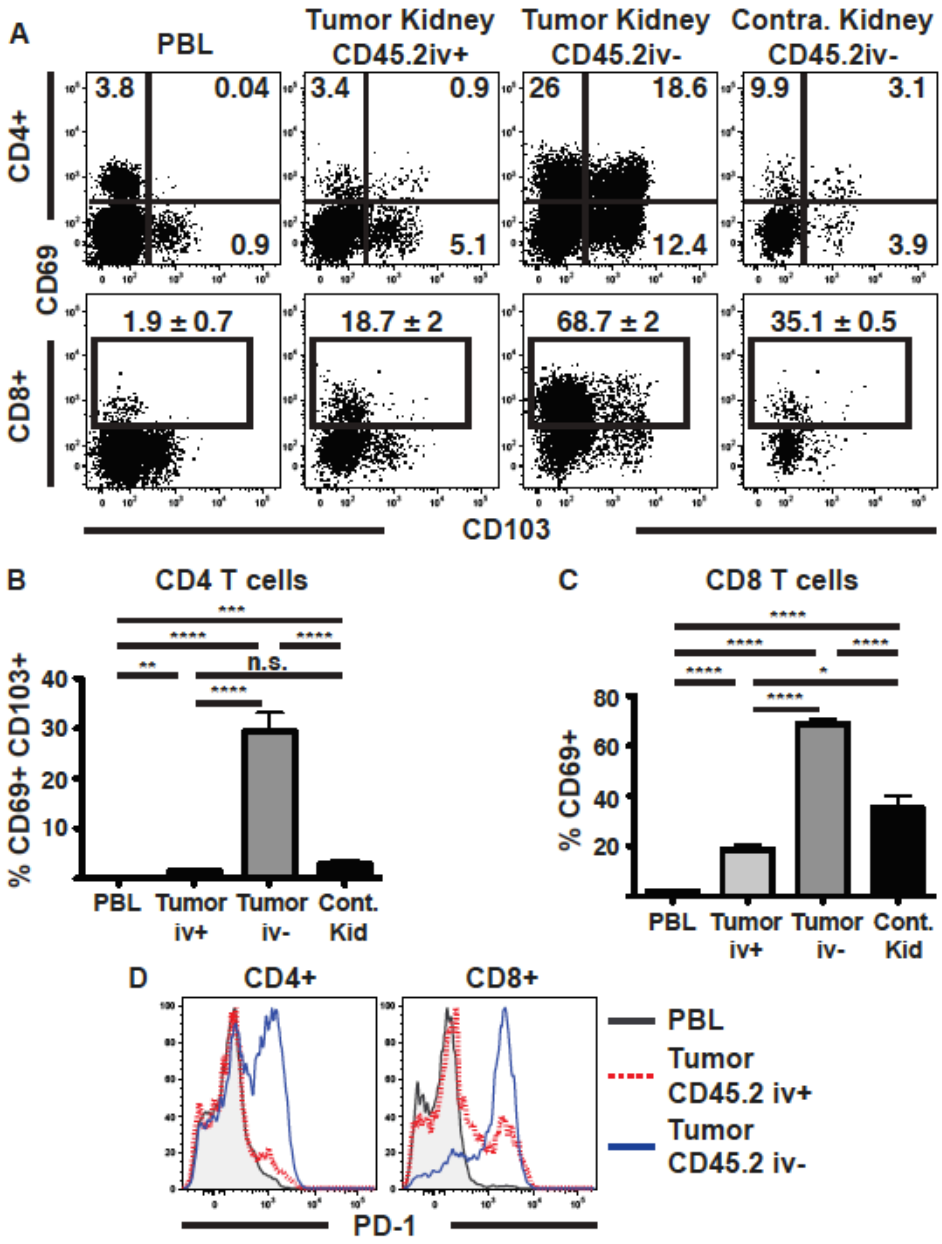

Figure 3-18: Intravascular staining reveals lymphoid tissue-specific subsets in a murine renal adenocarcinoma model. Non-metastatic Renca cells were injected into the kidney of Balb/c female mice in order to establish solid tumors. Anti-CD45.2 mAb was injected i.v. 14d after intrarenal Renca cell injection. (A) CD69 and CD103 expression on CD4 and CD8 T cells isolated from PBL, tumor-bearing kidney, and contralateral kidney. Frequency of (B) CD69+/CD103+ CD4 T cells and (C) CD69+ CD8 T cells from tumor-bearing mice. (D) PD-1 expression on CD4 and CD8 T cells isolated from PBL (gray) and tumor-bearing kidney (anti-CD45.2 i.v. mAb+ in red and anti-CD45.2 i.v. mAb- in blue). * $p < 0.05$, ** $p < 0.01$, *** $p < 0.0005$, **** $p < 0.0001$. Error bars indicate SEM.

Myeloid-derived suppressor cells (MDSCs) are immature myeloid cells that can both suppress anti-tumor immune responses as well as promote cancer (*221*, *295*). The presence and subsequent suppressive capacity of MDSC have been reported in both human renal cell patients and Renca murine models (*126*, *284*, *285*). Two main subsets of MDSC exist based on their Ly6G expression (*168*, *169*, *221*), which have been shown to be phenotypically and functionally distinct (*180*, *286*, *287*). Therefore, understanding where they reside within the tumor-bearing kidney can shed light on their functional capabilities and suppressive mechanisms. To determine whether certain subsets of MDSCs were more likely to be found in tumor-bearing kidney tissue or vasculature, we examined anti-CD45.2 i.v. mAb staining on CD11c- CD11b+ Ly6C+ MDSC subsets based on Ly6G expression (Figure 3-19). Ly6G+ MDSCs were predominantly found in Renca tumors whereas Ly6G- MDSCs were isolated from both tumor tissue and vasculature (Figure 3-19). Together, these data suggest that intravascular staining is also a useful tool to refine our understanding of anti-tumor immune responses.

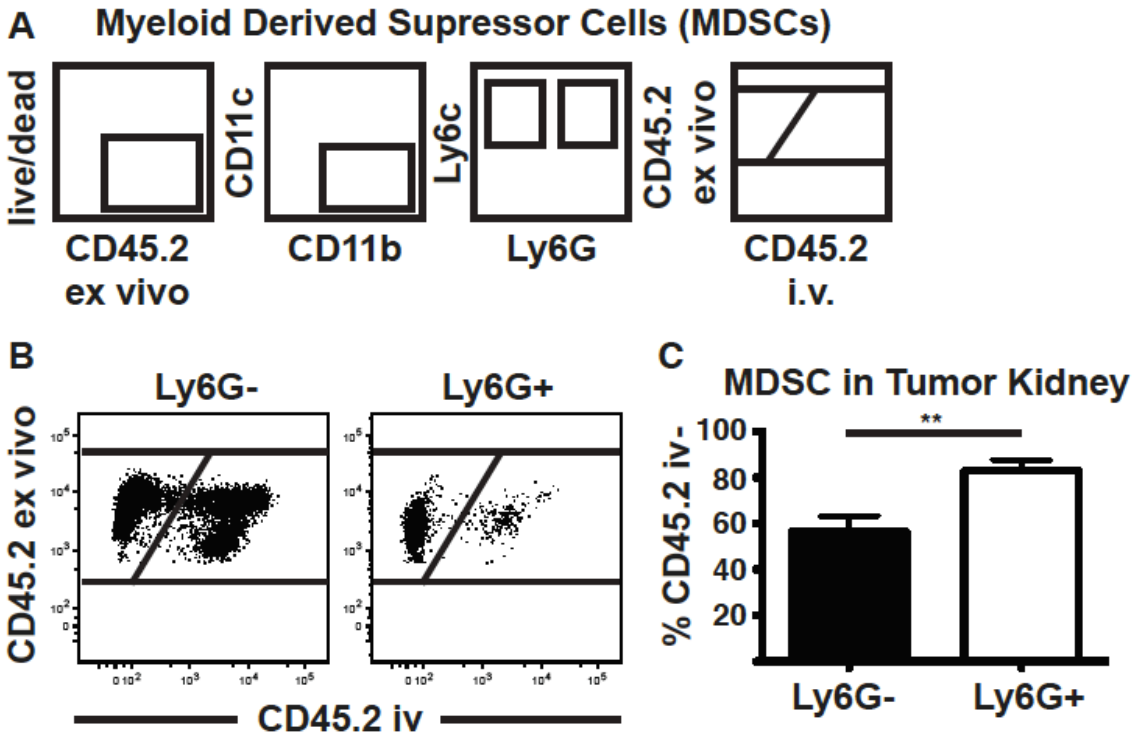

Figure 3-19: Intravascular staining reveals myeloid tissue-specific subsets in a murine renal adenocarcinoma model. Non-metastatic Renca cells were injected into the kidney of Balb/c female mice in order to establish solid tumors. MDSCs were isolated from tumor-bearing kidneys 14d after Renca cell injection. (A) Gating strategy for myeloid-derived suppressor cells (MDSCs). (B) CD45.2 i.v. mAb staining of Ly6G- and Ly6G+ MDSCs are shown. (C) Percentage of Ly6G- and Ly6G+ MDSCs from tumor-bearing kidneys protected from CD45.2 i.v. mAb staining. All plots are representative of 8-11 mice from three experiments. * $p < 0.05$, ** $p < 0.01$, *** $p < 0.0005$, **** $p < 0.0001$. Error bars indicate SEM.

Discussion

Intravascular staining has previously been used to distinguish between single populations of leukocytes in the vascular circulation and those in the tissue of the lung (*124*, *180*, *234*, *243*, *254*, *288*) or the red and white pulp of the spleen (*180*, *241*). Moreover, perfusion was shown to inefficiently remove CD8 T cells

from the lung vasculature (*254*, *296-300*). Here, we reveal the true scope of this issue by showing that cells of both the adaptive and innate immune system accumulate in the vasculature of many tissues and in the disease models examined. Perfusion not only fails to remove many vascular-bound leukocytes, but may also disrupt novel tissue populations such as alveolar lymphoid aggregates. Methods for intravascular staining in mice were delineated and validated. The strengths, considerations, and caveats of using different mAb combinations for studying various members of the innate and adaptive immune system were described. No specific problems with intravascular staining were encountered in any of the models presented.

These findings discourage the widely used practice of perfusion. Rather, they provide a compelling rationale for the incorporation of intravascular staining when possible, without perfusion, when studying any tissue leukocyte population. In fact, this approach may be absolutely necessary to capture an accurate and interpretable representation of the local participants in immune-mediated protection and disease.

Materials and Methods

Mice and Infections

Specific pathogen free (SPF) C57Bl/6 mice from Jackson Laboratories were used for analysis of immune responses to infection. Thy1.1+ P14 chimeric mice were generated as described (*254*, *301-304*). CD45.1+ SMARTA chimeric mice

were generated as described (*289*, *304*, *305*). Mice were infected intratracheally (i.t.) with 1 x 10^5 PFU LCMV (*126*, *254*). C57Bl/6 mice were infected with 100-150 CFU of aerosolized *Mycobacterium tuberculosis* (strain H37Rv) as described (*123*, *126*, *177*). SPF Balb/c mice from the National Cancer Institute were used for analysis of immune responses to solid tumors. All animal experiments were approved by the Institutional Animal Care and Use Committee (IACUC) at either the University of Minnesota or the National Institutes of Health.

Tumor cell line and challenge

The murine renal adenocarcinoma cell line, Renca, was obtained from Dr. Robert Wiltrout (National Cancer Institute, Frederick, MD), and maintained in Complete RPMI. For intrarenal tumor challenge a skin incision was made on the left flank, and 2 x 10^5 Renca cells were injected through the intact peritoneum into the left kidney (*282*, *283*, *294*).

Intravascular staining and cell isolations

Intravascular Ab was injected intravenously (i.v.). Three minutes later, the animals were sacrificed, lavaged to remove cells in the airway, bled, and perfused (as indicated) with 10 ml of cold phosphate buffered saline (PBS). The spleen, lymph nodes, lung, liver, kidney, salivary gland, female reproductive tract, small and large intestine were harvested within 12min, and lymphocytes were isolated as described (*126*, *155*).

Analysis	Marker	Fluorochrome	Clone	Company
CD8 T cells	CD8α	APC	53-6.7	eBioscience
	CD8α	PE	53-6.7	eBioscience
CD4 T cells	CD4	FITC	RM4-4	eBioscience
Endothelium	CD31	AF488	MEC13.3	Biolegend
Collagen basement membrane	Collagen IV	N/A Purified Ab	N/A Polyclonal goat anti-mouse	Millipore (Cat No: AB769)

Table 3-3: Antibodies for intravascular injection

Analysis	Marker	Fluorochrome	Clone	Company
Epithelial cells	cytokeratin 8	N/A Purified Ab	N/A Polyclonal rabbit anti-mouse	Novus Biologicals
	cytokeratin 18	N/A Purified Ab	N/A Polyclonal rabbit anti-mouse	Novus Biologicals
HEV	PNAd	N/A Purified Ab	MECA-7 Rat anti-mouse	BD Biosciences
Vascular Endothelium	CD31	AF488	MEC13.3	BioLegend
	CD31	AF647	MEC13.3	BioLegend
T cells	CD4	AF700	RM4-5	eBioscience
	CD4	AF647	RM4-5	BioLegend
	CD8α	PE-Cy7	53-6.7	eBioscience
	CD8β	AF647	YTS156.7.7	BioLegend
	CD44	APC-eF780	IM7	eBioscience
	CD45.2	BV650	104	BioLegend
	CD62L	PerCP-Cy5.5	MEL-14	BioLegend
	CD69	eF450	H1.2F3	eBioscience
	CD90.1 (Thy1.1)	eF450	HIS51	eBioscience
	CD90.1 (Thy1.1)	AF647	OX-7	BioLegend
	CD103	APC	2E7	eBioscience
B cells	CD11c	APC-eF780	N418	eBioscience
	CD19	AF700	eBio1D3	eBioscience
	CD38	PE-Cy7	90	BioLegend
	CD45.2	BV650	104	BioLegend
	CD90.2 (Thy1.2)	APC-eF780	53-2.1	eBioscience

	B220	V500	RA3-6B2	BD Biosciences
	F4/80	APC-AF750	REF: MF48027	Invitrogen
	GL7	eF450	GL-7	eBioscience
	Ig (H+L)	AF350	Cat: A11068	Invitrogen
	IgD	PerCP-Cy5.5	11-26c.2a	BioLegend
	IgM	APC	II/41	eBioscience
	Ly6G	APC-eF780	RB6-8C5	eBioscience
Myeloid cells	CD11b	APC-eF780	M1/70	eBioscience
	CD11c	PE-Cy7	N418	eBioscience
	CD45.2	BV650	104	BioLegend
	CD68	PerCP-Cy5.5	FA-11	BioLegend
	CD103	APC	2E7	eBioscience
	Ly6C	FITC	AL-21	BD Biosciences
	Ly6G	AF700	IA8	BioLegend
	MHC II I-A^b	eF450	M5/114.15.2	eBioscience
IHC	Goat anti-Rabbit	AF488	N/A	Invitrogen
	Goat anti-Rabbit	AF555	N/A	Invitrogen
	Donkey anti-Goat	AF488	N/A	Invitrogen
	Donkey anti-Goat	AF555	N/A	Invitrogen
	Donkey anti-Rat	AF488	N/A	Invitrogen
	Donkey anti-Rabbit	AF647	N/A	Jackson Immuno Research Laboratories

Table 3-4: Antibodies for ex vivo staining for flow cytometry or immunofluorescence

Immunofluorescence Microscopy

Immunofluorescence staining was performed as described (*123*, *126*, *155*). Briefly, tissues were frozen in O.C.T. on dry ice. 7μm frozen sections were cut using a Leica cryostat. Slides were fixed in cold acetone for 10 minutes. Prior to

staining, slides were rehydrated for 10 minutes in PBS. All slides were blocked for 60-90 minutes with 5% bovine serum albumin (BSA) in PBS. Secondary antibodies were used for 30 minutes at room temperature. DAPI staining was performed for 10 minutes. Cover slips were mounted with Prolong Gold Anti-Fade mounting reagent (Invitrogen). A Leica DM5500B epifluorescent microscope with Leica Acquisition Suite Advanced Fluorescence software was used for image acquisition. Adobe Photoshop was used for image analysis.

Confocal Microscopy

55µm frozen sections were cut using a Leica cryostat. A Leica SP5 laser scanning confocal microscope with Leica acquisition suite software was used for image acquisition. Imaris 7.6 (bitplane) software was used for image analysis.

Statistical Analysis

All statistical comparisons were performed using Prism 5 software (Graphpad). Analyses utilized a two-tailed unpaired t-test with 95% confidence intervals. All error bars represent standard error of the mean (SEM).

Chapter 4

The role of memory T cells during anamnestic responses to respiratory challenge

Myriad factors influence how leukocytes contribute to disease processes. While cell differentiation state accounts for some mechanistic differences between cell lineages, factors dependent on the physical location of the cell, such as the milieu of the tissue microenvironment, proximity to the site of infection, and physical barriers preventing cell-to-cell contact, also play a major role in immune responses to disease. In the lung, numerous leukocyte-containing tissue and blood compartments exist, and cells within these different microenvironments may play distinct roles during anamnestic responses to infection. Here we use intratracheal cell transfer and parabiotic methods along with intravascular staining to study the contributions of memory T cells within the airways or the tissue of the lung to secondary challenge. We demonstrate that the milieu of the lung airways significantly alters cell surface phenotype of memory T cells and inhibits division of T cells programmed to undergo proliferation. We also confirm the presence of a resident memory T cell population in the lung tissue. Finally, we show evidence that memory T cells within the lung tissue prior to secondary challenge are involved in recall of additional antigen-specific memory T cells to the site of infection. These findings have significant implications for the development of vaccines aimed at developing local T cell memory against respiratory infections.

Introduction

Leukocytes are found within numerous compartments of the respiratory tract: airspace, large blood vessels, alveolar capillaries, bronchiolar epithelium, inducible bronchus associated lymphoid tissue (iBALT), alveolar aggregates, pericapillary, and lamina propria. Cells in each of these locations are exposed to a different milieu of cytokines, such as TGF-β, and barrier surface conditions, such as surfactants and lung microbiota. Tissue milieu has been shown to affect leukocyte differentiation, proliferative capacity, and recruitment in numerous organs (*114*, *143*, *155*, *306*) including the lung (*123*, *126*, *290*). Further, it has been suggested that a paucity of direct cell-cell contact likely impacts the response time of cells during pathogen encounter (*291*, *307*). As cells in the lung vasculature are likely prevented from making cell-to-cell contacts with infected cells in the lung tissue or airways by endothelial cells and the underlying collagen matrix, cells in these distinct compartments of the lung may contribute differently during anamnestic responses.

Adoptive transfer of T cells expressing a traceable congenic marker, such as CD45.1/2 (Ly5.1/2) or CD90.1/2 (Thy1.1/2), or cells labeled with a detectable dye, such as carboxyfluorescin succinimidyl ester (CFSE) or cell tracker violet, into recipient mice can be used to study the role of distinct cell types during a memory response. Importantly, the route of cell transfer can also be utilized to focus on the role of cells in unique tissue locations. For instance, intratracheal (i.t.) transfer, followed by bronchioalveolar lavage (BAL), can be used to study the effects of the airway microenvironment on T cells and the role of these cells

in a response to airway challenge (*238*, *254*). On the other hand, intravenous (i.v.) transfer of a population of interest may be used to monitor migration, differentiation, and effector functions of cells circulating through secondary lymphoid organs and vasculature. While the presence of T cells within the lung airways correlates with protection against secondary challenge (*238*, *301*), and these have been shown to wane together over time (*168*, *169*, *307*), further studies are needed to fully characterize the contribution of airway T cells during immune responses to respiratory infections.

Airway memory T cells wane over time; however, memory T cells can be isolated from the lung many months after clearance of an infection, suggesting T cells within different compartments of the lung may have different retention capacities. Resident memory T cells (T_{RM}), a subset of effector memory T cell (T_{EM}), have been shown to be long-lived and play a role in both the recruitment of additional memory T cells as well as protection against local challenge within non-lymphoid tissues (*122-124*, *155*, *169*, *292*). One of the most definitive methods for defining T_{RM} is through the use of parabiotic experiments. In these systems, two congenically distinct partners are surgically conjoined for 2-4 weeks, allowing the circulatory systems of the partners to anastomose, or fuse. Cells originating from either parabiont partner can then be tracked for migration to the conjoined partner or retention within the original host. Use of parabiosis in combination with intravascular staining (*126*, *254*, *293*) allows for the characterization of intracellular and cell surface marker expression specific to T_{RM}.

One major regulator of T cell trafficking is the transcription factor Kruppel-like factor 2 (KLF2). In addition to directly regulating the expression of L-selectin (CD62L) and sphingosine 1 phosphate receptor 1 (S1PR1) (*238*, *294*), receptors that are required for lymph node entry and egress, respectively, KLF2 represses chemokine receptor expression (*138*, *155*, *254*, *295*). All of these molecules play distinct, yet critical roles in lymphocyte migration. In fact, reduced expression of KLF2 within CD8 T cells in non-lymphoid tissues results in the establishment of T_{RM} in the kidney, small intestine epithelium, salivary gland, and brain (*126*, *155*, *254*). While this mechanism ok KLF2 down-regulation is involved in the establishment of T_{RM} in several non-lymphoid tissues, investigation of this process in the lung to date is lacking.

Here we explore the contribution of memory CD8 T cells in the airspace and tissue of the lung to antigen-specific or antigen-irrelevant secondary responses. We demonstrate that environmental factors within the airway modulate the expression of cell surface molecules and inhibit T cell proliferation, and we utilize parabiosis in conjunction with intravascular staining to demonstrate the presence of a CD8 T_{RM} population within the lung tissue. Together, these data provide evidence that distinct populations of memory T cells exist within the lung.

Results

Intratracheal transfer of memory splenocytes alters cell surface phenotype

T cell memory within the lung airways wanes over time (*168*, *169*, *238*). To bypass the complications of low cell recoveries in endogenous systems, we adoptively transferred memory P14 splenocytes (>30 days after primary infection) intratracheally (i.t.) to study the behavior of airway cells (*119*, *180*, *254*). P14 T cells are transgenic CD8 T cells that express a T cell receptor (TCR) specific for the gp33-41 epitope of lymphocytic choriomeningitis virus (LCMV). Within 24 hours of transfer, donor P14 T cells displayed modest changes in the expression of cell surface molecules, consistent with previously published findings. For example, i.t. transfer of memory T cells primed with Sendai virus infection have reduced expression of the α_L integrin component of lymphocyte function-associated antigen 1 (LFA-1), also referred to as CD11a (*126*, *180*). We observed this same reduction in CD11a expression on memory T cells generated by LCMV infection and transferred into the airway of naïve mice (Figure 4-1). We also observed reduced expression of the tumor necrosis family (TNF) receptor CD27 and the interleukin 7 receptor-α (IL-7Rα) chain (CD127), consistent with observations by Woodland and colleagues (*107-109*, *111*, *180*). Importantly, this change begins to occur within 24 hours of transfer, but the reduction is most significant after greater duration in the airspace (Figure 4-1). As previously reported, expression of CD69, a marker correlated with antigen experience or residency, remained stable. However, expression of CD44, another marker

correlated with antigen experience and memory, was slightly reduced (Figure 4-1). Together, these findings are consistent with the hypothesis that the airway environment influences T cell phenotype.

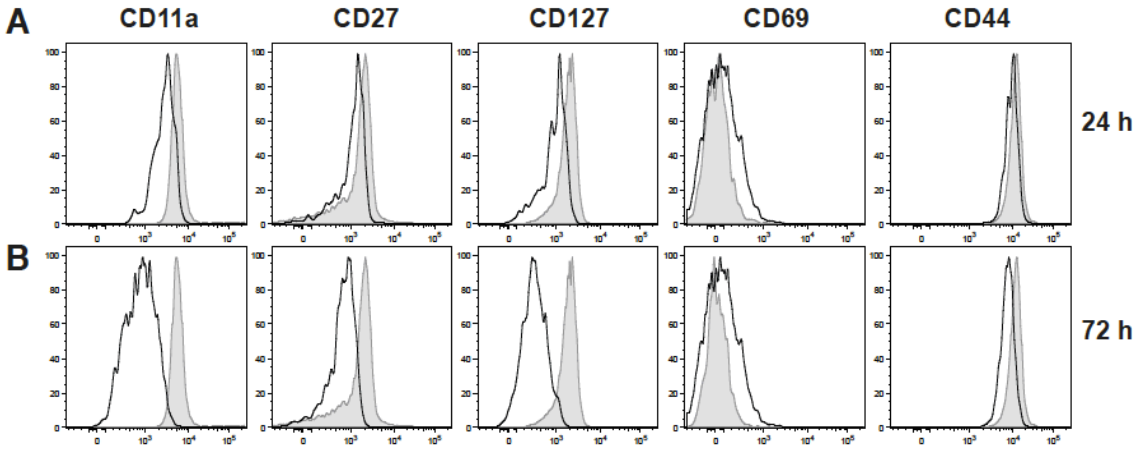

Figure 4-1: Intratracheal transfer of memory splenocytes alters cell surface phenotype. Memory P14 splenocytes were transferred i.t. into naïve C57Bl/6 recipients. 24 (a) or 72 (b) hours later, cells were isolated from the airway by bronchioalveolar lavage and assessed using flow cytometry for cell surface expression of CD11a, CD27, CD127, CD69, and CD44. Plots are representative of 3 mice per condition from 1 experiment.

T cell proliferation is inhibited within the lung airspace

To explore the effects of the airway environment on T cell proliferation, we treated memory P14 T cells with carboxyfluorescin succinimidyl ester (CFSE), initiated proliferation in vitro, and adoptively transferred the cells using either an intratracheal (i.t.) or intravenously (i.v.) route. CFSE is a green fluorescent dye commonly used to track cell proliferation (*108-110*, *296-300*). CFSE forms covalent bonds to amine groups within intracellular proteins; during cell division, the dye is dispersed in equal proportions to newly formed daughter cells.

Consequently, dilution of the dye within a population of cells results in a reduction of fluorescence intensity, indicative of the number of rounds of division the cells have experienced.

P14 T cells cultured in vitro with gp33-coated splenocytes begin to dilute CFSE as early as 24 hours (Figure 4-2A). By 48 hours in culture, the cells have undergone several rounds of division, and by 96 hours in culture, some P14 T cells have completely diluted CFSE, indicating they have undergone at least 6 rounds of division (Figure 4-2A). P14 T cells cultured with splenocytes lacking gp33 peptide remain CFSE high during the duration of in vitro culture. To assess the proliferation of P14 T cells in vivo, CFSE-coated P14s were stimulated in vitro for 24 or 48 hours and transferred i.v. via the tail vein. P14 splenocytes transferred i.v. continued to proliferate, and had fully diluted CFSE 1-2d after transfer (96 hours from initial stimulation). However, cells stimulated under the same conditions and transferred i.t. ceased CFSE dilution. Notably, when cells were transferred after 48 hours in culture, after several rounds of proliferation occurred and CFSE fluorescence intensity had been reduced, cells transferred i.t. failed to further dilute CFSE, indicating an arrest in cell division (Figure 4-2B).

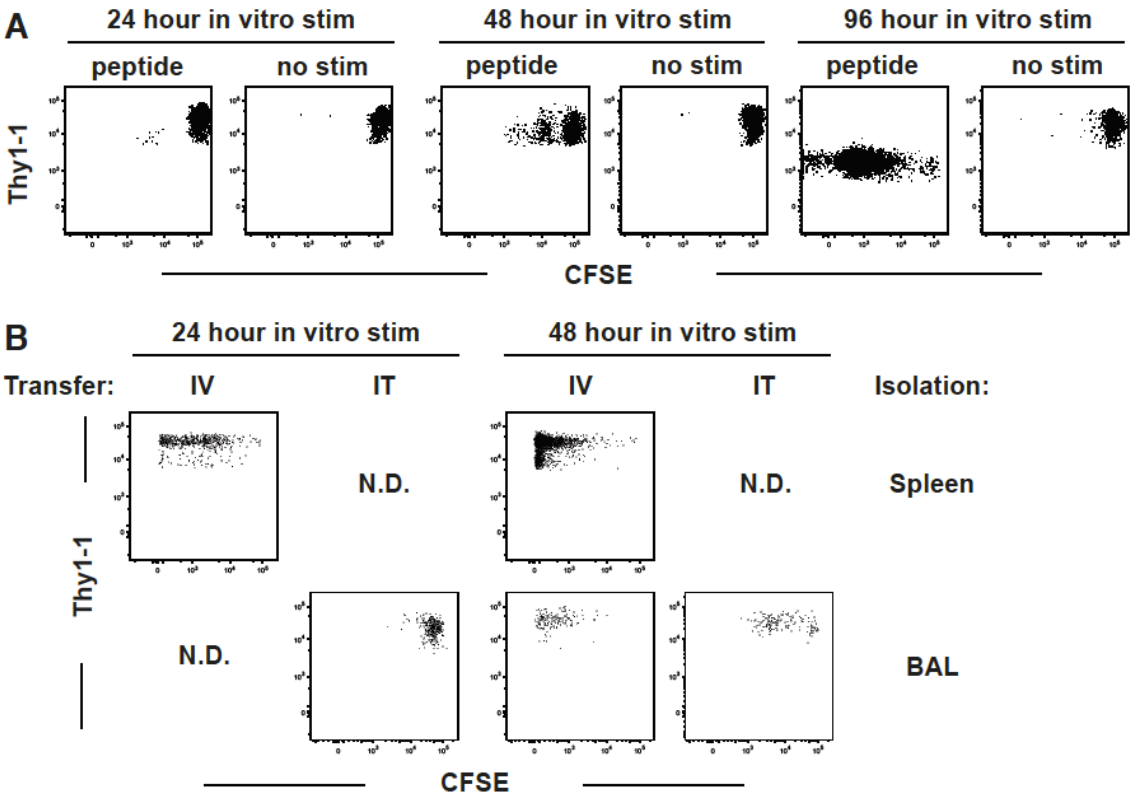

Figure 4-2: T cell proliferation is inhibited in the airways. (a) P14 splenocytes were treated with CFSE and stimulated in vitro using gp33-peptide-coated congenic splenocytes (peptide) or media alone (no stim). (b) After 24 or 48 hours, stimulated P14 splenocytes were transferred either i.v. or i.t. into naïve recipients. Cells were isolated from the spleen or airways 96 hours after initial stimulation and assessed for CFSE dilution using flow cytometry. Plots are representative of 6 recipient mice per condition from 2 independent experiments. N.D. = not detectable.

We noted that we were also able to isolate P14 T cells that had fully diluted CFSE from the airways of mice that received an i.v. transfer of donor cells. To examine whether these cells migrated to the airway and continued proliferation in the airways or completed proliferation prior to entry of the airway, we prepared P14 memory T cells with CFSE labeling and in vitro stimulation, as before, but we also treated the cells with media or pertussis toxin (PTx) prior to

i.t. transfer. Naïve P14 splenocytes were coated in CFSE prior to i.t. transfer as a negative control for CFSE dilution. Four days after transfer, only CFSE high cells could be isolated from the airways (Figure 4-3A, top row). However, very low numbers of donor memory P14 T cells (but not naïve P14 donor cells) treated with media could be recovered from spleen and mediastinal LN and displayed dilution of CFSE at both time points examined (Figure 4-3B and data not shown). Notably, naïve cells and P14 donor cells treated with PTx were not detected in any secondary lymphoid organs at any time point assessed (data not shown). By 7 days after transfer, memory cells treated with media alone could be isolated from the airways, and a fraction of these cells had completely diluted CFSE (Figure 4-3A, bottom row, center panel). However, only CFSE-high donor cells could be recovered from the airways of mice that received PTx-treated donor cells (Figure 4-3A, bottom row, right panel). These data suggest that memory T cell proliferation is indeed inhibited within the lung airways. Further, these data also support the hypothesis that chemokine signaling allows T cells to exit the airways and return to secondary lymphoid organs.

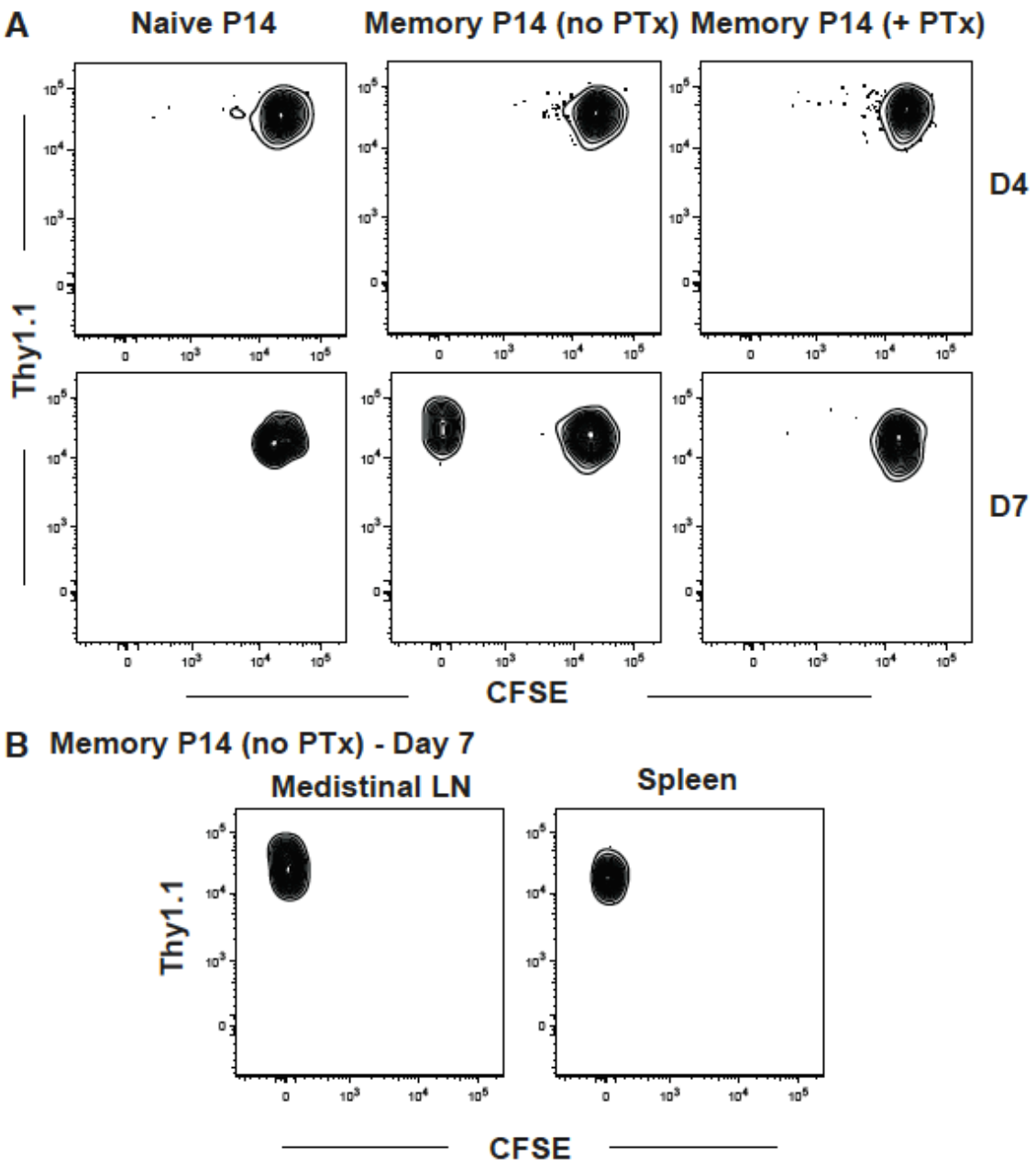

Figure 4-3: T cell proliferation occurs outside of lung airways. Memory P14 splenocytes were coated with CFSE and stimulated in vitro using gp33-peptide-coated splenocytes. Cells were treated with media (no PTx) or pertussis toxin (+ PTx) prior to i.t. transfer. Unstimulated naïve P14 T cells were transferred as a negative control for CFSE dilution. Cells were isolated from the (a) airway by lavage or (b) mediastinal lymph node or spleen 4 or 7 days after transfer and assessed for CFSE dilution by flow cytometry. Transferred Thy1.1 cells were not detectable in the mediastinal LNs or spleens of mice receiving naïve P14s of memory P14s treated with PTx. Plots are representative of 2 (Naïve and +PTx) or 3 (-PTx) mice per condition from 1-2 independent experiments.

In vivo peptide administration within lung airways results in cell loss

One mechanism by which CD8 T cells contribute to pathogen control is through secretion of cytokines such as interferon-γ (IFN-γ) and tumor necrosis factor-α (TNF-α). Since the cell surface phenotype and proliferative capacity of memory T cells in the airways is altered, we wished to assess the ability of memory T cells within the airways to secrete cytokines after re-stimulation in vivo. To this end, P14 memory splenocytes were transferred i.t. into naïve recipients. One day later, mice received an i.t. administration of media or gp33 peptide, and 2 hours later airway cells were isolated via BAL. Cells recovered from the airway were incubated in vitro with media or gp33 peptide and Golgi Plug (Golgi Plug is a chemical inhibitor of protein transport, which results in protein accumulation within the Golgi complex of the cell. This allows for detection of cytokine production using intracellular staining and flow cytometry). Donor P14 splenocytes were also stimulated with media or peptide in vitro as negative and positive controls, respectively. As expected, cells receiving no peptide stimulation produced neither cytokine (Figure 4-4, top left and bottom left panels), while cells receiving in vitro peptide stimulation readily produced both cytokines (Figure 4-4, right column). We observed cells within the airways that only received in vivo peptide stimulation were also able to produce both cytokines (Figure 4-4, left column, middle panel), although at a reduced frequency compared to those only stimulated in vitro.

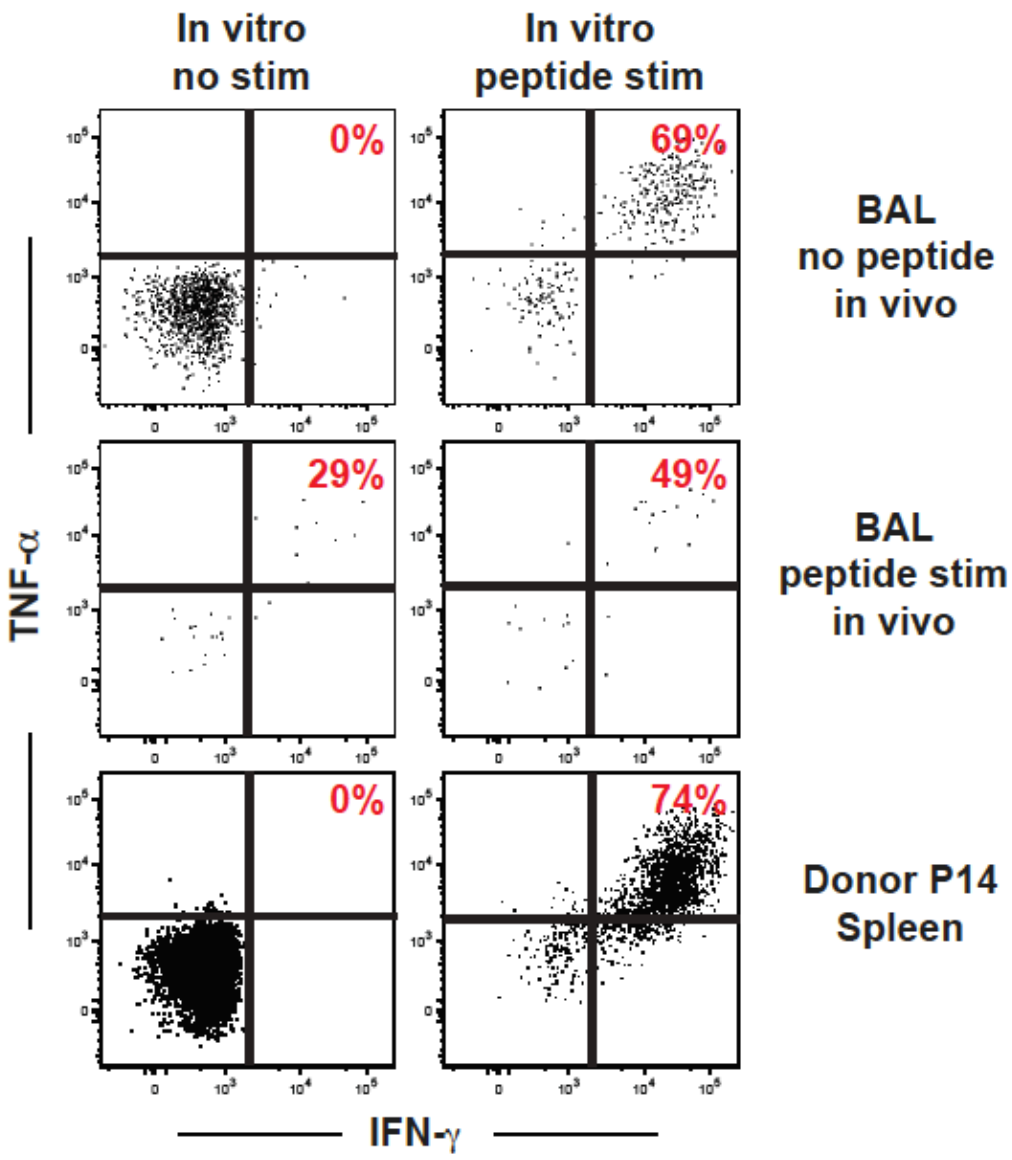

Figure 4-4: Splenocytes within lung airways secrete cytokines in response to peptide. 5 x 10^6 memory P14 donor splenocytes were transferred i.t. 1 day prior to peptide challenge. Recipient mice received media (top row) or gp33 peptide (middle row) i.t. 2 hours later, cells were recovered from airways via lavage and incubated in vitro with media (left column) or gp33 peptide (right column) for an additional 3 hours. Plots display concatamerized data from all mice (n = 3 per condition for BAL samples, n = 1 donor spleen) from 1 experiment. Percentages represent the average of all mice in each condition.

We also noted that the number of recoverable cells from BAL was significantly reduced in animals that received an i.t. administration of peptide. CD8 T cell fratricide has been reported under conditions of cognate ligand expression using in vitro model systems (*247*, *301-304*) and in vivo infectious systems (*148*, *304*, *305*). While T cell fratricide may explain these findings, it is also possible that in vivo stimulation with peptide results in rapid egress of antigen-specific T cells from the airway to secondary lymphoid tissue. Thus, we wished to determine if the reduced cell recovery was due to cell death upon peptide encounter or cell egress from the airway. To investigate this observation further, we transferred an equal number of CFSE-labeled memory P14 splenocytes i.t. into naïve mice and challenged one day later with either gp33 peptide or a recombinant form of *Listeria monocytogenes* expressing gp33 (LM-gp33).

Two hours or three days after challenge, CFSE high donor cells could be recovered from animals administered either challenge (Figure 4-5A, left and middle panels), but the number of recovered cells from the peptide challenged animals were markedly lower than the animals receiving the infection. By 8 days after challenge, CFSE-diluted donor cells could only be recovered from the airways of mice challenged with LM-gp33 (Figure 4-5A, right panels). In addition, donor cells could only be recovered from spleens of mice challenged with LM-gp33 (Figure 4-5B), and these cells had completely diluted CFSE by 8 days after infection (Figure 4-5C). Together, these data are consistent with the hypothesis that CD8 T cells in the airways exposed to peptide stimulation are undergoing

cell death rather than migration out of the airways. However, we cannot rule out the possibility that infection with a pathogen provides survival factors and/or migration cues that are absent during challenge with peptide alone. Further experiments are required to fully interpret these results.

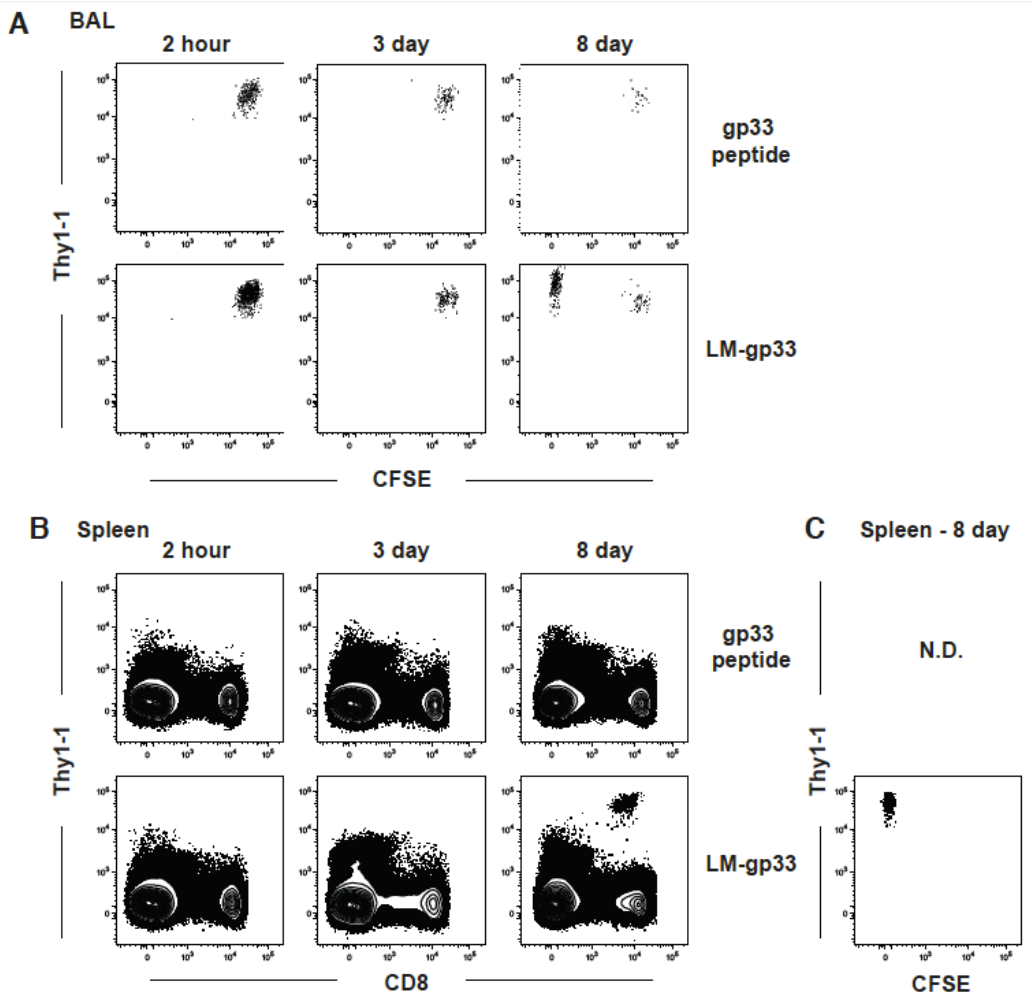

Figure 4-5: In vivo peptide administration results in P14 cell loss. Memory P14 splenocytes were coated with CFSE and transferred i.t. 1 day prior to challenge with gp33 peptide or LM-gp33. P14 donor cells were recovered from the airways via BAL (a) or the spleen (b&c) and assessed for CFSE dilution 2 hours, and 3 or 8 days after challenge. Plots in (a) display concatamerized data of all mice (n = 3 per condition) from 1 experiment. (b&c) Representative plots from 3-5 mice per condition in 1-2 independent experiments.

Lung tissue contains both non-recirculating T_{RM} and circulating T_{EM}

Reduction in the expression of the transcription factor KLF2 has been shown to result in the formation of T_{RM} populations within non-lymphoid tissues (*126*, *308*). To determine whether T_{RM} cells reside in the lung tissue, we generated congenically distinct P14 immune chimeric mice. After >30 days, infection-matched memory mice were conjoined through parabiosis to allow shared circulation to develop (Figure 4-6A). Three weeks after surgery, approximately equal ratios of P14 T cells from each animal could be found in the peripheral blood circulation (data not shown). To assess the presence of resident or circulating donor memory cells in tissues, we injected anti-CD8β Ab i.v., sacrificed the animals, and harvested lymphoid and non-lymphoid tissues to examine KLF2 expression in P14 T cells derived from either donor.

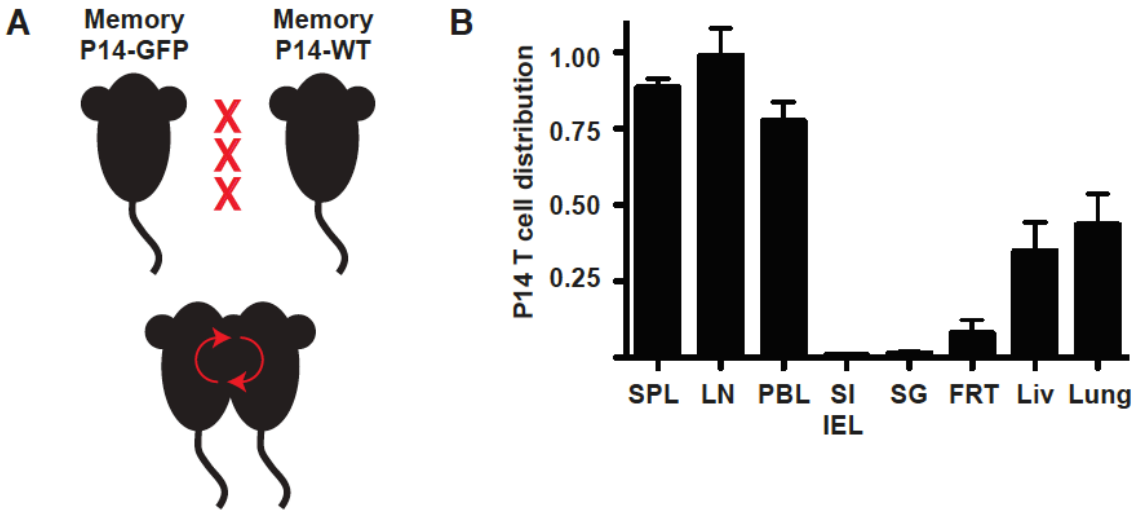

Figure 4-6: Lung tissue contains non-recirculating T_{RM}. Congenically distinct P14 memory mice were generated by transferring either naïve P14 T cells expressing a KLF2-GFP fusion protein (CD45.1/2) or naïve wild type (WT) P14s T cells (CD45.1) into naïve C57Bl/6 recipients (CD45.2) and infecting with LCMV i.p. 1 day later. >30d after infection, hosts containing distinct memory T cell populations were surgically conjoined. (a) Parabiosis schematic. (b) Four weeks later, intravascular staining was used to quantitate the proportion of recirculating memory cells in spleen (SPL), lymph node (LN), peripheral blood (PBL), small intestine epithelium (SI IEL), salivary gland (SG), female reproductive tract (FRT), liver, (Liv), and lung tissues. Results are presented as the frequency of P14 T cells among total CD8+ cells in the parabiont divided by the counterpart in the donor. Data are representative of 6 parabiont pairs (12 mice total) from 2 independent experiments. Error bars = SEM.

As expected, approximately equal proportions of P14-GFP to P14-WT cells could be found in the spleen, lymph nodes and peripheral blood of the WT memory animal after 4 weeks (Figure 4-6B). However, consistent with previously published results, P14-GFP memory cells failed to enter the small intestine epithelium (SI IEL), salivary gland (SG) and female reproductive tract (FRT) of the WT animal (*123*, *126*, *309*) (Figure 4-6B), confirming that memory cells within these tissues are non-recirculating T_{RM}. Non-lymphoid tissues such as the liver

and lung, however, neither completely equilibrated (like the lymph nodes), nor remained completely resident (such as the SI IEL, SG, and FRT), suggesting that these tissues may contain both populations of memory T cells: non-circulating T_{RM} and recirculating T_{EM} (Figure 4-6B).

KLF2 regulates the expression of the T cell migration markers CD62L and S1PR1 (*177*, *294*); consequently, a reduction in KLF2 expression correlates with a reduction in sensitivity to S1P signaling in the blood and lymph, resulting in cells that are refractory to egress signals. S1PR1 expression also inversely correlates with expression of CD69 (*126*, *251*). Consequently, KLF2 reduction and/or CD69 expression are used as surrogate markers for T_{RM}. To examine the expression of KLF2 and CD69 on resident and recirculating cells in the lung, we compared KFL2-GFP and CD69 expression levels from P14-GFP memory cells within the donor and parabiont partner. As expected, the lymph nodes of P14-GFP and P14-WT memory mice contained equivalent populations of $KLF2^{hi}$ $CD69^{lo}$ memory P14 cells from the donor P14-GFP mouse (Figure 4-7A, second row), confirming that the lymph node compartment contains recirculating memory cells. The SG and FRT of the P14-GFP donor mouse both contained $KLF2^{lo}$ $CD69^{hi}$ T_{RM} populations, which were lacking in the P14-WT mouse (Figure 4-7A), consistent with previously published reports of T cell residency within these tissues (*122*, *123*, *126*, *228*). Furthermore, the splenic white pulp of the P14-GFP donor mouse contained a sizeable fraction of $KLF2^{lo}$ $CD69^{hi}$ T_{RM}, consistent with recent findings regarding the presence of T_{RM} within lymphoid tissues (*156*).

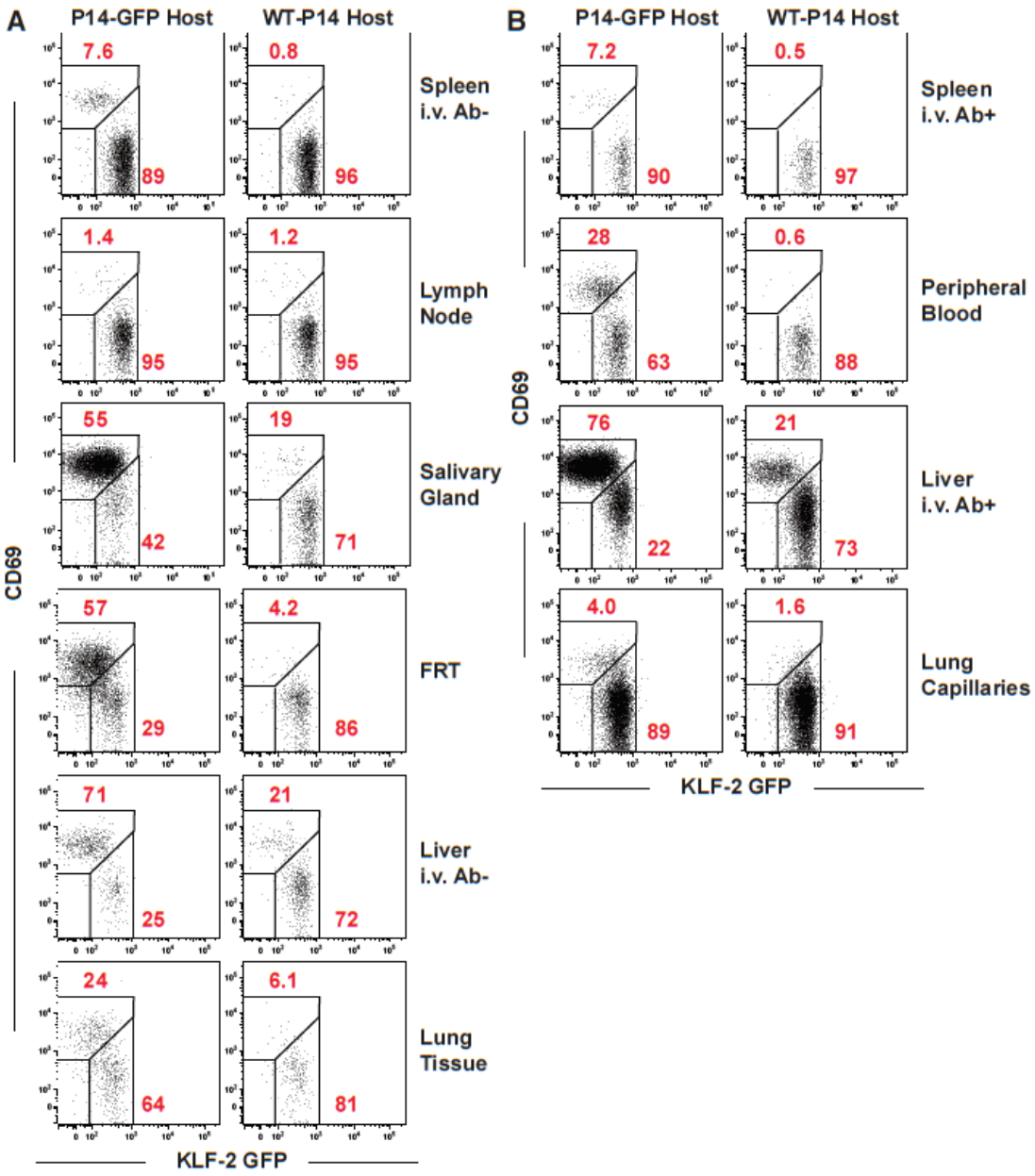

Figure 4-7: T_{RM} in the lung reduce expression of KLF2. Congenically distinct P14 memory mice were generated by transferring either naïve P14 T cells expressing a KLF2-GFP fusion protein (CD45.1/2) or naïve wild type (WT) P14s T cells (CD45.1) into naïve C57Bl/6 recipients (CD45.2) and infecting with LCMV i.p. 1 day later. >30d after infection, hosts containing distinct memory T cell populations were surgically conjoined. Four weeks later, intravascular staining was used to distinguish cells within tissue (a) and blood (b) compartments of the indicated tissues. Plots are concatamerized data from 3 mice per condition and are representative of 6 parabiont pairs (12 mice) from 2 independent experiments.

Notably, KLF2^{lo} CD69^{hi} T_{RM} populations were identified within the liver and lung tissue compartments of the P14-GFP donor mice (Figure 4-7A), although these populations constituted only 68% and 32% of the memory cells in the tissue, respectively (compared to P14-WT mice, which contained 17.3% and 9.4% in liver and lung, respectively). This further supports the interpretation that the liver and lung contain both non-recirculating T_{RM} and circulating T_{EM} populations. Interestingly, we observed that the P14-WT recipient liver tissue also contained a fraction of KLF2^{lo} CD69^{hi} T_{RM} derived from the parabiont partner (Figure 4-7A). While it is possible that some tissue compartments are accessible to circulating memory T cells and may be seeded with new T_{RM}, an alternative explanation is that additional S1P receptors, such as the other S1PR family members S1PR2, S1PR3, S1PR4, and S1PR5 (*124*, *306*), also play a role in T cell recirculation. Regardless of the mechanism, this finding is consistent with the notion that CD69 is an imperfect marker of T_{RM} (*123*, *126*). Finally, we noted that three compartments accessible by intravascular Ab, the peripheral blood, liver sinusoids and lung vasculature, also contained small populations of KLF2^{lo} CD69^{hi} T_{RM} (Figure 4-7B, left panels). Although resident populations of leukocytes in vascular compartments have previously been reported (*251*, *307*), we cannot rule out the possibility that additional S1P receptors also play a role in T cell recirculation. Further experiments are needed to fully understand the implications of these data.

Memory CD8 T cells are rapidly recalled to the lung tissue after local antigen challenge

Local antigen-specific memory CD8 T cells can secrete cytokines, elicit cytotoxic functions, and induce rapid recall of additional memory T cells upon exposure to antigen. We wished to asses whether the presence of antigen-specific memory T cells within the lung tissue would also be associated with rapid recall responses after a local lung challenge. To this end, we generated P14 memory mice containing memory T cells in the lung tissue via intratracheal (i.t.) infection with LCMV as previously described (*160*, *254*). After 140 days, mice were re-challenged i.t. with media (ø), irrelevant peptide (AL11, a peptide from the gag protein of simian immunodeficiency virus), LCMV-derived peptide (gp33), recombinant Vaccinia virus expressing an irrelevant antigen (VV-gag), or recombinant Vaccinia virus expressing an LCMV-specific antigen (VV-gp33). At 12, 24 and 48 hours after challenge, intravascular staining was performed and the lungs of mice were frozen for histological analysis.

No quantitative difference was observed between any groups by 12 hours after challenge (Figure 4-8A). However, by 24 hours, the lungs of mice challenged with Vaccinia containing a relevant P14 T cell epitope contained significantly more P14 T cells than unchallenged animals (Figure 4-8B). Notably, mice challenged with gp33 peptide also appear to have more cells than unchallenged animals; however, this difference is not statistically significant. We hypothesize, based on the previous peptide challenge experiments (Figure 4-4 and Figure 4-5), that the results observed in the animals challenged with peptide

alone may be a reflection of concurrent cell recall and cell death, although additional experiments are needed to thoroughly test this hypothesis.

By 48 hours after challenge, we observed a significant increase in P14 T cells within mice challenged with relevant antigen, regardless of form during administration. Notably, a small increase in P14 T cells was observed in animals challenged with an infection containing irrelevant antigen as well (Figure 4-8C). While this increase was not statistically significant over unchallenged controls, it is also not significantly different from the animals challenged with relevant antigen. Further experiments are needed to determine if irrelevant infection can also induce a minor recall response within the lung tissue. Future experiments examining the recall of other immune cell types will also significantly contribute to our understanding of the role of memory CD8 T cells during secondary responses to infection.

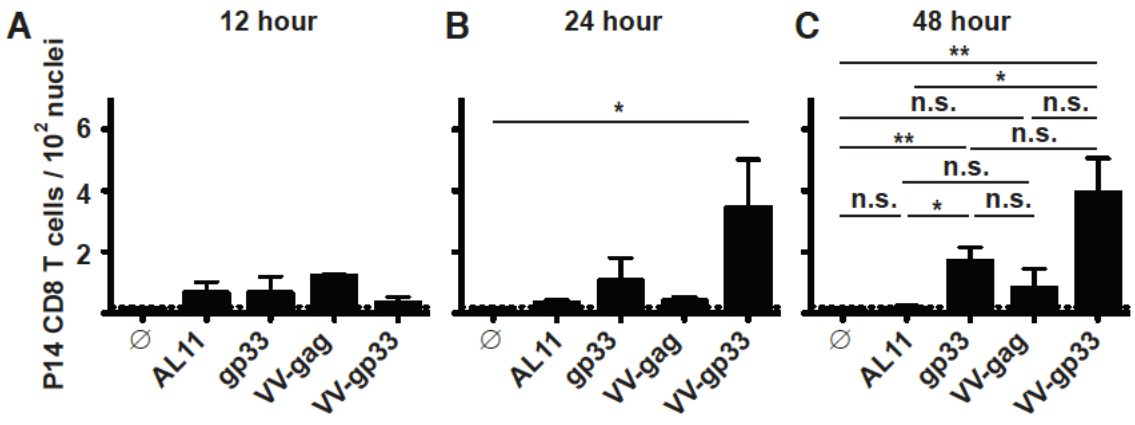

Figure 4-8: Rapid recall of antigen-specific memory T cells to lung tissue after local challenge with antigen. After 140 days, we re-challenged the mice i.t. with media (ø), irrelevant peptide (AL11, a peptide from the gag protein of simian immunodeficiency virus), relevant peptide (gp33), recombinant Vaccinia virus expressing an irrelevant antigen (VV-gag), or recombinant Vaccinia virus expressing a relevant antigen (VV-gp33). At 12 (a), 24 (b) and 48 (c) hours after challenge, intravascular staining was performed and the lungs of mice were frozen for histological analysis. Data are representative of 4-5 mice per condition from 2 independent experiments. * $p<0.05$, ** $p<0.01$, n.s. = not significant. Error bars indicate SEM.

Discussion

Within the lower respiratory tract, the pulmonary-alveolar barrier between airspace and vasculature consists of two cells, an endothelial cell and an alveolar epithelial cell, with a fused basal lamina. Hence, this interface constitutes a delicate barrier surface exposed to the external environment. Pulmonary alveolar epithelial cells are constantly exposed to environmental antigens, both innocuous and pathogenic. Consequently, a careful balance must be maintained between immune responses poised to contain infection and regulation of responses to minimize tissue pathology. Much like the dual-functionality that alveolar epithelial cells provide in both efficient gas exchange and as a barrier surface, other

factors unique to the lung environment, such as surfactant proteins, also play multiple roles in homeostatic maintenance. For instance, surfactant protein A (SP-A) reduces surface tension at the alveolar air-liquid interface, but SP-A also has an immunomodulatory role. SP-A serves as a scavenger receptor and opsonin (*124*, *310*-*314*) promoting innate immune responses, but SP-A also suppresses T cell proliferation (*119*, *121*, *122*, *155*, *290*, *315*-*317*) and IL-2 secretion (*155*, *158*, *159*, *318*). Our findings regarding modulation of memory T cell phenotype, proliferation, and cytokine secretion are consistent with previously published results, although further work is needed to elucidate whether SP-A or an alternate mechanism is responsible for the phenotypic modulation and cytokine suppression we observed.

Previous studies have suggested that the cells arriving in the lung airways were in a state of terminal differentiation (*169*, *180*, *311*, *319*, *320*), and speculated that these cells would eventually be expelled from the body, likely via the mucociliary escalator. Therefore, in our experiments involving i.t. transfer of memory cells, it was surprising to see memory cells retained the ability to egress and return to secondary lymphoid tissue. It could be argued that these observations are an artifact derived from the adoptive transfer system utilizing a large number of transgenic splenocytes, as the expression of migratory molecules, differentiation state, proliferative potential, and function of splenocytes and cells within the airway are notably different (*168*, *169*, *180*). However, in all experiments, the donor cells were parked in the airways at least 24 hours prior to challenge, which is enough time to allow the cells to modulate expression of cell

surface markers characteristics of splenocytes to resemble airway T cells (Figure 4-1). Thus, it is interesting to speculate that memory T cells migrating into the airways may not be on a “one-way trip”. Additional experiments involving the transfer of labeled airway cells may shed some light on the physiological relevance of this phenomenon.

Additionally, while cells in the airways have previously been described as a population of effector T cells poised to protect against infection at the respiratory interface, the experiments in which challenge with peptide resulted in cell loss may allude to another role for these cells. T cells engaged in the process of fratricide have been shown to express IFN-γ and TNF-α (*237*, *301*), consistent with our observations (Figure 4-4), yet they also mediate cytotoxic effects against other CD8 T cells via perforin-mediated mechanisms. Consequently, it is possible that cells within the airways also play a regulatory role during immune responses in the respiratory tract. Further investigation is needed to determine if memory T cells in the airways also play an immune-regulatory role in the lungs.

In light of the protective role T_{RM} have been shown to play, efforts to improve the generation of T_{RM} in the lung tissue may be critical for the development of T cell vaccines against respiratory pathogens, such as influenza and *Mycobacterium tuberculosis*. We have shown that a population of T_{RM} does exist in the lung tissue, but that not all memory cells in the lung are resident. The factors that make this tissue distinct from non-lymphoid tissues containing predominantly T_{RM} memory, such as the small intestine epithelium and female reproductive tract (which are also a barrier surfaces), remain to be elucidated.

Teleologically, perhaps the lung only contains a fraction of T_{RM} to preserve optimal gas exchange function. Alternatively, perhaps some cells lacking CD69 expression are also resident and are retained in the tissue by alternate mechanisms. Yet another explanation for these findings may be that local lung infection generates a more substantial population of lung-localized T_{RM}. These unresolved questions merit further investigation.

Although resident leukocyte populations have been described within vascular compartments previously (*307*, *321*), we were surprised to find such a large population of $KLF2^{lo}$ $CD69^{hi}$ T cells within the peripheral blood. Since the peripheral blood leukocytes in the parabiosis experiments were obtained via cardiac puncture, we cannot rule out the possibility that the isolated cells had recently re-entered the vascular circulation through the thoracic duct. For instance, if memory cells managed to egress from non-lymphoid tissue but lacked expression of the major lymph node homing molecule CCR7, they would likely travel through the sinuses of lymph nodes, back to the venous circulation, into the right atria and ventricle of the heart, and out to the pulmonary vasculature. This alternative scenario could explain the presence of T_{RM} phenotype cells within the vascular compartments of the peripheral blood, lung and liver of the parabiont partners. Further experiments are needed to determine the origin of these cells, as well as to refine the markers used to characterize true T_{RM}.

Fully elucidating the role of tissue localized memory T cells during a second exposure to antigen is an active area of interest. Our findings suggest

that local memory CD8 T cells may be involved in recall responses; however, the kinetics of the responses to different pathogens may vary significantly. For example, others have demonstrated that heterosubtypic responses to influenza virus do not result in accumulation of antigen-specific memory T cells until ~5 days after challenge (*169*). Thus, the kinetics of the memory T cell response may be heavily influenced by the agent used for secondary challenge. As these issues are all relevant for the development of efficacious vaccines, future work will need to address these unresolved questions.

Materials and Methods

Mice and infections

C57Bl/6 and CD45.1 congenic B6 mice were purchased from Jackson Laboratories or the National Cancer Institute and used at 6-8 weeks of age. P14 TCR transgenic mice expressing the H-2D^{b} restricted LCMV gp33-41 epitope [KAVYNFATC] expressing Thy1.1 or CD45.1/2 were used for the described studies. P14 chimeric immune mice were generated as described (*155*, *170*, *322*). CD45.1 P14 were crossed to KLF2^{GFP} reporter mice for parabiosis studies (*126*, *162*, *323-328*). Mice were either infected intraperitoneally (i.p.) with 2 x 10^5 PFU LCMV or intratracheally (i.t.) with 1 x 10^5 PFU LCMV (*238*). Mice challenged with pathogens received 5 x 10^3 cfu LM-gp33, 5 x 10^5 pfu VV-gp33, 5 x 10^5 pfu VV-OVA, or 5 x 10^5 pfu VV-SIV-gag i.t.. Mice challenged with peptide received 1μg/ml of gp33, SIINFEKL, or AL11 peptide in 100μl volume i.t. Animals were

maintained under specific pathogen-free conditions at the University of Minnesota, and the IACUC approved all experiments.

Intravascular staining and cell isolations

3 µg of Anti-CD8α-APC, anti-CD8α-PE, or purified anti-CD8α (clone: 53-6.7 from eBioscience) or anti-CD8β Pacific Blue (clone: 53-5.8 from Biolegend), were injected intravenously (i.v.). Three minutes later, the animals were sacrificed, lavaged to remove cells in the airway, bled, and perfused with 10 ml of cold phosphate buffered saline (PBS). The peripheral blood, spleen, LNs, lung, liver, kidney, brain, female reproductive tract, and small intestine were harvested within 12min, and lymphocytes were isolated as described (*138*, *155*, *254*). Spleen, lymph nodes and livers were homogenized through 70µm filter in RPMI 1640 containing 5% FBS. All tissue pieces were washed several times with 5% RPMI 1640 medium to remove excess of injected antibody prior to enzymatic digestion. Lung was removed, dissected into small pieces and the pieces were incubated with 1.3 mM EDTA in HBSS (30 min at 37°C, 400 rpm) followed by treatment with 100 U/ml Type I collagenase in 5% RPMI 1640 medium/2 mM $MgCl_2$/2 mM $CaCl_2$ (45 min/37°C, 400 rpm). For isolation of intraepithelial lymphocytes (IELs) from small and large intestine the organs were removed, fecal contents were removed, Peyer's Patches were excised (from small intestine only), the intestines were cut longitudinally and then into 1cm pieces. They were incubated in 10% 1xHBSS/Hepes Bicarbonate containing 15.4mg/100ml dithioerythritol (30 min at 37°C, 400 rpm) to extract IEL. After separating IELs,

the gut pieces were further treated with 100U/ml Type I Collagenase (Worthington) for lamina propria lymphocyte (LPL) isolation. Kidneys and female reproductive tract (containing uterine horns, cervix, and vaginal tissue) were removed and cut into small pieces followed by treatment with 100U/ml Type I (Worthington) and type IV (Sigma) Collagenase respectively in 5% RPMI 1640/2mM MgCl2/2mM CaCl2 (45 min at 37°C, 400rpm). The lymphocytes from liver, lung, gut, kidney and FRT were purified on a 44/67% Percoll gradient (800xg at 23°C for 20 min). Immunofluorescence staining was performed as described (*155*, *254*).

Intratracheal cell transfers

Splenocytes from memory P14 immune chimeras were collected >30d after LCMV infection. Donor cells were washed and resuspended in RPMI 1640. Naïve C57Bl/6 recipient mice were anesthetized with 0.4-0.75 mg/g 2-2-2-tribromoethanol (Avertin, Sigma Aldrich) in accordance with IACUC guidelines and 100 μl (5 x 10^6 cells) of the cell suspension were instilled into the lungs via a 1-ml syringe fitted with a 25-G needle (*238*).

CFSE Treatment

Purified splenocytes from P14 immune chimeric mice or naïve P14 transgenic mice were washed twice in PBS. Cells were resuspended in PBS at a concentration of 2 x 10^7 cells/ml. Equal volumes of cell suspension and 10 μM CFSE in PBS were combined, vortexed, and incubated for 10 minutes at room temperature (final CFSE concentration of 5μM). After 7 minutes, 1/10^{th} volume of

fetal bovine serum (FBS) was added. After 10 minutes, CFSE was diluted with RPMI 1640 containing 10% FBS and washed twice. Following incubation, cells were resuspended in RPMI for injection, and 3 - 5 x 10^6 cells were injected i.v. or i.t. into C57Bl/6 recipient mice.

Pertussis Toxin Treatment

Purified splenocytes from P14 immune chimeric mice were incubated in 25 ng/ml Pertussis Toxin (Sigma-Aldrich) in RPMI containing 10% FBS and 10 mM HEPES at a concentration of 30 x 10^6 cells/ml for 1h at 37°C as described (*119*, *254*). Following incubation, cells were washed to remove excess pertussis toxin and 5 x 10^6 cells were injected i.t. into C57Bl/6 recipient mice.

In vitro stimulation for proliferation induction

The medium used for cell cultures was RPMI 1640 supplemented with 10% FBS, 2mM L-glutamine, 100 U/ml penicillin, 100 mg/ml streptomycin, 0.25 mg/ml Amphotericin B, and 50 μM 2-mercaptoethanol (RP-10 media). Purified splenocytes from naïve congenic mice were incubated in RP-10 containing 0.1 μg/ml gp33-41 peptide in 15mL conical tube or flat-bottom 96 well plates for 30 minutes at 37°C (5% CO_2). Memory P14 T splenocytes were incubated in flat-bottom 96-well plates in RP-10 media co-cultured with media or peptide-treated congenic splenocytes for 16-96 hours at 37°C (5% CO_2).

In vitro re-stimulation and staining for intracellular cytokine production

The medium used for in vitro re-stimulation cell cultures was RPMI 1640 supplemented with 10% FBS, 2mM L-glutamine, 100 U/ml penicillin, 100 mg/ml

streptomycin, 1x non-essential amino acids (MEM NEAA 100x, Gibco, Life Technologies), 1 mM sodium pyruvate (Cellgro, Mediatech), 50 μM 2-mercaptoethanol, and 10 mM HEPES (Aliclone media). Donor P14 T cells recovered from airway or spleen were incubated in 15mL conical tube or flat-bottom 96-well plates in Aliclone media with or without 0.1μg/ml gp33-41 peptide for 4 hours at 37°C.

Parabiosis

Congenically marked KLF2^{GFP} P14 T cells were transferred into C57Bl/6 mice. One day later, the mice were infected with LCMV. 30-65 days later, mice underwent parabiotic surgery as per the schematic in Figure 4-6a, and as described (*126*). Briefly, mice were anesthetized with ketamine, flank hair removed using nair, and the skin cleaned using betadine. A lateral incision was made on each mouse from knee to elbow. Mice were joined using a continuous sub-cuticular suture on both the dorsal and ventral sides, with mattress and cruciate sutures joining the skin layer. Mattress sutures just under the armpit and knee were made to secure the parabiosed mice. 7-9 days after surgery, mice were bled via the retro-orbital route to ensure equilibrium between circulating cells. At 28 days after surgery, intravascular staining was performed and tissues were harvested from both mice. The number of non-vascular-associated P14 memory T cells was calculated in both “donor” and “parabiont” with respect to the original host for each cell type. A minimum threshold of 25 events was applied for calculation of P14 T cell KLF2^{GFP} and CD69 MFI.

Statistical analysis

Data were analyzed using Prism software 5 (GraphPad). For standard data sets, an unpaired two-tailed Student's t-test was used. The number of biological repeats is indicated in the figure legends. Asterisks indicate obtained P values: *, $p<0.05$; **, $p<0.01$; ***, $p<0.005$, ****, $p<0.001$

Chapter 5

Conclusions

Discussion

The work presented in this thesis validates a method of intravascular staining that distinguishes blood-borne from tissue-localized leukocytes and expands the utility of this technique to novel situations examining many leukocyte lineages and model systems of disease. One of the major recurrent observations within these studies is that perfusion of the heart and pulmonary vasculature with a saline buffer solution is insufficient to completely remove leukocytes from the vascular circulation. Even more surprising was the discovery that this method of flushing the vasculature actually removes tissue-localized cells, which may be of interest to investigators. Therefore, for thorough and accurate analysis of leukocyte contributions to disease processes in tissues, incorporation of intravascular staining in lieu of perfusion has notable advantages. Investigators can confidently exclude vascular cells from analysis of tissue-localized responses while comparing tissue- and blood-borne cells for a more complete and dynamic understanding of local biological processes.

The initial goal of this work was to examine the primary and anamnestic CD8 T cell responses to respiratory pathogens. However, our initial studies revealed an unexpected advantage of intravascular staining. Our data suggested that many outstanding conflicts within the literature regarding leukocyte differentiation state, migration pattern, and functional capacity within the lung could be explained by distinguishing between blood and tissue compartments. For instance, several studies have suggested that naïve lymphocytes enter the

lung tissue as a method of patrolling non-lymphoid tissues and maintaining peripheral tolerance (*107-109*, *111*). However, the studies with intravascular staining discussed in Chapter 3 suggest that naïve lymphocytes in the uninflamed lung are confined to the vasculature. Further, studies involving blockade of chemokine receptor signaling via pertussis toxin treatment suggest that migration to the lung parenchyma is distinct from the traditional paradigm of lymphocyte migration (*108-110*). The studies in Chapters 2 and 3 that incorporate intravascular staining refute these interpretations by confirming that blockade of chemokine receptor signaling results in obstructed tissue entry by lymphocytes. Thus, intravascular staining clarifies seemingly paradoxical findings with respect to lymphocyte differentiation and migration in the lung tissue.

In light of this new understanding of tissue compartments, previously published data can be revisited and considered in a new context. For example, monocytes have been shown to undergo differentiation into either macrophages or DCs upon entry of inflamed tissue (*247*). However, Jakubzick and colleagues recently proposed that monocytes circulate through non-lymphoid tissues, such as the lung, and return to lymph nodes in an undifferentiated state (*148*). Using various flow cytometric and transcriptome analyses, the investigators argue that monocytes isolated from the peripheral blood, lymph node and lung express comparable levels of the characteristic molecules of classical, undifferentiated monocytes. While the data are consistent with the investigators' hypothesis, an alternative explanation could also account for these results: monocytes in the lung vasculature that are refractory to perfusion have not been excluded from the

analysis. Incorporation of intravascular staining would allow for the exclusion of confounding blood-borne monocytes and warrant a more in depth analysis of true tissue-localized cells of the monocyte lineage. Thus, a new appreciation for leukocyte location within tissue compartments invites a re-visitation of previous work, especially of findings within vascular organs such as the lung, liver and kidneys. Moreover, the addition of a straightforward method for the identification of vascular leukocytes has the ability to enhance our understanding of dynamic processes within lymphoid and non-lymphoid tissues.

The data presented in Chapter 3 also indicate that intravascular staining has the potential to dramatically influence our understanding of immune responses to *Mycobacterium tuberculosis* (Mtb). The data demonstrate that T cells within the lung tissue of Mtb-infected mice have increased expression of the inhibitory ligand programmed death-1 (PD-1) over cells within the vascular circulation. While expression of this marker is indicative of recent antigen exposure and signaling through the T cell receptor (*308*), prolonged expression has also been correlated with a functionally impaired differentiation program in models of chronic infection (*309*). It may be that T cells primed during an Mtb infection enter the lung tissue and become less functional over the extended time frame required for containing the chronic infection. Perhaps while attempting to contribute to control of the pathogen, T cell function is dampened as a mechanism for controlling T cell-mediated pathology. Experiments examining IFN-γ secretion and perforin and granzyme expression within lymphocytes in the

lung tissue will add to our understanding of T cell mechanisms of immune control of Mtb infection.

Intravascular staining has also added to our understanding of myeloid immune responses to Mtb. The analysis of multiple subsets of myeloid cells in Chapter 3 suggests that inflammatory monocyte derived dendritic cells (moDCs) are the major myeloid cell type within the lung tissue during Mtb infection. While this subset of myeloid cells is known to produce the pro-inflammatory cytokines IL-1α, IL-1β, and TNF-α as well as inducible nitric oxide species (*177*), moDCs also produce the anti-inflammatory cytokine IL-10. Thus, additional studies are needed to fully elucidate the contribution of these cells to the response against Mtb.

Intravascular staining has also allowed for a much more thorough analysis of the phenomenon of resident memory within tissues. For some time, memory T cells were characterized as either central memory, which recirculate between blood, lymph, and secondary lymphoid organs, or effector memory, which were all thought to recirculate between blood, lymph, and non-lymphoid tissues. Recently, a non-recirculating subset of memory T cells that resides permanently in non-lymphoid tissues has been described in several organs, including the skin, intestine, kidney, brain, lung, and female reproductive tract (*251*). This subset is most often referred to as T resident memory (T_{RM}). T_{RM} cells have been shown to protect against viral infections in the skin (*122*, *228*) and lung (*124*), and precipitate local inflammatory cascades that recruit circulating T cells to sites of infection (*123*). Intravascular staining provides an added advantage to the study

of T_{RM}: circulating cells contained within the vasculature can be excluded from analysis, allowing for in depth analysis of true tissue lymphocytes.

A current controversy within the field of T_{RM} revolves around the way in which investigators identify non-recirculating cells. Studies using tissue grafts and parabiotic murine models identify T_{RM} by assessing the migratory capacity of memory T cells. However, these methods are complicated, laborious, and time consuming; thus, a major goal within the field has been to identify universal phenotypic markers of residency. Since intravascular staining in combination with parabiosis allows for the identification of true T_{RM}, this technique has the potential to greatly refine the phenotypic markers used in the field as surrogate indicators of residency.

It has been noted that T_{RM} cells often express the C-type lectin CD69 as well as the $\alpha_E\beta_7$ integrin heterodimer (which is most often identified by staining cells with antibodies specific for α_E, otherwise known as CD103) (*251*). CD69 may be associated with retention of T_{RM} because expression antagonizes expression of the cell surface molecule sphingosine-1 phosphate receptor 1 (S1PR1), a protein that promotes egress of lymphocytes into the circulation. $\alpha_E\beta_7$ may also contribute directly to the local maintenance of T_{RM} by anchoring T lymphocytes to epithelial cells through interactions with E-cadherin (*160*). However, many critical questions remain unanswered: What induces CD69 and CD103 expression among T cells in different tissue compartments? What is the longevity of resident tissue memory within different locations? How are T_{RM}

established within a particular location? And under what conditions do T_{RM} contribute to protection?

Data from the studies in this thesis and previously published work (*124*, *311*) demonstrates that T_{RM} within the lung do not universally express CD103. More often, T_{RM} within the lung express only CD69, which is a starkly different phenotype than T_{RM} isolated from the small intestine epithelium, skin epidermis and salivary gland (*119*, *121*, *122*, *155*). One possible explanation for the difference between tissues is in the regulation of CD103 itself. Many studies implicate a role for TGF-β in driving CD103 expression. TGF-β is constitutively expressed in the small intestinal mucosa, where CD103 is maintained on virtually all memory CD8 T cells within the epithelium. And interfering with either TGF-β signaling or CD103 expression results in a gradual loss of intestinal intraepithelial memory CD8 T cells (*155*, *158*, *159*). In contrast, CD103 is expressed by only a minority of CD8 T cells in the lung, and many of these cells are lost over time. Perhaps TGF-β is also the driver of CD103 expression in the respiratory tract, but available TGF-β is maximal only for transient periods after infection. Indeed, loss of CD103+ T_{RM} parallels the gradual loss of prolonged antigen-presentation and the loss of PD-1 expression (which may reflect recent T cell receptor engagement) that occurs within a few months after infection (*169*, *311*, *319*, *320*). This issue merits further investigation, and other factors may regulate T_{RM} maintenance within the respiratory mucosa.

Numerous studies have reported the waning of memory T cell numbers within the lung tissue over extended periods of time (*168*, *169*) (Figure 5-1). Thus

far, we have no definitive teleological explanation of why local memory in the lung wanes. Why would the host not be better served by maintaining protective immunity at this site indefinitely? Perhaps there is a cost to such a strategy. Indeed, unlike the gut or skin, the lung is a particularly inflammation intolerant organ given the delicate architecture necessary for efficient respiration. Once local infection has truly been cleared and the innate antiviral state wanes, exuberant re-activation of local memory T cells, however helpful for eliminating infected host cells, may also be harmful by promoting excessive inflammation and pathology. If that is the case, then it is imperative to understand the possible pathological consequences of retaining inducible bronchus associated lymphoid tissue (iBALT) and T_{RM} in the lung indefinitely. This will, in turn, allow us to identify strategies that strike a balance necessary for optimizing host fitness in the face of re-infection of the respiratory mucosa: maintaining critical contributors to protection without compromising host lung function.

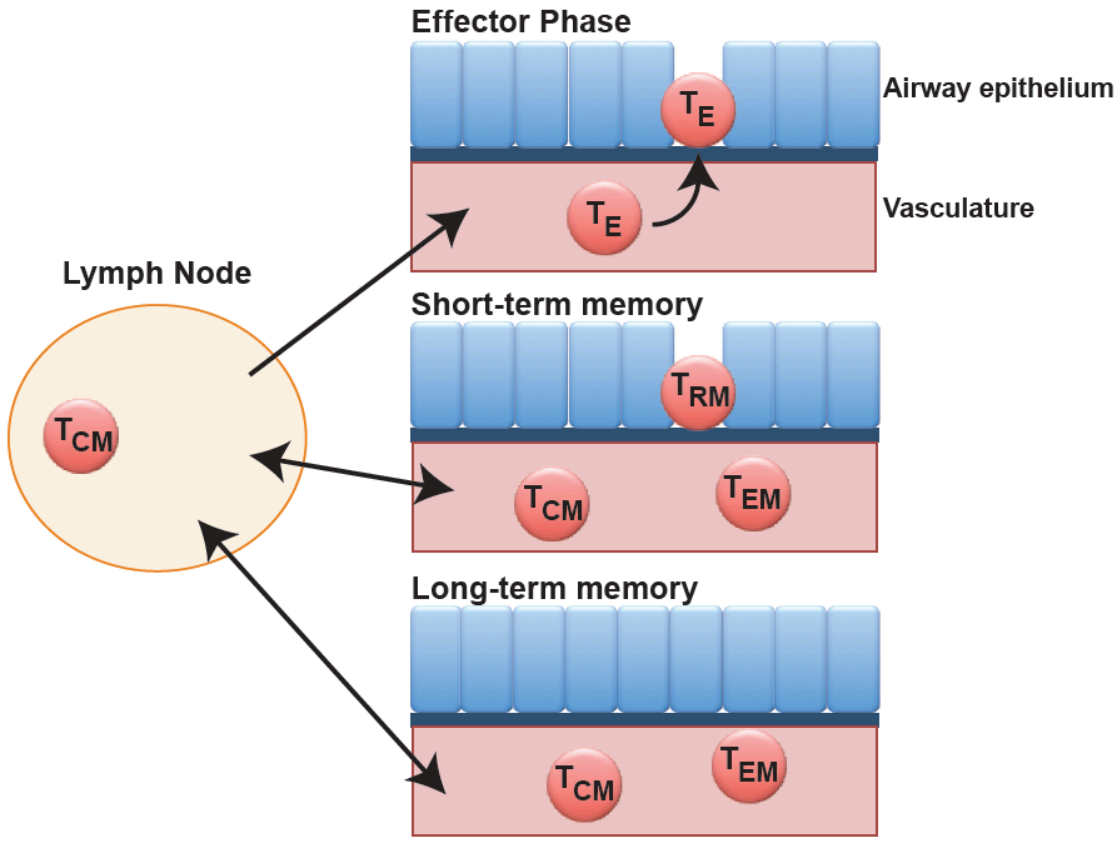

Figure 5-1: T_{RM} in the lung is short-lived. Top panel: Effector CD8 T cells enter the lung epithelium during the course of viral infection. Middle panel: Early after the infection is cleared, effector T cells in the lung epithelium differentiate into a specialized population of resident memory CD8 T cells (T_{RM}) that remain in the tissue without recirculating. The lung epithelium is not under routine surveillance by recirculating (T_{EM} and T_{CM}) memory CD8 T cell subsets. Bottom panel: Unlike longer lived memory CD8 T cell subsets, T_{RM} CD8 T cells gradually wane within the lung epithelium.

Since direct contact between antigen-specific T cells and the virally-infected epithelial cells is likely required for their function, the ratio of antigen-specific cytotoxic cells to target cells becomes an important consideration. How many antigen-specific T_{RM} are needed in the lung epithelium for considerable protection? Under physiological conditions that experience exposure to a wide

variety of pathogens (when a plethora of antigen-specificities are needed), how does the frequency of T_{RM} affect lung function? Questions regarding the threshold of T_{RM} cells required to optimally enhance local protection remain to be addressed (Figure 5-2).

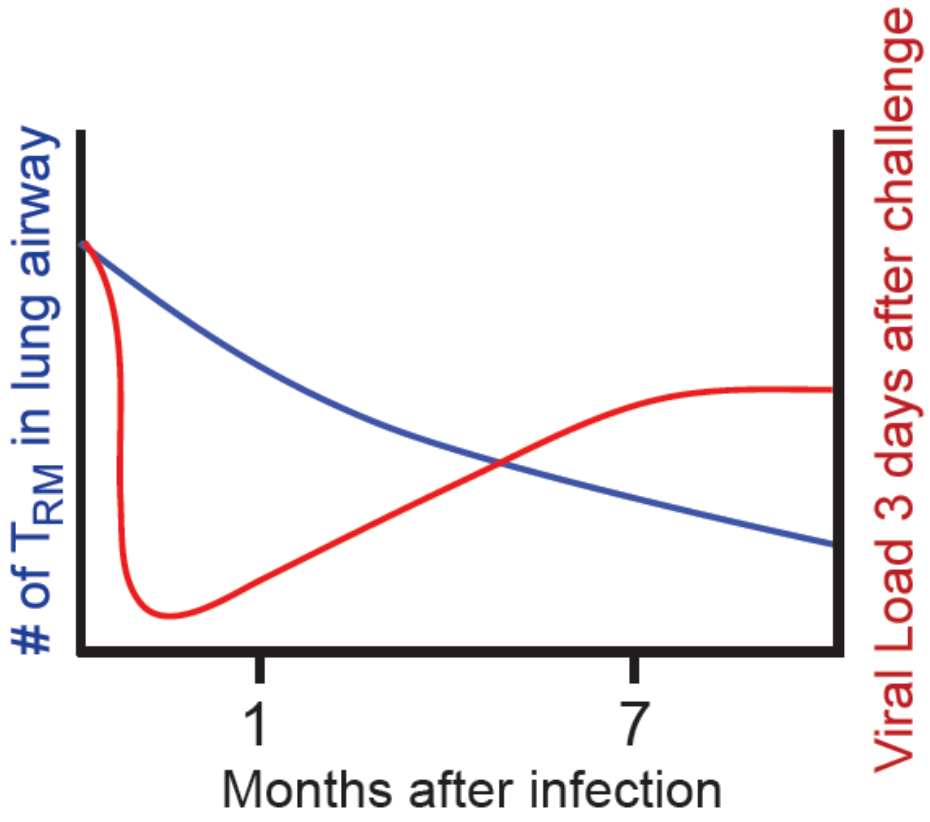

Figure 5-2: The loss of short-lived T_{RM} in the lung correlates with the erosion of heterosubtypic immunity against influenza virus. One month after primary infection, when T_{RM} in the lung epithelium are abundant, the host exhibits rapid control against a heterosubtypic influenza re-challenge. Seven months after priming, the number of T_{RM} in the lung airways is greatly reduced, which correlates with a pronounced reduction in heterosubtypic protection at this time point. This suggests that the maintenance of T_{RM} is critical for optimal interception of influenza virus at the primary site of secondary infection.

Perhaps one of the most interesting questions raised by recent work revolves around the mechanism by which T_{RM} in the lung tissue provide protection. It has been shown that memory CD4 T cells in the lung induce innate responses upon re-activation, which helps control influenza infection (*237*). Control of influenza A virus infections also depend on Fas and perforin-dependent cytotoxic processes (*321*), but T cells in the lung airways may have reduced cytolytic function (*170*, *322*). It has been speculated that this reduced cytotoxic functionality may be a mechanism for reducing excessive pathology in a vital, yet delicate, organ. Perhaps a compromise between maintaining local cell-mediated protection against pathogens and the need for preserving lung function may be related to the gradual waning of T_{RM} numbers in the lung.

Although antigen-specific T_{RM} in the lung play a critical role in protection in cross-reactive infections by direct cytotoxic activity and rapid recruitment of "reinforcements", T_{RM} may also play a significant role in protection by eliciting bystander activation. Memory T cells can adopt cytotoxic functionality in response to low-level TCR-stimulation as well as TCR-independent stimulation by alternative activating receptor ligation, inflammatory cytokines, and toll-like receptor (TLR) ligands (*162*, *323-328*). One intriguing possibility is that antigen recognition and cytokine secretion by T_{RM} could initiate local bystander activation of antigen-nonspecific cells. Bystander-activated cells, which have been shown to kill target cells through innate-like mechanisms, could temporarily control pathogen replication until additional antigen-specific cells are recruited to the tissue. Alternatively, TLR signaling within T_{RM} may also lead to antigen-

nonspecific T cell activation. Teleologically, bystander activation of T_{RM} may be one mechanism by which the immune system balances protection and homeostatic function within the delicate architecture of the lung: a minimal T_{RM} presence is maintained in the lung tissue to contain pathogens at the portal of entry while allowing for optimal gas exchange at alveolar surfaces. Further investigation is necessary to elucidate whether this is a possible additional role of T_{RM} in the lung.

Many exciting questions with respect to the establishment, regulation of longevity and the protective role of memory T cells in the lung remain to be addressed. Local T_{RM} cells promote rapid viral control at the point of viral exposure. Although the gradual disappearance of this protective population diminishes their potential for long-term protection against future infections, additional work may address whether the longevity of this memory population can be enhanced. Additionally, as T_{RM} are critical players in rapid pathogen clearance against local respiratory challenges, vaccines may be designed that optimize their generation. An improved understanding of the contribution of T_{RM} to protection during viral challenges has the potential to advance our application of this new knowledge to the fight against respiratory infections. As indicated by the work in Chapter 4, intravascular staining has the potential to greatly contribute to our understanding of resident immune cells within tissues.

In addition to a broader understanding of immune responses against infection, intravascular staining also reveals new insights about immune responses within solid tumors. The data in Chapter 3 demonstrate that a large

proportion of T cells are protected from intravascular staining, suggesting they are contained within the tumor. As in other systems of chronic antigen exposure, PD-1 expression is elevated on these T cells, further supporting the hypothesis that these cells are truly within the tumor. Interestingly, more than half of the CD8 T cells protected from intravascular staining express CD69. Without knowing the antigen specificity of these T cells, it is difficult to discern if this elevated expression is due to recent antigen exposure, similar to PD-1 expression, or if this is indicative of T_{RM} within the tumor.

It is important to note that intravascular staining is not without limitations. The studies presented in this thesis are restricted to murine models of disease. While the methodology may be adaptable for many small animal systems, the necessary modifications have not been examined or addressed in this work. Further, systems involving situations of vascular leakage, such as inflammatory states or angiogenic tumor models, may compromise the integrity of intravascular staining. Vascular permeability assays, such as histological analysis or Evans Blue Dye staining, must therefore be performed prior to the incorporation of intravascular staining as validating controls.

In conclusion, investigations of immune responses to viral and bacterial infections within most lymphoid and non-lymphoid tissues, as well as models of solid tumors, allergy and autoimmunity, and graft-versus-host-disease in small animal models may all benefit greatly from the application of intravascular staining. While the studies described here are limited to use of intravascular

staining in murine models of disease, this technique may be refined so as to be applicable in other setting and species.

Bibliography

1. World Health Organization, The top 10 causes of death, *The world health report*, 1–4 (2014).

2. M. C. Rose, J. A. Voynow, Respiratory tract mucin genes and mucin glycoproteins in health and disease, *Physiol. Rev.* **86**, 245–278 (2006).

3. J. M. Beck, V. B. Young, G. B. Huffnagle, The microbiome of the lung, *Translational Research* **160**, 258–266 (2012).

4. J. Rehwinkel *et al.*, RIG-I Detects Viral Genomic RNA during Negative-Strand RNA Virus Infection, *Cell* **140**, 397–408 (2010).

5. A. Baum, R. Sachidanandam, A. García-Sastre, Preference of RIG-I for short viral RNA molecules in infected cells revealed by next-generation sequencing, *Proc. Natl. Acad. Sci. U.S.A.* **107**, 16303–16308 (2010).

6. A. Nikonov *et al.*, B. Sherry, Ed. RIG-I and MDA-5 Detection of Viral RNA-dependent RNA Polymerase Activity Restricts Positive-Strand RNA Virus Replication, *PLoS Pathog* **9**, e1003610 (2013).

7. V. Hornung *et al.*, 5'-Triphosphate RNA Is the Ligand for RIG-I, *Science* **314**, 994–997 (2006).

8. A. U. Barlan, T. M. Griffin, K. A. Mcguire, C. M. Wiethoff, Adenovirus Membrane Penetration Activates the NLRP3 Inflammasome, *Journal of Virology* **85**, 146–155 (2010).

9. T. Fernandes-Alnemri, J.-W. Yu, P. Datta, J. Wu, E. S. Alnemri, AIM2 activates the inflammasome and cell death in response to cytoplasmic DNA, *Nature* **458**, 509–513 (2009).

10. D. A. Muruve *et al.*, The inflammasome recognizes cytosolic microbial and host DNA and triggers an innate immune response, *Nature* **452**, 103–107 (2008).

11. V. Hornung *et al.*, AIM2 recognizes cytosolic dsDNA and forms a caspase-1-activating inflammasome with ASC, *Nature* **458**, 514–518 (2009).

12. J. V. Rajan, D. Rodriguez, E. A. Miao, A. Aderem, The NLRP3 Inflammasome Detects Encephalomyocarditis Virus and Vesicular Stomatitis Virus Infection, *Journal of Virology* **85**, 4167–4172 (2011).

13. T. Bürckstümmer *et al.*, An orthogonal proteomic-genomic screen

identifies AIM2 as a cytoplasmic DNA sensor for the inflammasome, *Nature Publishing Group* **10**, 266–272 (2009).

14. A. Sabbah *et al.*, Activation of innate immune antiviral responses by Nod2, *Nature Publishing Group* **10**, 1073–1080 (2009).

15. F. S. Sutterwala, Y. Ogura, R. A. Flavell, The inflammasome in pathogen recognition and inflammation, *Journal of Leukocyte Biology* **82**, 259–264 (2007).

16. L. Alexopoulou, A. C. Holt, R. Medzhitov, R. A. Flavell, Recognition of double-stranded RNA and activation of NF-kappaB by Toll-like receptor 3, *Nature* **413**, 732–738 (2001).

17. S. S. Diebold, T. Kaisho, H. Hemmi, S. Akira, C. Reis e Sousa, Innate antiviral responses by means of TLR7-mediated recognition of single-stranded RNA, *Science* **303**, 1529–1531 (2004).

18. F. Heil *et al.*, Species-specific recognition of single-stranded RNA via toll-like receptor 7 and 8, *Science* **303**, 1526–1529 (2004).

19. T. Haas *et al.*, The DNA Sugar Backbone 2′ Deoxyribose Determines Toll-like Receptor 9 Activation, *Immunity* **28**, 315–323 (2008).

20. J. Lund, A. Sato, S. Akira, R. Medzhitov, A. Iwasaki, Toll-like Receptor 9-mediated Recognition of Herpes Simplex Virus-2 by Plasmacytoid Dendritic Cells, *Journal of Experimental Medicine* **198**, 513–520 (2003).

21. G. Trinchieri, Type I interferon: friend or foe? *Journal of Experimental Medicine* **207**, 2053–2063 (2010).

22. C. Asselin-Paturel *et al.*, Mouse type I IFN-producing cells are immature APCs with plasmacytoid morphology, *Nat Immunol* **2**, 1144–1150 (2001).

23. Y.-J. Liu, IPC: Professional Type 1 Interferon-Producing Cells and Plasmacytoid Dendritic Cell Precursors, *Annu. Rev. Immunol.* **23**, 275–306 (2005).

24. M. Colonna, G. Trinchieri, Y.-J. Liu, Plasmacytoid dendritic cells in immunity, *Nat Immunol* **5**, 1219–1226 (2004).

25. P. Lindahl, I. Gresser, P. Leary, M. Tovey, Interferon treatment of mice: enhanced expression of histocompatibility antigens on lymphoid cells, *Proc. Natl. Acad. Sci. U.S.A.* **73**, 1284–1287 (1976).

26. D. P. Simmons *et al.*, Type I IFN Drives a Distinctive Dendritic Cell Maturation Phenotype That Allows Continued Class II MHC Synthesis

and Antigen Processing, *The Journal of Immunology* **188**, 3116–3126 (2012).

27. M. Montoya *et al.*, Type I interferons produced by dendritic cells promote their phenotypic and functional activation, *Blood* **99**, 3263–3271 (2002).

28. M. Gidlund, A. Orn, H. Wigzell, A. Senik, I. Gresser, Enhanced NK cell activity in mice injected with interferon and interferon inducers, *Nature* **273**, 759–761 (1978).

29. E. Padovan, G. C. Spagnoli, M. Ferrantini, M. Heberer, IFN-alpha2a induces IP-10/CXCL10 and MIG/CXCL9 production in monocyte-derived dendritic cells and enhances their capacity to attract and stimulate CD8+ effector T cells, *Journal of Leukocyte Biology* **71**, 669–676 (2002).

30. M. Nakano *et al.*, Type I interferon induces CX3CL1 (fractalkine) and CCL5 (RANTES) production in human pulmonary vascular endothelial cells, *Clinical & Experimental Immunology* **170**, 94–100 (2012).

31. T. Jia, I. Leiner, G. Dorothee, K. Brandl, E. G. Pamer, MyD88 and Type I Interferon Receptor-Mediated Chemokine Induction and Monocyte Recruitment during Listeria monocytogenes Infection, *The Journal of Immunology* **183**, 1271–1278 (2009).

32. B. Moser, P. Loetscher, Lymphocyte traffic control by chemokines, *Nat Immunol* **2**, 123–128 (2001).

33. M. K. Jenkins *et al.*, In vivo activation of antigen-specific CD4 T cells, *Annu. Rev. Immunol.* **19**, 23–45 (2001).

34. R. H. Schwartz, T-lymphocyte recognition of antigen in association with gene products of the major histocompatibility complex, *Annu. Rev. Immunol.* **3**, 237–261 (1985).

35. M. A. Williams, M. J. Bevan, Effector and Memory CTL Differentiation, *Annu. Rev. Immunol.* **25**, 171–192 (2007).

36. O. Acuto, F. Michel, CD28-mediated co-stimulation: a quantitative support for TCR signalling, *Nature Publishing Group* **3**, 939–951 (2003).

37. R. J. Greenwald, G. J. Freeman, A. H. Sharpe, THE B7 FAMILY REVISITED, *Annu. Rev. Immunol.* **23**, 515–548 (2005).

38. S. J. Szabo, B. M. Sullivan, S. L. Peng, L. H. Glimcher, Molecular mechanisms regulating TH1 immune responses, *Annu. Rev. Immunol.* **21**, 713–758 (2003).

39. J. N. Blattman *et al.*, Estimating the precursor frequency of naive antigen-specific CD8 T cells, *J. Exp. Med.* **195**, 657–664 (2002).

40. J. J. Moon *et al.*, Naive CD4+ T Cell Frequency Varies for Different Epitopes and Predicts Repertoire Diversity and Response Magnitude, *Immunity* **27**, 203–213 (2007).

41. E. A. Butz, M. J. Bevan, Massive expansion of antigen-specific CD8+ T cells during an acute virus infection, *Immunity* **8**, 167–175 (1998).

42. K. Murali-Krishna *et al.*, Counting antigen-specific CD8 T cells: a reevaluation of bystander activation during viral infection, *Immunity* **8**, 177–187 (1998).

43. J. J. Obar, K. M. Khanna, L. Lefrançois, Endogenous Naive CD8+ T Cell Precursor Frequency Regulates Primary and Memory Responses to Infection, *Immunity* **28**, 859–869 (2008).

44. S. M. Kaech, E. J. Wherry, R. Ahmed, Effector and memory T-cell differentiation: implications for vaccine development, *Nat Rev Immunol* **2**, 251–262 (2002).

45. J. T. Harty, V. P. Badovinac, Shaping and reshaping CD8+ T-cell memory, *Nat Rev Immunol* **8**, 107–119 (2008).

46. R. H. Schwartz, T Cell Anergy, *Annu. Rev. Immunol.* **21**, 305–334 (2003).

47. E. Teixeiro *et al.*, Different T cell receptor signals determine CD8+ memory versus effector development, *Science* **323**, 502–505 (2009).

48. M. A. Williams, E. V. Ravkov, M. J. Bevan, Rapid Culling of the CD4+ T Cell Repertoire in the Transition from Effector to Memory, *Immunity* **28**, 533–545 (2008).

49. J. J. O'Shea, W. E. Paul, Mechanisms Underlying Lineage Commitment and Plasticity of Helper CD4+ T Cells, *Science* **327**, 1098–1102 (2010).

50. C.-S. Hsieh *et al.*, Development of TH1 CD4+ T cells through IL-12 produced by Listeria-induced macrophages, *Science* **260**, 547–549 (1993).

51. M. Moser, K. M. Murphy, Dendritic cell regulation of TH1-TH2 development, *Nat Immunol* **1**, 199–205 (2000).

52. F. Sallusto *et al.*, Switch in chemokine receptor expression upon TCR stimulation reveals novel homing potential for recently activated T cells, *Eur. J. Immunol.* **29**, 2037–2045 (1999).

53. D. C. Parker, T cell-dependent B cell activation, *Annu. Rev. Immunol.* **11**, 331–360 (1993).

54. L. J. McHeyzer-Williams, M. G. McHeyzer-Williams, Antigen-specific memory B cell development, *Annu. Rev. Immunol.* **23**, 487–513 (2005).

55. A. I. Jaiswal, M. Croft, CD40 ligand induction on T cell subsets by peptide-presenting B cells: implications for development of the primary T and B cell response, *J. Immunol.* **159**, 2282–2291 (1997).

56. S. K. Yoshinaga *et al.*, T-cell co-stimulation through B7RP-1 and ICOS, *Nature* **402**, 827–832 (1999).

57. A. Hutloff *et al.*, ICOS is an inducible T-cell co-stimulator structurally and functionally related to CD28, *Nature* **397**, 263–266 (1999).

58. F. Mackay, J. L. Browning, BAFF: A fundamental survival factor for B cells, *Nat Rev Immunol* **2**, 465–475 (2002).

59. T. Okada, J. G. Cyster, B cell migration and interactions in the early phase of antibody responses, *Current Opinion in Immunology* **18**, 278–285 (2006).

60. T. G. Phan, E. E. Gray, J. G. Cyster, The microanatomy of B cell activation, *Current Opinion in Immunology* **21**, 258–265 (2009).

61. K. A. Pape *et al.*, Visualization of the Genesis and Fate of Isotype-switched B Cells during a Primary Immune Response, *Journal of Experimental Medicine* **197**, 1677–1687 (2003).

62. J. Jacob, G. Kelsoe, K. Rajewsky, U. Weiss, Intraclonal generation of antibody mutants in germinal centres, (1991).

63. V. H. Odegard, D. G. Schatz, Targeting of somatic hypermutation, *Nature Publishing Group* **6**, 573–583 (2006).

64. J. Stavnezer, Immunoglobulin class switching, *Current Opinion in Immunology* **8**, 199–205 (1996).

65. A. Radbruch *et al.*, Competence and competition: the challenge of becoming a long-lived plasma cell, *Nature Publishing Group* **6**, 741–750 (2006).

66. F. Nimmerjahn, J. V. Ravetch, Divergent immunoglobulin g subclass activity through selective Fc receptor binding, *Science* **310**, 1510–1512 (2005).

67. H. P. Roost *et al.*, Early high-affinity neutralizing anti-viral IgG responses without further overall improvements of affinity, *Proc. Natl. Acad. Sci. U.S.A.* **92**, 1257–1261 (1995).

68. M. F. Bachmann *et al.*, The role of antibody concentration and avidity in antiviral protection, *Science* **276**, 2024–2027 (1997).

69. P. Brandtzaeg, Role of secretory antibodies in the defence against infections, *Int. J. Med. Microbiol.* **293**, 3–15 (2003).

70. J. H. Russell, T. J. Ley, L YMPHOCYTE-M EDIATEDC YTOTOXICITY, *Annu. Rev. Immunol.* **20**, 323–370 (2002).

71. D. R. Green, N. Droin, M. Pinkoski, Activation-induced cell death in T cells, *Immunol. Rev.* **193**, 70–81 (2003).

72. R. D. Stout, J. Suttles, J. Xu, I. S. Grewal, R. A. Flavell, Impaired T cell-mediated macrophage activation in CD40 ligand-deficient mice, *J. Immunol.* **156**, 8–11 (1996).

73. M. H. Kaplan, J. R. Whitfield, D. L. Boros, M. J. Grusby, Th2 cells are required for the Schistosoma mansoni egg-induced granulomatous response, *J. Immunol.* **160**, 1850–1856 (1998).

74. M. C. Siracusa, M. R. Comeau, D. Artis, New insights into basophil biology: initiators, regulators, and effectors of type 2 inflammation, *Annals of the New York Academy of Sciences* **1217**, 166–177 (2011).

75. H. Park *et al.*, A distinct lineage of CD4 T cells regulates tissue inflammation by producing interleukin 17, *Nat Immunol* **6**, 1133–1141 (2005).

76. R. L. Reinhardt, H.-E. Liang, R. M. Locksley, Cytokine-secreting follicular T cells shape the antibody repertoire, *Nat Immunol* **10**, 385–393 (2009).

77. J. B. McLachlan, D. M. Catron, J. J. Moon, M. K. Jenkins, Dendritic Cell Antigen PresentationDrives Simultaneous Cytokine Productionby Effector and Regulatory T Cells in Inflamed Skin, *Immunity* **30**, 277–288 (2009).

78. Y. Zheng *et al.*, Regulatory T-cell suppressor program co-opts transcription factor IRF4 to control T, *Nature* **458**, 351–356 (2009).

79. A. Chaudhry *et al.*, CD4+ Regulatory T Cells Control TH17 Responses in a Stat3-Dependent Manner, *Science* **326**, 986–991 (2009).

80. Y. Belkaid, B. T. Rouse, Natural regulatory T cells in infectious disease, *Nat Immunol* **6**, 353–360 (2005).

81. C. Sun, C. Migliorini, L. L. Munn, Red blood cells initiate leukocyte rolling in postcapillary expansions: a lattice Boltzmann analysis, *Biophys. J.* **85**, 208–222 (2003).

82. G. W. Schmid-Schönbein, R. Skalak, S. Usami, S. Chien, Cell distribution in capillary networks, *Microvasc. Res.* **19**, 18–44 (1980).

83. M. B. Lawrence, T. A. Springer, Leukocytes roll on a selectin at physiologic flow rates: distinction from and prerequisite for adhesion through integrins, *Cell* **65**, 859–873 (1991).

84. C. Potsch, D. Vöhringer, H. Pircher, Distinct migration patterns of naive and effector CD8 T cells in the spleen: correlation with CCR7 receptor expression and chemokine reactivity, *Eur. J. Immunol.* **29**, 3562–3570 (1999).

85. R. Yoshida *et al.*, EBI1-ligand chemokine (ELC) attracts a broad spectrum of lymphocytes: activated T cells strongly up-regulate CCR7 and efficiently migrate toward ELC, *International Immunology* **10**, 901–910 (1998).

86. J. J. Campbell *et al.*, 6-C-kine (SLC), a lymphocyte adhesion-triggering chemokine expressed by high endothelium, is an agonist for the MIP-3β receptor CCR7, *The Journal of Cell Biology* **141**, 1053–1059 (1998).

87. R. F. Bargatze, M. A. Jutila, E. C. Butcher, Distinct roles of L-selectin and integrins alpha 4 beta 7 and LFA-1 in lymphocyte homing to Peyer's patch-HEV in situ: the multistep model confirmed and refined, *Immunity* **3**, 99–108 (1995).

88. C. H. GeurtsvanKessel *et al.*, Dendritic cells are crucial for maintenance of tertiary lymphoid structures in the lung of influenza virus-infected mice, *Journal of Experimental Medicine* **206**, 2339–2349 (2009).

89. J. E. Kohlmeier *et al.*, The Chemokine Receptor CCR5 Plays a Key Role in the Early Memory CD8+ T Cell Response to Respiratory Virus Infections, *Immunity* **29**, 101–113 (2008).

90. L. N. Lee *et al.*, CXCR6 Is a Marker for Protective Antigen-Specific Cells in the Lungs after Intranasal Immunization against Mycobacterium tuberculosis, *Infection and Immunity* **79**, 3328–3337 (2011).

91. K. Ley, G. S. Kansas, Selectins in T-cell recruitment to non-lymphoid tissues and sites of inflammation, *Nature Publishing Group* **4**, 325–336 (2004).

92. C. Agostini *et al.*, Role for CXCR6 and Its Ligand CXCL16 in the

Pathogenesis of T-Cell Alveolitis in Sarcoidosis, *American Journal of Respiratory and Critical Care Medicine* **172**, 1290–1298 (2005).

93. A. J. Morgan *et al.*, CXCR6 identifies a putative population of retained human lung T cells characterised by co-expression of activation markers, *Immunobiology* **213**, 599–608 (2008).

94. J. E. Kohlmeier *et al.*, CXCR3 Directs Antigen-Specific Effector CD4+ T Cell Migration to the Lung During Parainfluenza Virus Infection, *The Journal of Immunology* **183**, 4378–4384 (2009).

95. T. A. Springer, Traffic signals for lymphocyte recirculation and leukocyte emigration: the multistep paradigm, *Cell* **76**, 301–314 (1994).

96. E. J. Kunkel *et al.*, Expression of the Chemokine Receptors CCR4, CCR5, and CXCR3 by Human Tissue-Infiltrating Lymphocytes, *AJPA* **160**, 347–355 (2010).

97. L. M. Bradley, S. R. Watson, S. L. Swain, Entry of naive CD4 T cells into peripheral lymph nodes requires L-selectin, *J. Exp. Med.* **180**, 2401–2406 (1994).

98. S. J. Ray *et al.*, The collagen binding alpha1beta1 integrin VLA-1 regulates CD8 T cell-mediated immune protection against heterologous influenza infection, *Immunity* **20**, 167–179 (2004).

99. T. J. Chapman, D. J. Topham, Identification of a Unique Population of Tissue-Memory CD4+ T Cells in the Airways after Influenza Infection That Is Dependent on the Integrin VLA-1, *The Journal of Immunology* **184**, 3841–3849 (2010).

100. J. Thatte, V. Dabak, M. B. Williams, T. J. Braciale, K. Ley, LFA-1 is required for retention of effector CD8 T cells in mouse lungs, *Blood* **101**, 4916–4922 (2003).

101. J. C. Hogg *et al.*, Erythrocyte and polymorphonuclear cell transit time and concentration in human pulmonary capillaries, *J. Appl. Physiol.* **77**, 1795–1800 (1994).

102. M. Plantinga, H. Hammad, B. N. Lambrecht, Origin and functional specializations of DC subsets in the lung, *Eur. J. Immunol.* **40**, 2112–2118 (2010).

103. G. W. Schmid-Schönbein, Y. Y. Shih, S. Chien, Morphometry of human leukocytes, *Blood* **56**, 866–875 (1980).

104. M.-L. del Rio, J.-I. Rodriguez-Barbosa, E. Kremmer, R. Förster, CD103-

and CD103+ bronchial lymph node dendritic cells are specialized in presenting and cross-presenting innocuous antigen to CD4+ and CD8+ T cells, *Multiple values selected* **178**, 6861–6866 (2007).

105. M. P. Ainslie, C. A. McNulty, T. Huynh, F. A. Symon, A. J. Wardlaw, Characterisation of adhesion receptors mediating lymphocyte adhesion to bronchial endothelium provides evidence for a distinct lung homing pathway, *Thorax* **57**, 1054–1059 (2002).

106. F. M. Wolber *et al.*, Endothelial selectins and alpha4 integrins regulate independent pathways of T lymphocyte recruitment in the pulmonary immune response, *J. Immunol.* **161**, 4396–4403 (1998).

107. J. R. Harp, T. M. Onami, Naïve T cells re-distribute to the lungs of selectin ligand deficient mice, *PLoS ONE* **5**, e10973 (2010).

108. S. Cose, C. Brammer, K. M. Khanna, D. Masopust, L. Lefrançois, Evidence that a significant number of naive T cells enter non-lymphoid organs as part of a normal migratory pathway, *Eur. J. Immunol.* **36**, 1423–1433 (2006).

109. C. F. Inman, T. Z. Murray, M. Bailey, S. Cose, Most B cells in non-lymphoid tissues are naïve, *Immunol Cell Biol* **90**, 235–242 (2012).

110. K. D. Klonowski *et al.*, Dynamics of blood-borne CD8 memory T cell migration in vivo, *Immunity* **20**, 551–562 (2004).

111. S. M. Caucheteux, P. Torabi-Parizi, W. E. Paul, Analysis of naive lung CD4 T cells provides evidence of functional lung to lymph node migration, *Proc. Natl. Acad. Sci. U.S.A.* **110**, 1821–1826 (2013).

112. J. Hataye, J. J. Moon, A. Khoruts, C. Reilly, M. K. Jenkins, Naive and memory CD4+ T cell survival controlled by clonal abundance, *Science* **312**, 114–116 (2006).

113. E. J. Wherry *et al.*, Lineage relationship and protective immunity of memory CD8 T cell subsets, *Nat Immunol* **4**, 225–234 (2003).

114. S. C. Jameson, D. Masopust, Diversity in T Cell Memory: An Embarrassment of Riches, *Immunity* **31**, 859–871 (2009).

115. F. L. Black, L. Rosen, Patterns of measles antibodies in residents of Tahiti and their stability in the absence of re-exposure, *J. Immunol.* **88**, 725–731 (1962).

116. E. Hammarlund *et al.*, Duration of antiviral immunity after smallpox vaccination, *Nature Medicine* **9**, 1131–1137 (2003).

117. K. Murali-Krishna *et al.*, Persistence of memory CD8 T cells in MHC class I-deficient mice, *Science* **286**, 1377–1381 (1999).

118. F. Sallusto, D. Lenig, R. Förster, M. Lipp, A. Lanzavecchia, Two subsets of memory T lymphocytes with distinct homing potentials and effector functions, *Nature* **401**, 708–712 (1999).

119. D. Masopust *et al.*, Dynamic T cell migration program provides resident memory within intestinal epithelium, *Journal of Experimental Medicine* **207**, 553–564 (2010).

120. L. M. Wakim, A. Woodward-Davis, M. J. Bevan, Memory T cells persisting within the brain after local infection show functional adaptations to their tissue of residence, *Proc. Natl. Acad. Sci. U.S.A.* **107**, 17872–17879 (2010).

121. M. Hofmann, H. Pircher, E-cadherin promotes accumulation of a unique memory CD8 T-cell population in murine salivary glands, *Proc. Natl. Acad. Sci. U.S.A.* **108**, 16741–16746 (2011).

122. T. Gebhardt *et al.*, Memory T cells in nonlymphoid tissue that provide enhanced local immunity during infection with herpes simplex virus, *Nat Immunol* **10**, 524–530 (2009).

123. J. M. Schenkel, K. A. Fraser, V. Vezys, D. Masopust, Sensing and alarm function of resident memory CD8+ T cells, *Nat Immunol* **14**, 509–513 (2013).

124. J. R. Teijaro *et al.*, Cutting Edge: Tissue-Retentive Lung Memory CD4 T Cells Mediate Optimal Protection to Respiratory Virus Infection, *The Journal of Immunology* **187**, 5510–5514 (2011).

125. L. K. Mackay *et al.*, Long-lived epithelial immunity by tissue-resident memory T (TRM) cells in the absence of persisting local antigen presentation, *Proc. Natl. Acad. Sci. U.S.A.* **109**, 7037–7042 (2012).

126. C. N. Skon *et al.*, Transcriptional downregulation of S1pr1 is required for the establishment of resident memory CD8, *Nat Immunol* **14**, 1285–1293 (2013).

127. F. Sallusto, J. Geginat, A. Lanzavecchia, Central memory and effector memory T cell subsets: function, generation, and maintenance, *Annu. Rev. Immunol.* **22**, 745–763 (2004).

128. A. Scholer, S. Hugues, A. Boissonnas, L. Fetler, S. Amigorena, Intercellular Adhesion Molecule-1-Dependent Stable Interactions between T Cells and Dendritic Cells Determine CD8+ T Cell Memory, *Immunity* **28**,

258–270 (2008).

129. A. V. Gett, F. Sallusto, A. Lanzavecchia, J. Geginat, T cell fitness determined by signal strength, *Nat Immunol* **4**, 355–360 (2003).

130. M. J. B. van Stipdonk *et al.*, Dynamic programming of CD8+ T lymphocyte responses, *Nat Immunol* **4**, 361–365 (2003).

131. M. A. Williams, M. J. Bevan, Shortening the infectious period does not alter expansion of CD8 T cells but diminishes their capacity to differentiate into memory cells, *J. Immunol.* **173**, 6694–6702 (2004).

132. D. A. Blair, L. Lefrançois, Increased competition for antigen during priming negatively impacts the generation of memory CD4 T cells, *Proc. Natl. Acad. Sci. U.S.A.* **104**, 15045–15050 (2007).

133. S. M. Kaech, E. J. Wherry, Heterogeneity and Cell-Fate Decisions in Effector and Memory CD8+ T Cell Differentiation during Viral Infection, *Immunity* **27**, 393–405 (2007).

134. W. W. Agace, Tissue-tropic effector T cells: generation and targeting opportunities, *Nat Rev Immunol* **6**, 682–692 (2006).

135. J. R. Mora, M. Iwata, U. H. von Andrian, Vitamin effects on the immune system: vitamins A and D take centre stage, *Nat Rev Immunol* **8**, 685–698 (2008).

136. H. Sigmundsdottir, E. C. Butcher, Environmental cues, dendritic cells and the programming of tissue-selective lymphocyte trafficking, *Nat Immunol* **9**, 981–987 (2008).

137. G. Kassiotis, B. Stockinger, Anatomical heterogeneity of memory CD4+ T cells due to reversible adaptation to the microenvironment, *J. Immunol.* **173**, 7292–7298 (2004).

138. D. Masopust, V. Vezys, E. J. Wherry, D. L. Barber, R. Ahmed, Cutting edge: gut microenvironment promotes differentiation of a unique memory CD8 T cell population, *J. Immunol.* **176**, 2079–2083 (2006).

139. R. G. van der Most, K. Murali-Krishna, R. Ahmed, Prolonged presence of effector-memory CD8 T cells in the central nervous system after dengue virus encephalitis, *International Immunology* **15**, 119–125 (2003).

140. J. E. Kohlmeier, S. C. Miller, D. L. Woodland, Cutting edge: Antigen is not required for the activation and maintenance of virus-specific memory CD8+ T cells in the lung airways, *J. Immunol.* **178**, 4721–4725 (2007).

141. A. L. Marzo, H. Yagita, L. Lefrançois, Cutting edge: migration to nonlymphoid tissues results in functional conversion of central to effector memory CD8 T cells, *J. Immunol.* **179**, 36–40 (2007).

142. N. S. Joshi *et al.*, Inflammation Directs Memory Precursor and Short-Lived Effector CD8+ T Cell Fates via the Graded Expression of T-bet Transcription Factor, *Immunity* **27**, 281–295 (2007).

143. S. Yona, S. Jung, Monocytes: subsets, origins, fates and functions, *Curr. Opin. Hematol.* **17**, 53–59 (2010).

144. E. L. Pearce, H. Shen, Generation of CD8 T cell memory is regulated by IL-12, *J. Immunol.* **179**, 2074–2081 (2007).

145. A. Kallies, A. Xin, G. T. Belz, S. L. Nutt, Blimp-1 Transcription Factor Is Requiredfor the Differentiationof Effector CD8, *Immunity* **31**, 283–295 (2009).

146. R. L. Rutishauser *et al.*, Transcriptional Repressor Blimp-1 Promotes CD8+ T Cell Terminal Differentiation and Represses the Acquisition of Central Memory T Cell Properties, *Immunity* **31**, 296–308 (2009).

147. K. Araki *et al.*, mTOR regulates memory CD8 T-cell differentiation, *Nature* **460**, 108–112 (2009).

148. C. Jakubzick *et al.*, Minimal Differentiation of Classical Monocytes as They Survey Steady-State Tissuesand Transport Antigen to Lymph Nodes, *Immunity* **39**, 599–610 (2013).

149. E. L. Pearce *et al.*, Enhancing CD8 T-cell memory by modulating fatty acid metabolism, *Nature* **460**, 103–107 (2009).

150. M. A. Suni *et al.*, CD4(+)CD8(dim) T lymphocytes exhibit enhanced cytokine expression, proliferation and cytotoxic activity in response to HCMV and HIV-1 antigens, *Eur. J. Immunol.* **31**, 2512–2520 (2001).

151. A. Harari, F. B. Enders, C. Cellerai, P. A. Bart, G. Pantaleo, Distinct Profiles of Cytotoxic Granules in Memory CD8 T Cells Correlate with Function, Differentiation Stage, and Antigen Exposure, *Journal of Virology* **83**, 2862–2871 (2009).

152. M. A. Williams, A. J. Tyznik, M. J. Bevan, Interleukin-2 signals during priming are required for secondary expansion of CD8+ memory T cells, *Nature* **441**, 890–893 (2006).

153. S. K. Kim, K. S. Schluns, L. Lefrancois, Induction and visualization of mucosal memory CD8 T cells following systemic virus infection, *J.*

Immunol. **163**, 4125–4132 (1999).

154. D. Masopust *et al.*, Activated primary and memory CD8 T cells migrate to nonlymphoid tissues regardless of site of activation or tissue of origin, *J. Immunol.* **172**, 4875–4882 (2004).

155. K. A. Casey *et al.*, Antigen-Independent Differentiation and Maintenance of Effector-like Resident Memory T Cells in Tissues, *The Journal of Immunology* **188**, 4866–4875 (2012).

156. J. M. Schenkel, K. A. Fraser, D. Masopust, Cutting Edge: Resident Memory CD8 T Cells Occupy Frontline Niches in Secondary Lymphoid Organs, *The Journal of Immunology* (2014), doi:10.4049/jimmunol.1400003.

157. D. Masopust, L. J. Picker, Hidden Memories: Frontline Memory T Cells and Early Pathogen Interception, *The Journal of Immunology* **188**, 5811–5817 (2012).

158. M. P. Schön *et al.*, Mucosal T lymphocyte numbers are selectively reduced in integrin alpha E (CD103)-deficient mice, *J. Immunol.* **162**, 6641–6649 (1999).

159. S. Y. Koyama, D. K. Podolsky, Differential expression of transforming growth factors alpha and beta in rat intestinal epithelial cells, *Journal of Clinical Investigation* **83**, 1768–1773 (1989).

160. K. L. Cepek *et al.*, Adhesion between epithelial cells and T lymphocytes mediated by E-cadherin and the alpha E beta 7 integrin, *Nature* **372**, 190–193 (1994).

161. L. K. Mackay *et al.*, The developmental pathway for CD103, *Nat Immunol* **14**, 1294–1301 (2013).

162. T. Chu *et al.*, Bystander-Activated Memory CD8 T Cells Control Early Pathogen Loadin an Innate-like, NKG2D-Dependent Manner, *CellReports* **3**, 701–708 (2013).

163. D. L. Barber, E. J. Wherry, R. Ahmed, Cutting edge: rapid in vivo killing by memory CD8 T cells, *J. Immunol.* **171**, 27–31 (2003).

164. J. A. Olson, C. McDonald-Hyman, S. C. Jameson, S. E. Hamilton, Effector-like CD8+ T Cells in the Memory Population Mediate Potent Protective Immunity, *Immunity* **38**, 1250–1260 (2013).

165. R. E. Berg, E. Crossley, S. Murray, J. Forman, Memory CD8+ T Cells Provide Innate Immune Protection against Listeria monocytogenes in the

Absence of Cognate Antigen, *Journal of Experimental Medicine* **198**, 1583–1593 (2003).

166. T. Kambayashi, E. Assarsson, A. E. Lukacher, H.-G. Ljunggren, P. E. Jensen, Memory CD8+ T cells provide an early source of IFN-gamma, *J. Immunol.* **170**, 2399–2408 (2003).

167. S. Bauer *et al.*, Activation of NK cells and T cells by NKG2D, a receptor for stress-inducible MICA, *Science* **285**, 727–729 (1999).

168. S. Liang, K. Mozdzanowska, G. Palladino, W. Gerhard, Heterosubtypic immunity to influenza type A virus in mice. Effector mechanisms and their longevity, *J. Immunol.* **152**, 1653–1661 (1994).

169. T. Wu *et al.*, Lung-resident memory CD8 T cells (TRM) are indispensable for optimal cross-protection against pulmonary virus infection, *Journal of Leukocyte Biology* **95**, 215–224 (2014).

170. J. E. Kohlmeier, T. Cookenham, A. D. Roberts, S. C. Miller, D. L. Woodland, Type I Interferons regulate cytolytic activity of memory CD8+ T cells in the lung airways during respiratory virus challenge, *Immunity* **33**, 96–105 (2010).

171. T. Mogues, M. E. Goodrich, L. Ryan, R. LaCourse, R. J. North, The relative importance of T cell subsets in immunity and immunopathology of airborne Mycobacterium tuberculosis infection in mice, *J. Exp. Med.* **193**, 271–280 (2001).

172. A. A. Chackerian, T. V. Perera, S. M. Behar, Gamma Interferon-Producing CD4+ T Lymphocytes in the Lung Correlate with Resistance to Infection with Mycobacterium tuberculosis, *Infection and Immunity* **69**, 2666–2674 (2001).

173. H. Shams, B. Wizel, S. E. Weis, B. Samten, P. F. Barnes, Contribution of CD8+ T Cells to Gamma Interferon Production in Human Tuberculosis, *Infection and Immunity* **69**, 3497–3501 (2001).

174. A. M. Gallegos *et al.*, L. Ramakrishnan, Ed. A Gamma Interferon Independent Mechanism of CD4 T Cell Mediated Control of M. tuberculosis Infection in vivo, *PLoS Pathog* **7**, e1002052 (2011).

175. N. Markowitz *et al.*, Incidence of tuberculosis in the United States among HIV-infected persons. The Pulmonary Complications of HIV Infection Study Group, *Ann. Intern. Med.* **126**, 123–132 (1997).

176. R. J. North, Y.-J. Jung, Immunity to Tuberculosis, *Annu. Rev. Immunol.* **22**, 599–623 (2004).

177. K. D. Mayer-Barber *et al.*, Innate and Adaptive Interferons Suppress IL-1 alpha and IL-1 beta Production by Distinct Pulmonary Myeloid Subsets during *Mycobacterium tuberculosis* Infection, *Immunity* **35**, 1023–1034 (2011).

178. D. Hanahan, R. A. Weinberg, Hallmarks of Cancer: The Next Generation, *Cell* **144**, 646–674 (2011).

179. T. F. Gajewski, H. Schreiber, Y.-X. Fu, Innate and adaptive immune cells in the tumor microenvironment, *Nat Immunol* **14**, 1014–1022 (2013).

180. K. H. Ely, T. Cookenham, A. D. Roberts, D. L. Woodland, Memory T cell populations in the lung airways are maintained by continual recruitment, *J. Immunol.* **176**, 537–543 (2006).

181. L. Yang, Y. Pang, H. L. Moses, and immune cells: an important regulatory axis in the tumor microenvironment and progression, *Trends in Immunology* **31**, 220–227 (2010).

182. J. D. Shields, I. C. Kourtis, A. A. Tomei, J. M. Roberts, M. A. Swartz, Induction of Lymphoidlike Stroma and Immune Escape by Tumors That Express the Chemokine CCL21, *Science* **328**, 749–752 (2010).

183. M. Kraman *et al.*, Suppression of Antitumor Immunity by Stromal Cells Expressing Fibroblast Activation Protein, *Science* **330**, 827–830 (2010).

184. Y. Wen *et al.*, Immunotherapy targeting fibroblast activation protein inhibits tumor growth and increases survival in a murine colon cancer model, *Cancer Science* **101**, 2325–2332 (2010).

185. H. Salmon *et al.*, Matrix architecture defines the preferential localization and migration of T cells into the stroma of human lung tumors, *Journal of Clinical Investigation* **122**, 899–910 (2012).

186. H. Salmon, E. Donnadieu, Within tumors, interactions between T cells and tumor cells are impeded by the extracellular matrix, *oncoimmunology* **1**, 992–994 (2012).

187. L. E. Kandalaft, A. Facciabene, R. J. Buckanovich, G. Coukos, Endothelin B Receptor, a New Target in Cancer Immune Therapy, *Clinical Cancer Research* **15**, 4521–4528 (2009).

188. S. Spranger *et al.*, Up-Regulation of PD-L1, IDO, and Tregs in the Melanoma Tumor Microenvironment Is Driven by CD8+ T Cells, *Science Translational Medicine* **5**, 200ra116–200ra116 (2013).

189. T. F. Gajewski, Failure at the Effector Phase: Immune Barriers at the

Level of the Melanoma Tumor Microenvironment, *Clinical Cancer Research* **13**, 5256–5261 (2007).

190. D. M. Brown, A. M. Dilzer, D. L. Meents, S. L. Swain, CD4 T cell-mediated protection from lethal influenza: perforin and antibody-mediated mechanisms give a one-two punch, *J. Immunol.* **177**, 2888–2898 (2006).

191. J. Kline *et al.*, Homeostatic Proliferation Plus Regulatory T-Cell Depletion Promotes Potent Rejection of B16 Melanoma, *Clinical Cancer Research* **14**, 3156–3167 (2008).

192. D. Mougiakakos, A. Choudhury, A. Lladser, R. Kiessling, C. C. Johansson, *Regulatory T Cells in Cancer* (Elsevier Inc., ed. 1, 2010), pp. 57–117.

193. S. Ostrand-Rosenberg, P. Sinha, Myeloid-Derived Suppressor Cells: Linking Inflammation and Cancer, *The Journal of Immunology* **182**, 4499–4506 (2009).

194. M. J. Berendt, R. J. North, T-cell-mediated suppression of anti-tumor immunity. An explanation for progressive growth of an immunogenic tumor, *J. Exp. Med.* **151**, 69–80 (1980).

195. E. S. Dye, R. J. North, T cell-mediated immunosuppression as an obstacle to adoptive immunotherapy of the P815 mastocytoma and its metastases, *J. Exp. Med.* **154**, 1033–1042 (1981).

196. E. Y. Woo *et al.*, Regulatory CD4(+)CD25(+) T cells in tumors from patients with early-stage non-small cell lung cancer and late-stage ovarian cancer, *Cancer Research* **61**, 4766–4772 (2001).

197. E. Y. Woo *et al.*, Cutting edge: Regulatory T cells from lung cancer patients directly inhibit autologous T cell proliferation, *J. Immunol.* **168**, 4272–4276 (2002).

198. A. M. Wolf *et al.*, Increase of regulatory T cells in the peripheral blood of cancer patients, *Clin. Cancer Res.* **9**, 606–612 (2003).

199. S. Kalathil, A. A. Lugade, A. Miller, R. Iyer, Y. Thanavala, Higher Frequencies of GARP+CTLA-4+Foxp3+ T Regulatory Cells and Myeloid-Derived Suppressor Cells in Hepatocellular Carcinoma Patients Are Associated with Impaired T-Cell Functionality, *Cancer Research* **73**, 2435–2444 (2013).

200. S. A. Joosten *et al.*, Identification of a human CD8+ regulatory T cell subset that mediates suppression through the chemokine CC chemokine ligand 4, *Proc. Natl. Acad. Sci. U.S.A.* **104**, 8029–8034 (2007).

201. C.-T. Huang *et al.*, Role of LAG-3 in regulatory T cells, *Immunity* **21**, 503–513 (2004).

202. K. Wing *et al.*, CTLA-4 control over Foxp3+ regulatory T cell function, *Science* **322**, 271–275 (2008).

203. M. I. Garin *et al.*, Galectin-1: a key effector of regulation mediated by CD4+CD25+ T cells, *Blood* **109**, 2058–2065 (2007).

204. M.-L. Chen *et al.*, Regulatory T cells suppress tumor-specific CD8 T cell cytotoxicity through TGF-beta signals in vivo, *Proc. Natl. Acad. Sci. U.S.A.* **102**, 419–424 (2005).

205. F. Ghiringhelli, CD4+CD25+ regulatory T cells inhibit natural killer cell functions in a transforming growth factor- -dependent manner, *Journal of Experimental Medicine* **202**, 1075–1085 (2005).

206. F. Fallarino *et al.*, The combined effects of tryptophan starvation and tryptophan catabolites down-regulate T cell receptor zeta-chain and induce a regulatory phenotype in naive T cells, *J. Immunol.* **176**, 6752–6761 (2006).

207. M. Mahic, S. Yaqub, C. C. Johansson, K. Taskén, E. M. Aandahl, FOXP3+CD4+CD25+ adaptive regulatory T cells express cyclooxygenase-2 and suppress effector T cells by a prostaglandin E2-dependent mechanism, *J. Immunol.* **177**, 246–254 (2006).

208. D. C. Gondek, L.-F. Lu, S. A. Quezada, S. Sakaguchi, R. J. Noelle, Cutting edge: contact-mediated suppression by CD4+CD25+ regulatory cells involves a granzyme B-dependent, perforin-independent mechanism, *J. Immunol.* **174**, 1783–1786 (2005).

209. W. J. Grossman *et al.*, Human T regulatory cells can use the perforin pathway to cause autologous target cell death, *Immunity* **21**, 589–601 (2004).

210. D.-M. Zhao, A. M. Thornton, R. J. DiPaolo, E. M. Shevach, Activated CD4+CD25+ T cells selectively kill B lymphocytes, *Blood* **107**, 3925–3932 (2006).

211. K. Kono *et al.*, CD4(+)CD25high regulatory T cells increase with tumor stage in patients with gastric and esophageal cancers, *Cancer Immunol Immunother* **55**, 1064–1071 (2005).

212. D. Wolf, The Expression of the Regulatory T Cell-Specific Forkhead Box Transcription Factor FoxP3 Is Associated with Poor Prognosis in Ovarian Cancer, *Clinical Cancer Research* **11**, 8326–8331 (2005).

213. Q. Gao *et al.*, Intratumoral Balance of Regulatory and Cytotoxic T Cells Is Associated With Prognosis of Hepatocellular Carcinoma After Resection, *Journal of Clinical Oncology* **25**, 2586–2593 (2007).

214. N. Leffers *et al.*, Prognostic significance of tumor-infiltrating T-lymphocytes in primary and metastatic lesions of advanced stage ovarian cancer, *Cancer Immunol Immunother* **58**, 449–459 (2008).

215. E. Sato *et al.*, Intraepithelial CD8+ tumor-infiltrating lymphocytes and a high CD8+/regulatory T cell ratio are associated with favorable prognosis in ovarian cancer, *Proc. Natl. Acad. Sci. U.S.A.* **102**, 18538–18543 (2005).

216. X. Yao *et al.*, Levels of peripheral CD4+FoxP3+ regulatory T cells are negatively associated with clinical response to adoptive immunotherapy of human cancer, *Blood* **119**, 5688–5696 (2012).

217. S. Sakaguchi, D. A. A. Vignali, A. Y. Rudensky, R. E. Niec, H. Waldmann, The plasticity and stability of regulatory T cells, *Nature Publishing Group* **13**, 461–467 (2013).

218. M. Kleinewietfeld, D. A. Hafler, Seminars in Immunology, *Seminars in Immunology* **25**, 305–312 (2013).

219. M. D. Sharma *et al.*, Reprogrammed Foxp3, *Immunity* **33**, 942–954 (2010).

220. N. Komatsu *et al.*, Heterogeneity of natural Foxp3+ T cells: a committed regulatory T-cell lineage and an uncommitted minor population retaining plasticity, *Proc. Natl. Acad. Sci. U.S.A.* **106**, 1903–1908 (2009).

221. D. I. Gabrilovich, S. Nagaraj, Myeloid-derived suppressor cells as regulators of the immune system, *Nat Rev Immunol* **9**, 162–174 (2009).

222. J.-I. Youn, S. Nagaraj, M. Collazo, D. I. Gabrilovich, Subsets of myeloid-derived suppressor cells in tumor-bearing mice, *The Journal of Immunology* **181**, 5791–5802 (2008).

223. P. Boros, J. C. Ochando, S. H. Chen, J. S. Bromberg, Myeloid-derived suppressor cells: Natural regulators for transplant tolerance, *HIM* **71**, 1061–1066 (2010).

224. J.-I. Youn, D. I. Gabrilovich, The biology of myeloid-derived suppressor cells: The blessing and the curse of morphological and functional heterogeneity, *Eur. J. Immunol.* **40**, 2969–2975 (2010).

225. K. Movahedi *et al.*, Different Tumor Microenvironments Contain

Functionally Distinct Subsets of Macrophages Derived from Ly6C(high) Monocytes, *Cancer Research* **70**, 5728–5739 (2010).

226. World Health Organization, Annex Table 2: Deaths by cause, sex and mortality stratum in WHO regions, estimates for 2002, *The world health report* (2004).

227. S. T. Holgate, Innate and adaptive immune responses in asthma, *Nature Medicine* **18**, 673–683 (2012).

228. X. Jiang *et al.*, Skin infection generates non-migratory memory CD8+ TRM cells providing global skin immunity, *Nature* **483**, 227–231 (2012).

229. D. Masopust, V. Vezys, A. L. Marzo, L. Lefrançois, Preferential Localization of Effector Memory Cells in Nonlymphoid Tissue, *Science* **291**, 2413–2417 (2001).

230. D. R. Marshall *et al.*, Measuring the diaspora for virus-specific CD8+ T cells, *Proc. Natl. Acad. Sci. U.S.A.* **98**, 6313–6318 (2001).

231. S. K. Bromley, T. R. Mempel, A. D. Luster, Orchestrating the orchestrators: chemokines in control of T cell traffic, *Nat Immunol* **9**, 970–980 (2008).

232. M. Hofmann, V. Brinkmann, H.-G. Zerwes, FTY720 preferentially depletes naive T cells from peripheral and lymphoid organs, *International Immunopharmacology* **6**, 1902–1910 (2006).

233. J. E. Childs, G. E. Glass, G. W. Korch, T. G. Ksiazek, J. W. Leduc, Lymphocytic choriomeningitis virus infection and house mouse (Mus musculus) distribution in urban Baltimore, *Am. J. Trop. Med. Hyg.* **47**, 27–34 (1992).

234. E. Galkina *et al.*, Preferential migration of effector CD8+ T cells into the interstitium of the normal lung, *Journal of Clinical Investigation* **115**, 3473–3483 (2005).

235. A. M. Gallegos, E. G. Pamer, M. S. Glickman, Delayed protection by ESAT-6-specific effector CD4+ T cells after airborne M. tuberculosis infection, *Journal of Experimental Medicine* **205**, 2359–2368 (2008).

236. J. E. Moyron-Quiroz *et al.*, Role of inducible bronchus associated lymphoid tissue (iBALT) in respiratory immunity, *Nature Medicine* **10**, 927–934 (2004).

237. T. M. Strutt *et al.*, Memory CD4+ T cells induce innate responses independently of pathogen, *Nature Medicine* **16**, 558–564 (2010).

238. R. J. Hogan *et al.*, Protection from respiratory virus infections can be mediated by antigen-specific CD4(+) T cells that persist in the lungs, *J. Exp. Med.* **193**, 981–986 (2001).

239. L. Yang *et al.*, Expansion of myeloid immune suppressor Gr+CD11b+ cells in tumor-bearing host directly promotes tumor angiogenesis, *Cancer Cell* **6**, 409–421 (2004).

240. L. Yang *et al.*, Abrogation of TGFβ Signaling in Mammary Carcinomas Recruits Gr-1+CD11b+ Myeloid Cells that Promote Metastasis, *Cancer Cell* **13**, 23–35 (2008).

241. T. I. Arnon, R. M. Horton, I. L. Grigorova, J. G. Cyster, Visualization of splenic marginal zone B-cell shuttling and follicular B-cell egress, *Nature* **493**, 684–688 (2013).

242. K. E. Barletta *et al.*, Leukocyte compartments in the mouse lung: distinguishing between marginated, interstitial, and alveolar cells in response to injury, *Journal of Immunological Methods* **375**, 100–110 (2012).

243. J. Reutershan, Sequential recruitment of neutrophils into lung and bronchoalveolar lavage fluid in LPS-induced acute lung injury, *AJP: Lung Cellular and Molecular Physiology* **289**, L807–L815 (2005).

244. U. H. von Andrian, C. R. Mackay, T-cell function and migration. Two sides of the same coin, *N. Engl. J. Med.* **343**, 1020–1034 (2000).

245. S. A. Islam, A. D. Luster, T cell homing to epithelial barriers in allergic disease, *Nature Medicine* **18**, 705–715 (2012).

246. S. Manicassamy, B. Pulendran, Dendritic cell control of tolerogenic responses, *Immunol. Rev.* **241**, 206–227 (2011).

247. T. A. Wynn, A. Chawla, J. W. Pollard, Macrophage biology in development, homeostasis and disease, *Nature* **496**, 445–455 (2013).

248. L. Lefrançois, L. Puddington, Intestinal and Pulmonary Mucosal T Cells: Local Heroes Fight to Maintain the Status Quo, *Annu. Rev. Immunol.* **24**, 681–704 (2006).

249. N. Zhang, M. J. Bevan, CD8+ T Cells: Foot Soldiers of the Immune System, *Immunity* **35**, 161–168 (2011).

250. B. S. Sheridan, L. Lefrançois, Regional and mucosal memory T cells, *Nat Immunol* **12**, 485–491 (2011).

251. S. N. Mueller, T. Gebhardt, F. R. Carbone, W. R. Heath, Memory T Cell Subsets, Migration Patterns, and Tissue Residence, *Annu. Rev. Immunol.* **31**, 137–161 (2013).

252. T. Gebhardt, S. N. Mueller, W. R. Heath, F. R. Carbone, Peripheral tissue surveillance and residency by memory T cells, *Trends in Immunology* **34**, 27–32 (2013).

253. M. Guilliams, B. N. Lambrecht, H. Hammad, Division of labor between lung dendritic cells and macrophages in the defense against pulmonary infections, *Mucosal Immunology* **6**, 464–473 (2013).

254. K. G. Anderson *et al.*, Cutting Edge: Intravascular Staining Redefines Lung CD8 T Cell Responses, *The Journal of Immunology* **189**, 2702–2706 (2012).

255. F. Geissmann *et al.*, Intravascular Immune Surveillance by CXCR6+ NKT Cells Patrolling Liver Sinusoids, *Plos Biol* **3**, e113 (2005).

256. W.-Y. Lee *et al.*, An intravascular immune response to *Borrelia burgdorferi* involves Kupffer cells and iNKT cells, *Nat Immunol* **11**, 295–302 (2010).

257. S. Y. Thomas *et al.*, T cell receptor signal strength in Treg and iNKT cell development demonstrated by a novel fluorescent reporter mouse, *Journal of Experimental Medicine* **208**, 1179–1188 (2011).

258. S. T. Scanlon *et al.*, Airborne lipid antigens mobilize resident intravascular NKT cells to induce allergic airway inflammation, *Journal of Experimental Medicine* **208**, 2113–2124 (2011).

259. G. B. Segel, G. R. Cokelet, M. A. Lichtman, The measurement of lymphocyte volume: importance of reference particle deformability and counting solution tonicity, *Blood* **57**, 894–899 (1981).

260. H. Unsoeld, H. Pircher, Complex Memory T-Cell Phenotypes Revealed by Coexpression of CD62L and CCR7, *Journal of Virology* **79**, 4510–4513 (2005).

261. C. Berlin-Rufenach *et al.*, Lymphocyte migration in lymphocyte function-associated antigen (LFA)-1-deficient mice, *J. Exp. Med.* **189**, 1467–1478 (1999).

262. M. Radu, J. Chernoff, An in vivo Assay to Test Blood Vessel Permeability, *JoVE* (2013), doi:10.3791/50062.

263. S. O. Sharrow, Overview of flow cytometry, *Curr Protoc Immunol* **Chapter**

5, Unit 5.1 (2002).

264. M. Roederer, Multiparameter FACS analysis, *Curr Protoc Immunol* **Chapter 5**, Unit 5.8 (2002).

265. J. G. Donaldson, Immunofluorescence staining, *Curr Protoc Cell Biol* **Chapter 4**, Unit 4.3 (2001).

266. C. A. Combs, *Fluorescence Microscopy: A Concise Guide to Current Imaging Methods* (John Wiley & Sons, Inc., Hoboken, NJ, USA, 2001).

267. B. Herman, Fluorescence Microscopy, *Curr Protoc Immunol* (2002).

268. K. Neyt, F. Perros, C. H. GeurtsvanKessel, H. Hammad, B. N. Lambrecht, Structure, development and function of tertiary lymphoid organs in infection and autoimmunity, *Trends in Immunology* **33**, 297–305 (2012).

269. B. A. Hart, A. G. Harmsen, R. B. Low, R. Emerson, Biochemical, cytological, and histological alterations in rat lung following acute beryllium aerosol exposure, *Toxicol. Appl. Pharmacol.* **75**, 454–465 (1984).

270. D. L. Woodland, T. D. Randall, Anatomical features of anti-viral immunity in the respiratory tract, *Seminars in Immunology* **16**, 163–170 (2004).

271. J. Moyron-Quiroz, J. Rangel-Moreno, D. M. Carragher, T. D. Randall, The function of local lymphoid tissues in pulmonary immune responses, *Adv. Exp. Med. Biol.* **590**, 55–68 (2007).

272. D. M. Carragher, J. Rangel-Moreno, T. D. Randall, Ectopic lymphoid tissues and local immunity, *Seminars in Immunology* **20**, 26–42 (2008).

273. T. D. Randall, *Chapter 7 - Bronchus-Associated Lymphoid Tissue (BALT): Structure and Function* (Elsevier Inc., ed. 1, 2010), pp. 187–241.

274. L. M. Carlin *et al.*, Nr4a1-Dependent Ly6Clow Monocytes Monitor Endothelial Cells and Orchestrate Their Disposal, *Cell* **153**, 362–375 (2013).

275. M. A. Daniels, S. C. Jameson, Critical role for CD8 in T cell receptor binding and activation by peptide/major histocompatibility complex multimers, *J. Exp. Med.* **191**, 335–346 (2000).

276. D. Allman, S. Pillai, Peripheral B cell subsets, *Current Opinion in Immunology* **20**, 149–157 (2008).

277. J. P. Pereira, L. M. Kelly, J. G. Cyster, Finding the right niche: B-cell

migration in the early phases of T-dependent antibody responses, *International Immunology* **22**, 413–419 (2010).

278. F. D. Batista, N. E. Harwood, The who, how and where of antigen presentation to B cells, *Nat Rev Immunol* **9**, 15–27 (2009).

279. E. Wissinger, J. Goulding, T. Hussell, Immune homeostasis in the respiratory tract and its impact on heterologous infection, *Seminars in Immunology* **21**, 147–155 (2009).

280. A. J. Wolf *et al.*, Mycobacterium tuberculosis infects dendritic cells with high frequency and impairs their function in vivo, *J. Immunol.* **179**, 2509–2519 (2007).

281. F. Geissmann *et al.*, Development of Monocytes, Macrophages, and Dendritic Cells, *Science* **327**, 656–661 (2010).

282. L. A. Norian *et al.*, E. J. Kremer, Ed. Eradication of Metastatic Renal Cell Carcinoma after Adenovirus-Encoded TNF-Related Apoptosis-Inducing Ligand (TRAIL)/CpG Immunotherapy, *PLoS ONE* **7**, e31085 (2012).

283. B. R. James *et al.*, Diet-Induced Obesity Alters Dendritic Cell Function in the Presence and Absence of Tumor Growth, *The Journal of Immunology* **189**, 1311–1321 (2012).

284. J. S. Ko *et al.*, Direct and Differential Suppression of Myeloid-Derived Suppressor Cell Subsets by Sunitinib Is Compartmentally Constrained, *Cancer Research* **70**, 3526–3536 (2010).

285. J. Finke *et al.*, MDSC as a mechanism of tumor escape from sunitinib mediated anti-angiogenic therapy, *International Immunopharmacology* **11**, 856–861 (2011).

286. T. A. Dietlin *et al.*, Mycobacteria-induced Gr-1+ subsets from distinct myeloid lineages have opposite effects on T cell expansion, *Journal of Leukocyte Biology* **81**, 1205–1212 (2007).

287. K. Movahedi *et al.*, Identification of discrete tumor-induced myeloid-derived suppressor cell subpopulations with distinct T cell-suppressive activity, *Blood* **111**, 4233–4244 (2008).

288. S. S. Kang *et al.*, Migration of cytotoxic lymphocytes in cell cycle permits local MHC I-dependent control of division at sites of viral infection, *Journal of Experimental Medicine* **208**, 747–759 (2011).

289. J. S. Hale *et al.*, Distinct Memory CD4+ T Cells with Commitment to T Follicular Helper- and T Helper 1-Cell Lineages Are Generated after

Acute Viral Infection, *Immunity* **38**, 805–817 (2013).

290. S. Mukherjee *et al.*, Surfactant protein A integrates activation signal strength to differentially modulate T cell proliferation, *The Journal of Immunology* **188**, 957–967 (2012).

291. D. Masopust, Developing an HIV cytotoxic T-lymphocyte vaccine: issues of CD8 T-cell quantity, quality and location, *Journal of Internal Medicine* **265**, 125–137 (2009).

292. T. Gebhardt, Local immunity by tissue-resident CD8,, 1–12 (2012).

293. K. G. Anderson *et al.*, Intravascular staining for discrimination of vascular and tissue leukocytes, *Nat Protoc* **9**, 209–222 (2014).

294. C. M. Carlson *et al.*, Kruppel-like factor 2 regulates thymocyte and T-cell migration, *Nature* **442**, 299–302 (2006).

295. E. Sebzda, Z. Zou, J. S. Lee, T. Wang, M. L. Kahn, Transcription factor KLF2 regulates the migration of naive T cells by restricting chemokine receptor expression patterns, *Nat Immunol* **9**, 292–300 (2008).

296. P. K. Wallace *et al.*, F. Kern, J. W. Gratama, F. Manca, M. Roederer, Eds. Tracking antigen-driven responses by flow cytometry: Monitoring proliferation by dye dilution, *Cytometry* **73A**, 1019–1034 (2008).

297. H. Veiga-Fernandes, U. Walter, C. Bourgeois, A. McLean, B. Rocha, Response of naïve and memory CD8+ T cells to antigen stimulation in vivo, *Nat Immunol* **1**, 47–53 (2000).

298. E. D. Hawkins *et al.*, Measuring lymphocyte proliferation, survival and differentiation using CFSE time-series data, *Nat Protoc* **2**, 2057–2067 (2007).

299. B. J. C. Quah, H. S. Warren, C. R. Parish, Monitoring lymphocyte proliferation in vitro and in vivo with the intracellular fluorescent dye carboxyfluorescein diacetate succinimidyl ester, *Nat Protoc* **2**, 2049–2056 (2007).

300. B. J. C. Quah, C. R. Parish, The Use of Carboxyfluorescein Diacetate Succinimidyl Ester (CFSE) to Monitor Lymphocyte Proliferation, *JoVE* (2010), doi:10.3791/2259.

301. M. W.-C. Su *et al.*, Fratricide of CD8+ cytotoxic T lymphocytes is dependent on cellular activation and perforin-mediated killing, *Eur. J. Immunol.* **34**, 2459–2470 (2004).

302. M. W. Su, P. R. Walden, D. B. Golan, H. N. Eisen, Cognate peptide-induced destruction of CD8+ cytotoxic T lymphocytes is due to fratricide, *J. Immunol.* **151**, 658–667 (1993).

303. P. R. Walden, H. N. Eisen, Cognate peptides induce self-destruction of CD8+ cytolytic T lymphocytes, *Proc. Natl. Acad. Sci. U.S.A.* **87**, 9015–9019 (1990).

304. D. Kyburz, D. E. Speiser, T. Aebischer, H. Hengartner, R. M. Zinkernagel, Virus-specific cytotoxic T cell-mediated lysis of lymphocytes in vitro and in vivo, *J. Immunol.* **150**, 5051–5058 (1993).

305. E. Hanon *et al.*, Fratricide among CD8(+) T lymphocytes naturally infected with human T cell lymphotropic virus type I, *Immunity* **13**, 657–664 (2000).

306. S. Spiegel, S. Milstien, The outs and the ins of sphingosine- 1-phosphate in immunity, *Nature Publishing Group* **11**, 403–415 (2011).

307. I. N. Crispe, Hepatic T cells and liver tolerance, *Nat Rev Immunol* **3**, 51–62 (2003).

308. A. H. Sharpe, E. J. Wherry, R. Ahmed, G. J. Freeman, The function of programmed cell death 1 and its ligands in regulating autoimmunity and infection, *Nat Immunol* **8**, 239–245 (2007).

309. E. J. Wherry, J. N. Blattman, K. Murali-Krishna, R. van der Most, R. Ahmed, Viral Persistence Alters CD8 T-Cell Immunodominance and Tissue Distribution and Results in Distinct Stages of Functional Impairment, *Journal of Virology* **77**, 4911–4927 (2003).

310. M. Saitoh *et al.*, Importance of the Carboxy-Terminal 25 Amino Acid Residues of Lung Collectins in Interactions with Lipids and Alveolar Type II Cells †, *Biochemistry* **39**, 1059–1066 (2000).

311. Y. T. Lee *et al.*, Environmental and Antigen Receptor-Derived Signals Support Sustained Surveillance of the Lungs by Pathogen-Specific Cytotoxic T Lymphocytes, *Journal of Virology* **85**, 4085–4094 (2011).

312. A. J. Tenner, S. L. Robinson, J. Borchelt, J. R. Wright, Human pulmonary surfactant protein (SP-A), a protein structurally homologous to C1q, can enhance FcR- and CR1-mediated phagocytosis, *J. Biol. Chem.* **264**, 13923–13928 (1989).

313. M. J. Tino, J. R. Wright, Surfactant protein A stimulates phagocytosis of specific pulmonary pathogens by alveolar macrophages, *Am. J. Physiol.* **270**, L677–88 (1996).

314. J. M. Hohlfeld, V. J. Erpenbeck, N. Krug, Surfactant proteins SP-A and SP-D as modulators of the allergic inflammation in asthma, *Pathobiology* (2003).

315. A. M. Pastva *et al.*, Lung effector memory and activated CD4+ T cells display enhanced proliferation in surfactant protein A-deficient mice during allergen-mediated inflammation, *The Journal of Immunology* **186**, 2842–2849 (2011).

316. S. T. Scanlon *et al.*, Surfactant protein-A inhibits Aspergillus fumigatus-induced allergic T-cell responses, *Respir. Res.* **6**, 97 (2005).

317. P. J. Borron *et al.*, Pulmonary surfactant proteins A and D directly suppress CD3+/CD4+ cell function: evidence for two shared mechanisms, *J. Immunol.* **169**, 5844–5850 (2002).

318. P. Borron *et al.*, Surfactant associated protein-A inhibits human lymphocyte proliferation and IL-2 production, *American Journal of Respiratory Cell and Molecular Biology* **15**, 115–121 (1996).

319. D. M. Jelley-Gibbs *et al.*, Unexpected prolonged presentation of influenza antigens promotes CD4 T cell memory generation, *Journal of Experimental Medicine* **202**, 697–706 (2005).

320. D. J. Zammit, D. L. Turner, K. D. Klonowski, L. Lefrançois, L. S. Cauley, Residual Antigen Presentation after Influenza Virus Infection Affects CD8 T Cell Activation and Migration, *Immunity* **24**, 439–449 (2006).

321. D. J. Topham, R. A. Tripp, P. C. Doherty, CD8+ T cells clear influenza virus by perforin or Fas-dependent processes, *J. Immunol.* **159**, 5197–5200 (1997).

322. S. Vallbracht, H. Unsöld, S. Ehl, Functional impairment of cytotoxic T cells in the lung airways following respiratory virus infections, *Eur. J. Immunol.* **36**, 1434–1442 (2006).

323. H. O'Donnell *et al.*, Toll-like Receptor and Inflammasome Signals Converge to Amplify the Innate Bactericidal Capacity of T Helper 1 Cells, *Immunity* **40**, 213–224 (2014).

324. J.-M. Doisne *et al.*, CD8+ T cells specific for EBV, cytomegalovirus, and influenza virus are activated during primary HIV infection, *J. Immunol.* **173**, 2410–2418 (2004).

325. O. A. Odumade *et al.*, Primary Epstein-Barr virus infection does not erode preexisting CD8+ T cell memory in humans, *Journal of Experimental Medicine* **209**, 471–478 (2012).

326. S. M. Soudja, A. L. Ruiz, J. C. Marie, G. Lauvau, Inflammatory Monocytes Activate Memory CD8, *Immunity* **37**, 549–562 (2012).

327. D. F. Tough, P. Borrow, J. Sprent, Induction of bystander T cell proliferation by viruses and type I interferon in vivo, *Science* **272**, 1947–1950 (1996).

328. J. M. Reynolds, C. Dong, Toll-like receptor regulation of effector T lymphocyte function, *Trends in Immunology* **34**, 511–519 (2013).